

**PRODUCTION AND CHARACTERIZATION OF ACTIVATED  
CARBON FROM PALM SHELL BY USING MICROWAVE HEATING  
METHOD**

**ROOZBEH HOSEINZADEH HESAS**

**THESIS SUBMITTED IN FULFILLMENT OF  
THE REQUIREMENT FOR THE DEGREE OF  
DOCTOR OF PHILOSOPHY**

**FACULTY OF ENGINEERING  
UNIVERSITY OF MALAYA  
KUALA LUMPUR**

**2014**

# UNIVERSITI MALAYA

## PERAKUAN KEASLIAN PENULISAN

Nama: *Roozbeh Hoseinzadeh Hesas*

(No. K.P/Pasport:

No. Pendaftaran/Matrik: *KHA100113*

Nama Ijazah: *Doktor Falsafah*

Tajuk Kertas Projek/Laporan Penyelidikan/Disertasi/Tesis ("Hasil Kerja ini"):

*PENGELUARAN KARBON DIAKTIFKAN DARIPADA SAWIT SHELL DENGAN MENGGUNAKAN  
GELOMBANG MEMANASKAN KAEDAH*

Bidang Penyelidikan: *Kejuruteraan Tindak Balas*

Saya dengan sesungguhnya dan sebenarnya mengaku bahawa:

- (1) Saya adalah satu-satunya pengarang/penulis Hasil Kerja ini;
- (2) Hasil Kerja ini adalah asli;
- (3) Apa-apa penggunaan mana-mana hasil kerja yang mengandungi hakcipta telah dilakukan secara urusan yang wajar dan bagi maksud yang dibenarkan dan apa-apa petikan, ekstrak, rujukan atau pengeluaran semula daripada atau kepada mana-mana hasil kerja yang mengandungi hakcipta telah dinyatakan dengan sejelasnya dan secukupnya dan satu pengiktirafan tajuk hasil kerja tersebut dan pengarang/penulisnya telah dilakukan di dalam Hasil Kerja ini;
- (4) Saya tidak mempunyai apa-apa pengetahuan sebenar atau patut semunasabahnya tahu bahawa penghasilan Hasil Kerja ini melanggar suatu hakcipta hasil kerja yang lain;
- (5) Saya dengan ini menyerahkan kesemua dan tiap-tiap hak yang terkandung di dalam hakcipta Hasil Kerja ini kepada Universiti Malaya ("UM") yang seterusnya mula dari sekarang adalah tuan punya kepada hakcipta di dalam Hasil Kerja ini dan apa-apa pengeluaran semula atau penggunaan dalam apa jua bentuk atau dengan apa juga cara sekalipun adalah dilarang tanpa terlebih dahulu mendapat kebenaran bertulis dari UM;
- (6) Saya sedar sepenuhnya sekiranya dalam masa penghasilan Hasil Kerja ini saya telah melanggar suatu hakcipta hasil kerja yang lain sama ada dengan niat atau sebaliknya, saya boleh dikenakan tindakan undang-undang atau apa-apa tindakan lain sebagaimana yang diputuskan oleh UM.

Tandatangan Calon

Tarikh      Nov 2014

Diperbuat dan sesungguhnya diakui di hadapan,

Tandatangan Saksi

Tarikh

Nama:

Jawatan:

# UNIVERSITI MALAYA

## ORIGINAL LITERARY WORK DECLARATION

Name of Candidate: *Roosbeh Hoseinzadeh Hesa* (I.C./Passport No: *L95236862* )

Registration/Matric No: *KHA100113*

Name of Degree: *Doctor of Philosophy (PhD)*

Title of Project Paper/Research Report/Dissertation/Thesis ("this Work"):

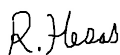
*PRODUCTION OF ACTIVATED CARBON FROM PALM SHELL BY USING  
MICROWAVE HEATING METHOD*

Field of Study: *Reaction Engineering*

I do solemnly and sincerely declare that:

- (1) I am the sole author/writer of this Work;
- (2) This Work is original;
- (3) Any use of any work in which copyright exists was done by way of fair dealing and for permitted purposes and any excerpt or extract from, or reference to or reproduction of any copyright work has been disclosed expressly and sufficiently and the title of the Work and its authorship have been acknowledged in this Work;
- (4) I do not have any actual knowledge nor do I ought reasonably to know that the making of this work constitutes an infringement of any copyright work;
- (5) I hereby assign all and every rights in the copyright to this Work to the University of Malaya ("UM"), who henceforth shall be owner of the copyright in this Work and that any reproduction or use in any form or by any means whatsoever is prohibited without the written consent of UM having been first had and obtained;
- (6) I am fully aware that if in the course of making this Work I have infringed any copyright whether intentionally or otherwise, I may be subject to legal action or any other action as may be determined by UM.

Candidate's Signature



Date

Nov 2014

Subscribed and solemnly declared before,

Witness's Signature

Date

Name:

Designation:

## ABSTRACT

Activated carbon (AC) demonstrated significant adsorption of pollutants in gas and liquid phases due to its high micropore volume, large specific surface area, favorable pore size distribution, thermal stability, capability for rapid adsorption and low acid/base reactivity. Palm shell (agricultural waste) is used as a raw material in this study due to its inherent characteristics such as high carbon content, low ash, and almost negligible sulfur content.

In the present work, microwave heating was applied instead of conventional heating techniques as a heat source of AC preparation. This method reveals higher sintering temperatures and shorter processing times which result in higher efficiency and more energy saving. The effects of significant parameters such as microwave radiation time and power level, different types of chemical and physical agents, chemical impregnation ratio and particle size in production of ACs were investigated. Accordingly, the effects of these variables on the structural and surface chemical properties of the ACs were explored.

Several methods of characterization were utilized to examine the prepared ACs including nitrogen adsorption-desorption at  $-196\text{ }^{\circ}\text{C}$ , proximate and ultimate analysis, Fourier transform infrared spectroscopy (FTIR) and scanning electron microscopy (SEM). Moreover,  $\text{CO}_2$  adsorption at different temperatures and methylene blue (MB) adsorption were carried out. The response surface methodology was used to optimize the preparation conditions of palm shell based ACs with microwave heating methods by zinc chloride chemical activation. The influence of variances on MB adsorption capacity and AC yield was investigated.

Based on the analysis of variance, microwave power and microwave radiation time were identified as the most influential factors for AC yield and MB adsorption capacity, respectively.

In this study, effects of different heating methods of microwave and conventional on textural and surface chemical properties of the ACs were compared. The  $\text{ZnCl}_2$  chemical activation at different weight ratio of  $\text{ZnCl}_2$  to precursors were applied. The results indicated that for both the microwave and conventionally prepared samples, the BET surface area ( $S_{\text{BET}}$ ) is enhanced to a maximum value at optimum impregnation ratio and then decreased with further increases in the agent ratio. The total pore volume in the microwave samples increased continuously with increasing zinc chloride, while in the conventional samples, the total pore volume increased up to the optimum impregnation ratio and then decreased.

Oil palm shell based ACs were also prepared using KOH as an activation agent under the microwave irradiation. The effects of the activation time, chemical impregnation ratio and microwave power on the AC properties were investigated. To study the effects of the nature of the physical agent, the impregnated precursors were activated under a flow of carbon dioxide or nitrogen. The results demonstrates that the  $\text{CO}_2$  activation requires a shorter activation time to reach the maximum  $S_{\text{BET}}$  than the activation under  $\text{N}_2$  since  $\text{CO}_2$  reacts with the carbon to develop the porosity.

## ABSTRAK

Diaktifkan karbon (AC) menunjukkan penjerapan bahan pencemar ketara dalam fasa gas dan fasa cecair akibat kelantangan micropore tinggi, kawasan permukaan tertentu yang besar, baik taburan saiz liang, kestabilan terma, keupayaan untuk penjerapan pesat dan rendah asid / asas kereaktifan. Kelapa shell (sisa pertanian) digunakan sebagai bahan mentah dalam kajian ini kerana ciri-ciri yang sedia ada seperti kandungan tinggi karbon, abu yang rendah, dan kandungan sulfur hampir diabaikan.

Dalam kajian ini, pemanasan gelombang mikro telah sebaliknya digunakan teknik pemanasan konvensional sebagai sumber haba penyediaan AC. Kaedah ini mendedahkan suhu pensinteran yang lebih tinggi dan masa pemprosesan yang lebih pendek yang mengakibatkan kecekapan yang lebih tinggi dan lebih penjimatan tenaga. Kesan parameter penting seperti masa radiasi gelombang mikro dan tahap kuasa, pelbagai jenis bahan kimia dan fizikal, nisbah hal memberi kimia dan saiz zarah dalam pengeluaran PB telah disiasat. Oleh itu, kesan pembolehubah pada sifat-sifat kimia dan struktur permukaan PB telah diteroka.

Beberapa kaedah pencirian telah digunakan untuk mengkaji PB disediakan termasuk nitrogen penjerapan-desorption pada  $-196\text{ }^{\circ}\text{C}$ , proksimat dan kandungan utama, Spektroskopi (FTIR) dan imbasan mikroskop elektron (SEM). Lebih-lebih lagi, penjerapan  $\text{CO}_2$  pada suhu yang berbeza dan penjerapan metilena biru (MB) telah dijalankan.

Ini kaedah gerak balas permukaan telah digunakan untuk mengoptimumkan keadaan penyediaan tempurung kelapa PB berasaskan dengan kaedah pemanasan gelombang mikro oleh pengaktifan zink klorida kimia. Pengaruh perbezaan kapasiti penjerapan metilena biru dan hasil AC telah dikaji.

Berdasarkan analisis varians, kuasa gelombang mikro dan ketuhar gelombang mikro radiasi masa telah dikenal pasti sebagai faktor yang paling berpengaruh untuk hasil AC dan kapasiti penjerapan MB, masing-masing.

Dalam kajian ini, kesan kaedah pemanasan yang berbeza gelombang mikro dan konvensional pada sifat-sifat kimia dan tekstur permukaan PB berbanding. Dalam seksyen ini,  $\text{ZnCl}_2$  pengaktifan kimia pada nisbah berat badan yang berbeza  $\text{ZnCl}_2$  untuk prekursor telah digunakan. Keputusan menunjukkan bahawa bagi kedua-dua gelombang mikro dan sampel konvensional disediakan, kawasan permukaan BET ( $S_{\text{BET}}$ ) dipertingkatkan kepada nilai maksimum pada nisbah hal memberi optimum dan kemudian menurun dengan peningkatan lebih lanjut dalam nisbah ejen itu. Jumlah isi padu liang dalam sampel gelombang mikro meningkat secara berterusan dengan peningkatan zink klorida, manakala dalam sampel konvensional, jumlah isi padu liang meningkat sehingga nisbah hal memberi optimum dan kemudian berkurangan.

PB tempurung kelapa sawit berasaskan juga telah disediakan dengan menggunakan KOH sebagai agen pengaktifan di bawah penyinaran gelombang mikro. Kesan masa pengaktifan, nisbah hal memberi kimia dan kuasa gelombang mikro pada sifat-sifat AC telah disiasat. Untuk mengkaji kesan sifat ejen fizikal, prekursor impregnated telah diaktifkan di bawah aliran karbon dioksida atau nitrogen. Keputusan menunjukkan bahawa pengaktifan  $\text{CO}_2$  memerlukan masa pengaktifan yang lebih pendek untuk mencapai  $S_{\text{BET}}$  maksimum daripada pengaktifan di bawah  $\text{N}_2$  sejak  $\text{CO}_2$  bertindak balas dengan karbon untuk membangunkan keliangan.

## ACKNOWLEDGEMENTS

I would like to express my special appreciation and thanks to my advisor Professor Dr. Wan Mohd Ashri Wan Daud, you have been a tremendous mentor for me. I would like to thank you for encouraging my research and for allowing me to grow as a research scientist. Your advice on both research as well as on my career have been priceless.

I also acknowledge the support provided by the laboratory technicians and office staff during the entire period of my study. I will like to thank University of Malaya for providing me with sufficient research grants and excellent analytical facility.

I will thank my parents, and my friends, especially Arash Arami-Niya and for his constant help throughout the thesis.

Roozbeh Hoseinzadeh Hesas

Dept of Chemical Engineering,

University of Malaya, Kuala Lumpur, Malaysia.



# TABLE OF CONTENTS

ABSTRACT .....	i
ABSTRAK .....	iii
ACKNOWLEDGEMENTS .....	vi
TABLE OF CONTENTS .....	vii
LIST OF FIGURES .....	xi
LIST OF TABLES .....	xiv
LIST OF SYMBOLS AND ABBREVIATIONS .....	xvi
CHAPTER 1: GENERAL INTRODUCTION .....	1
1.1 Background .....	1
1.2 Research Objectives .....	2
1.3 Thesis Organization .....	3
CHAPTER 2: LITERATURE REVIEW .....	4
2.1 Introduction .....	4
2.2 Microwave heating methods .....	6
2.3 Effects of the microwave heating method on the physical properties of AC .....	8
2.4 Effects of microwave power on the physical structure of chemically AC .....	10
2.5 Effects of microwave radiation time on the physical structure of chemically AC .....	14
2.6 Effects of impregnation ratio on the physical structure of chemically AC .....	20
2.7 Effects of microwave power and radiation time on the physical structure of physically AC .....	21

2.8 Effects of different agents and agent flow rates on the physical structure of physically AC .....	23
2.9 Effects of microwave-induced method on carbon yield .....	25
2.10 Effects of the microwave-induced method on the chemical properties of AC	29
CHAPTER 3: METHODOLOGY .....	35
3.1 PART 1: Palm shell based AC prepared by zinc chloride chemical activation using response surface methodology.....	35
3.1.1 Materials.....	35
3.1.2 Activation method.....	35
3.1.3 Characterization methods.....	36
3.1.4 Experimental design.....	37
3.1.5 Batch equilibrium studies.....	40
3.2 PART 2: Comparison of oil palm shell-based ACs produced by microwave and conventional heating methods using zinc chloride activation.....	41
3.2.1 Material .....	41
3.2.1 Activation method.....	41
3.2.3 Characterization methods.....	42
3.3 PART 3: Microwave-assisted production of ACs from oil palm shell in the presence of CO <sub>2</sub> or N <sub>2</sub> for CO <sub>2</sub> adsorption .....	43
3.3.1 Material .....	43
3.3.1 Activation method.....	43
3.3.3 CO <sub>2</sub> capture measurements .....	44
CHAPTER 4: RESULTS AND DISCUSSION.....	45
4.1 PART 1: Palm shell based AC prepared by zinc chloride chemical activation using response surface methodology .....	45
4.1.1 Development of regression model equation and statistical analysis.....	45

4.1.2	Effects of the preparation variables on the AC yield .....	49
4.1.3	Effect of preparation variables on MB adsorption capacity .....	53
4.1.4	Process optimization .....	55
4.1.5	Characterization of the AC prepared under the optimized conditions .....	56
4.2	PART 2: Comparison of oil palm shell-based ACs produced by microwave and conventional heating methods using zinc chloride activation.....	60
4.2.1	Surface textural properties .....	60
4.2.2	Pore size distribution.....	66
4.2.3	Proximate and ultimate analysis .....	68
4.2.4	FTIR analysis .....	70
4.2.5	Surface morphology .....	75
4.3	PART 3: Production of ACs from oil palm shell via microwave-assisted KOH activation in the presence of CO <sub>2</sub> or N <sub>2</sub> for CO <sub>2</sub> adsorption .....	77
4.3.1	Effects of radiation time.....	77
4.3.2	Effects of the impregnation ratio.....	80
4.3.3	Effects of the microwave power .....	85
4.3.4	Extra surface characterizations .....	87
4.3.4.1	Surface morphology.....	88
4.3.4.2	Proximate and ultimate analysis.....	89
4.3.4.3	FTIR analysis .....	91
4.3.4.4	CO <sub>2</sub> adsorption.....	94
	CHAPTER 5: CONCLUSION.....	98
5.1	PART 1: Palm shell based AC prepared by zinc chloride chemical activation using response surface methodology.....	98

5.2	PART 2: Comparison of oil palm shell-based ACs produced by microwave and conventional heating methods using zinc chloride activation.....	98
5.3	PART 3: Production of ACs from oil palm shell via microwave-assisted KOH activation in the presence of CO <sub>2</sub> or N <sub>2</sub> for CO <sub>2</sub> adsorption .....	99
	REFERENCES .....	100

## LIST OF FIGURES

Figure 4.1	Predicted vs. experimental value of (a) AC yield (%) and (b) MB adsorption capacity.....	46
Figure 4.2	The three-dimensional response surfaces (a) the effect of activation time and microwave power (b) the effect of activation time and particle size (c) the effect of impregnation ratio and microwave power on the AC yield.....	52
Figure 4.3	The three-dimensional response surfaces (a) the effect of activation time and particle size (b) the effect of microwave power and particle size (c) the effect of impregnation ratio and activation time on the AC yield.....	54
Figure 4.4	(a) SEM image of the raw palm shell. (b) SEM image of the prepared AC under optimum conditions .....	57
Figure 4.5	Nitrogen adsorption isotherm of prepared AC under optimum conditions	57
Figure 4.6	Pore width vs. pore volume of prepared AC under optimum conditions.	58
Figure 4.7	Fourier transforms infrared spectra of raw palm shell and prepared AC under optimum conditions. ....	59
Figure 4.8	Nitrogen adsorption isotherms of ACs by microwave heating.....	62
Figure 4.9	Nitrogen adsorption isotherms of ACs by conventional heating.....	62
Figure 4.10	Variation of the total pore volume and micropore volume of ACs prepared by microwave and conventional heating methods .....	65
Figure 4.11	Pore size distribution of ACs prepared by microwave heating. ....	68
Figure 4.12	Pore size distribution of ACs prepared by conventional heating .....	68
Figure 4.13	FTIR spectra of (a) palm shell, (b) prepared ACs by microwave heating and (c) prepared ACs by conventional heating.....	73

Figure 4.14	SEM micrographs (3000X) of the (a) palm shell, (b) MW0.65, (c) C0.65	74
Figure 4.15	N <sub>2</sub> adsorption isotherms of ACs prepared using different activation times and a microwave power of 750 W and impregnation ratio of 1.5 in the presence of CO <sub>2</sub> (a) and N <sub>2</sub> (b).	78
Figure 4.16	Pore size distributions of ACs prepared using different activation times and a microwave power of 750 W and agent ratio of 1.5 in the presence of CO <sub>2</sub> (a) and N <sub>2</sub> (b) derived from the N <sub>2</sub> adsorption results at -196 °C.	81
Figure 4.17	N <sub>2</sub> adsorption isotherms of ACs prepared using different impregnation ratios and an irradiation time of 15 min and microwave input power of 750 W in the presence of CO <sub>2</sub> (a) and an activation time of 30 min and microwave power of 750 W in the presence of and N <sub>2</sub> (b).	82
Figure 4.18	Pore size distributions of ACs prepared using different impregnation ratios and an irradiation time of 15 min and microwave input power of 750 W in the presence of CO <sub>2</sub> (a) and an activation time of 30 min and microwave power of 750 W in the presence of N <sub>2</sub> (b) derived from the N <sub>2</sub> adsorption results at -196 °C.	84
Figure 4.19	N <sub>2</sub> adsorption isotherms of ACs prepared using different microwave powers and an irradiation time of 15 min and impregnation ratio of 1.5 Xk in the presence of CO <sub>2</sub> (a) and an activation time of 30 min and impregnation ratio of 2.5 Xk in the presence of N <sub>2</sub> (b).	86
Figure 4.20	Pore size distributions of ACs prepared using different microwave powers and an irradiation time of 15 min and impregnation ratio of 1.5 Xk in the presence of CO <sub>2</sub> (a) and an activation time of 30 min and impregnation ratio of 2.5 Xk in the presence of N <sub>2</sub> (b).	88
Figure 4.21	SEM images of the raw palm shell (a) and the ACs with the highest surface areas prepared under CO <sub>2</sub> (b) and N <sub>2</sub> (c).	90

Figure 4.22	Fourier transform infrared spectra of the raw palm shell and the ACs with the highest surface areas prepared under CO <sub>2</sub> and N <sub>2</sub> .....	93
Figure 4.23	Carbon dioxide adsorption isotherms of the ACs with the highest surface areas prepared under (a) CO <sub>2</sub> and (b) N <sub>2</sub> at 0 °C, 25 °C and 50 °C; solid lines, Toth model.....	96
Figure 4.24	Deviations between the measured and the calculated carbon dioxide adsorption capacities of Toth Model for the ACs prepared under CO <sub>2</sub> ; filled symbols; and under N <sub>2</sub> , empty symbols .....	97

## LIST OF TABLES

Table 2.1	Summary of the yield and physical properties of the ACs produced by the microwave method under optimum conditions with chemical activation .....	11
Table 2.2	Summary of the yield and physical properties of the ACs produced by the microwave method under optimum conditions with physical activation .....	12
Table 2.3	Maximum adsorption capacity of ACs prepared from agricultural wastes by chemical activation under the optimum preparation conditions .....	20
Table 2.4	Maximum adsorption capacity of ACs prepared from agricultural waste by physical activation under the optimum preparation conditions .....	23
Table 2.5	Functional groups characterized by FTIR in different agricultural-based ACs produced under optimum conditions.....	33
Table 3.1	Independent variables and their coded levels for the CCD.....	37
Table 3.2	Experimental design matrix and response results .....	39
Table 4.1	Analysis of variance (ANOVA) for response surface quadratic model for AC yield .....	48
Table 4.2	Analysis of variance (ANOVA) for response surface quadratic model for MB adsorption capacity .....	49
Table 4.3	Proximate and ultimate analysis of oil palm shell and prepared AC under optimum conditions.....	56
Table 4.4	Surface characteristics of AC prepared by microwave and conventional methods .....	65
Table 4.5	Proximate and elemental analysis of raw material and ACs prepared under optimum impregnation ratio.....	70



Table 4.6	Wave numbers and ascription of the principal bands in the FTIR Spectra of palm shell and prepared ACs .....	76
Table 4.7	Textural characteristics of ACs prepared using different activation times in the presence of either CO <sub>2</sub> or N <sub>2</sub> measured by N <sub>2</sub> adsorption at -196 °C.....	79
Table 4.8	Textural characteristics of ACs prepared using different impregnation ratios in the presence of either CO <sub>2</sub> or N <sub>2</sub> measured by N <sub>2</sub> adsorption at -196 °C.....	83
Table 4.9	Textural characteristics of ACs prepared using different microwave powers in the presence of either CO <sub>2</sub> or N <sub>2</sub> measured by N <sub>2</sub> adsorption at -196 °C.....	87
Table 4.10	Proximate and elemental analyses of the raw palm shell and ACs prepared under the optimum CO <sub>2</sub> and N <sub>2</sub> gasification conditions .....	91
Table 4.11	Wave numbers and descriptions of the principal FTIR bands of the palm shell and the ACs with the highest surface areas .....	93
Table 4.12	Textural parameters of the ACs with the highest surface areas obtained from N <sub>2</sub> adsorption at -196 °C and CO <sub>2</sub> adsorption at 0 °C .....	94
Table 4.13	Fitting parameters of the Toth model .....	97

## LIST OF SYMBOLS AND ABBREVIATIONS

Symbol	Meaning
Å	Angstrom
AC	Activated carbon
ANOVA	Analysis of variance
(CCD)	Central composite design
Dp	average pore diameter (nm)
(DH)	Dollimore–Heal
(DOE)	Design expert software
(DR)	Dubinin–Radushkevich
FG	Functional group
FI	Factor interaction
FT-IR	Fourier transform infra red
g	gram
h	hour
IR	Impregnation ratio (wt%)
IUPAC	International union of pure and applied chemistry
K	Degree Kelvin
KOH	potassium hydroxide
kPa	kilopascal
l	liter
m	meter
MB	Methylene blue
mg	milligram
min	minute
n <sub>C</sub>	centre runs
nm	nanometre
OTC	oxytetracycline
°C	Degree Celsius
P	relative pressure (mmHg)
P <sub>0</sub>	absolute pressure (mmHg)

---

pH	Negative logarithm of the hydrogen ion concentration
PSD	pore size distribution
Symbol	Meaning
ppm	part per million
rpm	Rate per minute
SD	Standard deviation
RSM	Response surface method
$S_{\text{BET}}$	BET surface area
$S_{\text{external}}$	External surface area
$S_{\text{micro}}$	Micropores surface area
SEM	Scanning electron microscope
t	time (min)
$V_{\text{tot}}$	total pore volume ( $\text{cm}^3/\text{g}$ )
$V_{\text{mic}}$	micropore pore volume ( $\text{cm}^3/\text{g}$ )
$V_{\text{meso}}$	mesopores volume ( $\text{cm}^3/\text{g}$ )
W	watt
Y	Yield
Zn	Zinc
$\text{ZnCl}_2$	Zinc chloride

---

# CHAPTER 1: GENERAL INTRODUCTION

## 1.1 Background

In recent years, microwave irradiation has attracted the attention of chemists due to its capability of molecular level heating, which leads to homogeneous and quick thermal reactions (Ania, Parra, Menéndez, & Pis, 2007; Zhang-Steenwinkel et al., 2005). Yet, in the particular case of carbon materials, the efficiency of applying microwave heating technology to regenerate industrial waste AC has been investigated. The results are very promising (Yuen & Hameed, 2009) due to the rapid heating of the AC by microwave energy. In addition, microwave technology allowed the carbon to be recycled and reused for a large number of times. This technique does not damage the carbon; rather, it increases the surface area allowing more contaminants to adhere, thereby increasing the value (Ania, Menéndez, Parra, & Pis, 2004). The main difference between microwave and conventional heating methods is in the way the heat is generated (Ania, Parra, Menéndez, & Pis, 2005). In the former approaches, thermal regeneration is conventionally performed in rotary kilns or vertical furnaces, the heat source is located outside the carbon bed, and the bed is heated by conduction and/or convection. A temperature gradient is established in the material until conditions of steady state are reached (Menéndez, Menéndez, Iglesias, García, & Pis, 1999).

Nevertheless, in some cases, the thermal process may take long processing time, involve high energy consumption, require larger equipment size and generate improper heating rate, thereby resulting in a detrimental effect on the quality of the ACs prepared (Thostenson & Chou, 1999). Compared with conventional heating techniques, microwave heating has the additional advantages as follows: interior heating, higher heating rates, selective heating, greater control of the heating process, no direct contact between the heating source and heated materials, and reduced equipment size and waste

(Appleton, Colder, Kingman, Lowndes, & Read, 2005; Jones, Lelyveld, Mavrofidis, Kingman, & Miles, 2002; Venkatesh & Raghavan, 2004; Yu, 2001). With continued development of ACs technologies, the new applications of microwave heating in preparing ACs are succeeding and expanding.

The study attempts for potential applications of microwave-assisted preparation of ACs from agricultural waste like as: palm shell, coconuts shell and rubber plant wood etc. Synthesis of AC from agricultural waste at different operating conditions i.e. microwave radiation power, activation time, and flow rate of  $N_2/CO_2$  and impregnation ratio of  $ZnCl_2/KOH$ . Applications test for removal of organic and inorganic pollutants dissolved in aqueous media (MB), or from gaseous environment ( $CO_2$ ).

## **1.2 Research Objectives**

This project promotes preparation of AC by using palm shell (agricultural wastes) as a precursor using microwave-irradiation methods. The objectives of this study are:

- I. To produce AC from palm shell using microwave heating method
- II. To optimize  $ZnCl_2$  activation process conditions using microwave heating method.
- III. To characterize the produced AC, using microwave and conventional heating methods.
- IV. To study the effects of chemical and physical agents on the textural and surface properties of the produced AC by microwave heating method.

### **1.3 Thesis Organization**

This thesis is composed of five chapters. The chapters contain their specified content as follow:

- CHAPTER 1: In this chapter, the differences between microwave and conventional heating method on preparation of AC and the use of microwave irradiation in production of AC are briefly introduced in their turn to justify attention paid to the objective of this study.
- CHAPTER 2: This chapter presents a comprehensive literature review on the effects of more significant variables; Microwave power, radiation time, impregnation ratio and particle size on the adsorption capacity and carbon yield of the agricultural based of AC, advantages and disadvantages of microwave and conventional heating method, and the effects of these parameters in preparation of AC using microwave method on the end products were investigated.
- CHAPTER 3: Materials, equipment, methodologies, procedures and experimental design used for this study are described in this chapter.
- CHAPTER 4: This chapter presents experimental results and data analysis and discusses them based on firm evidences and reasons extracted from literature.
- CHAPTER 5: The conclusions constructed from the results and discussion chapter are explained part by part.

## CHAPTER 2: LITERATURE REVIEW

### 2.1 Introduction

Various technologies have been applied recently to remove toxic components such as anions, heavy metals, organic compounds and dyes from water sources (Namasivayam & Sangeetha, 2006; Timur, Kantarli, Onenc, & Yanik, 2010; Yuen & Hameed, 2009). Adsorption technology is one of the applicable and simple methods for water treatment (Hejazifar, Azizian, Sarikhani, Li, & Zhao, 2011). AC is used as a potential adsorbent in processes such as the purification of industrial effluents (Albin, 2003), groundwater treatment (El-Sheikh, Newman, Al-Daffaee, Phull, & Cresswell, 2004) and the removal of volatile organic compounds from air and mercury vapors from a gas mixture (Vitolo & Seggiani, 2002). AC demonstrated significant adsorption in gas and liquid phases due to its high micropore volume ( $V_{mic}$ ), large specific surface area ( $S_{BET}$ ), favorable pore size distribution, thermal stability, capability for rapid adsorption and low acid/base reactivity (W. Li et al., 2009). Essentially, the high cost of AC production is one of the most important challenges for commercial manufacturers, and using inexpensive raw materials with high carbon content and low levels of inorganic compounds to produce low cost AC has been a focus of research efforts in recent years. Agricultural by-products and waste materials such as rice husk (Y. Guo et al., 2005), coconut husks (Tan, Ahmad, & Hameed, 2008b) and oil palm fibers (Tan, Hameed, & Ahmad, 2007) are among the low cost precursors for the production of AC. In addition to the raw materials, the preparation method significantly affects the quality, properties and cost of AC. A conventional heating method is one of the most applicable and usual techniques of AC preparation. In the conventional method, the heat source is located outside the carbon bed, and the heat generated by the heat source is transferred to the particles by convection, conduction and radiation mechanisms.

The surface of the sample is heated before the internal parts. There is a temperature gradient from the surface to the interior of each particle (Thostenson & Chou, 1999; Yadoji, Peelamedu, Agrawal, & Roy, 2003). Using a microwave radiation method is a possible way to solve the problems of the thermal gradient and the high cost of AC preparation. Over the last several years, many promising results have been obtained by using a microwave irradiation method for the preparation of relatively homogeneous inexpensive AC particles with high surface area and significant adsorption capacity. Microwaves interact directly with the particles inside the pressed compact material and are not conducted into the sample from an external heat source, thus providing quick volumetric heating (Xie, Yang, Huang, & Huang, 1999). The use of microwave radiation causes higher sintering temperatures, shorter processing times and, therefore, higher energy savings (Thakur, Kong, & Gupta, 2007). The different mechanisms of heat transfer in microwave and conventional methods and the advantages and disadvantages of these methods were reviewed in this section.

On the other hand, the activation process also has significant effects on the pore structure and adsorption capacity of the prepared AC. Chemical and physical activation are two types of activation processes used in the preparation of ACs. Physical activation is the partial gasification of the carbonaceous material, where the carbonaceous material is carbonized at high temperatures in a furnace under an inert atmosphere such as nitrogen to eliminate most of the hydrogen and oxygen content and produce char with the desired porosity. The prepared char from the carbonization process is then activated in the presence of oxidizing gases, such as steam, carbon dioxide, air or mixtures of these gases, to produce AC (Rodríguez-Reinoso & Molina-Sabio, 1992). Chemical activation involves mixing an acidic or basic solution with the carbonaceous material to influence the pyrolytic decomposition of the starting materials, suppress tar formation and lower the pyrolysis temperature.



To exclusively review the effects of the microwave method due to the different mechanisms of chemical and physical activation procedures, the effects of preparation conditions on chemical activation and the effects of different types of physical activation agents are presented separately. The effects of variables in the microwave heating method on the carbon yield and the physical and chemical properties of prepared agricultural waste-based ACs were reviewed in this thesis.

## **2.2 Microwave heating methods**

As mentioned above, in the conventional method of heating, there is a temperature gradient from the surface to the interior of each particle. To avoid this thermal gradient at high synthesis temperatures inside the material, a slower rate of heating with isothermal holding is used. This slow heating rate at intermediate temperatures increases the duration of the preparation process in the conventional heating method, resulting in greater energy consumption (Kubota, Hata, & Matsuda, 2009; Oghbaei & Mirzaee, 2010). This thermal gradient impedes the effective removal of gaseous products to the surroundings (W. Li, Zhang, Peng, Li, & Zhu, 2008), and therefore, some light components may remain inside the samples and pyrolyze, giving rise to carbon deposition. The deposited carbon might obstruct the microporous network, leading to low values of  $V_{\text{tot}}$  and BET surface area (D. Li, Zhang, Quan, & Zhao, 2009). The thermal gradient also leads to distortion and inhomogeneous microstructure in the prepared AC (Oghbaei & Mirzaee, 2010). On the other hand, the conventional thermal process may take several hours or even up to a week to reach the desired level of activation.

This slow thermal process increases the expense associated with the process (Hui Deng, Li, Yang, Tang, & Tang, 2010; W. Li et al., 2009; Yuen & Hameed, 2009). Conventional fast firing is also a disadvantage of the thermal heating method that is solved by using a microwave heating method (W. Li et al., 2009).

In the microwave method, microwave irradiation interacts directly with the particles inside the pressed compact material and changes electromagnetic energy into heat transfer inside the dielectric materials. Microwave irradiation is not conducted into the sample from an external heat source, providing quick volumetric heating (Thakur et al., 2007; Xie et al., 1999). Microwave synthesis is an alternative technique that overcomes the problems of conventional fast firing because microwave synthesis is a non-contact technique where the heat is transferred to the product via electromagnetic waves, and large amounts of heat can be transferred to the interior of the material, minimizing the effects of differential synthesis (Jones et al., 2002; Kazi E, 1999). On the other hand, microwave radiation method is both internal and volumetric, where the huge thermal gradient from the interior of the sample to the cool surface allows the microwave-induced reaction to proceed more quickly and effectively at a lower bulk temperature, providing shorter processing time and saving energy ((Hui Deng, Zhang, Xu, Tao, & Dai, 2010). Among the many types of materials, carbon materials are very good microwave absorbents. This characteristic allows carbonaceous materials to be transformed by microwave heating, giving rise to new carbonaceous materials with modified properties (Menéndez et al., 2010). The thermal gradient in the microwave radiation method decreases gradually from the center to the surface of the sample due to higher temperatures in the interior than at the surface of the sample (Foo & Hameed, 2011a; G.Chih-Ju, 1998; Ji, Li, Zhu, Wang, & Lin, 2007). Because of this temperature gradient, the light components are easily released to create more pores (Ania, Parra, Menéndez, & Pis, 2005; J. Yang, Shen, & Hao, 2004). Microwave radiation offers other advantages over conventional heating methods such as: energy transfer instead of heat transfer; selective heating; improved efficiency; immediate startup and shutdown; smaller steps; lower activation temperature; improved safety; simplicity; smaller

equipment size and less automation (Foo & Hameed, 2011e; Menezes, Souto, & Kiminami, 2007; Oghbaei & Mirzaee, 2010; Xie et al., 1999).

Microwave radiation can generate hot spots (as a consequence of mineral impurities) inside the carbon particles where the temperature is much higher than the overall temperature of the sample (Menéndez et al., 1999). This temperature difference usually causes heterogeneous reactions between the sample and the inert gases that are taking part in the reaction (Menéndez et al., 2010). Additionally, it is nearly impossible to accurately measure the sample temperature, and only the surface temperature of the sample is measurable using an infrared pyrometer. The internal temperature of the sample may be tens or hundreds of degrees higher than the sample surface temperature due to the internal and volumetric nature of microwave heating. Hence, the temperature could not be a variable condition in the preparation of AC using the microwave irradiation method (J. Guo & Lua, 2000; W. Li et al., 2008). Finally, much more dedicated work and further exploration are needed to expand this research, to improve the performance of microwave techniques and to scale-up the microwave production of AC particles (Yuen & Hameed, 2009).

### **2.3 Effects of the microwave heating method on the physical properties of AC**

The specific surface area and pore structure are two main properties of porous carbon that determine its applications (Figueiredo, Pereira, Freitas, & Órfão, 1999; Rodríguez-Reinoso & Molina-Sabio, 1998). Porous materials include micropores (<2 nm), mesopores (2–50 nm) and macropores (>50 nm), in accord with the classification adopted by the International Union of Pure and Applied Chemistry (IUPAC) (J. Guo & Lua, 2000; X. He et al., 2010). Although a microporous AC is generally desired for adsorption purposes, the presence of mesopores is also valuable for the adsorption of large molecules or where a faster adsorption rate is required (Huang, Sun, Wang, Yue, & Yang, 2011; Q.S. Liu, T. Zheng, P. Wang, & L. Guo, 2010).

Different conditions and routes, such as the raw material, activation time and temperature and types of activation agents (Biniak, Szymański, Siedlewski, & Świątkowski, 1997), could control the pore structure. The BET surface area ( $S_{\text{BET}}$ ) of AC is one of the most important physical properties that may strongly affect the reactivity and combustion behavior of the carbon (Pütün, Özbay, Önal, & Pütün, 2005). By using the microwave heating method, a higher  $S_{\text{BET}}$  value can be obtained compared with that reached using an electric furnace heating method in an initial short stage. The difference in BET surface areas may be due to the different heating mechanisms used in these two methods. The adsorption capacity is another property of AC that is related mainly to the specific surface area, pore size distributions and pore volume. Because of the high internal pore structure that makes a large area available for adsorption, AC has significant adsorptive properties (El-Hendawy, Samra, & Girgis, 2001). The increase in the adsorption capacity in the microwave method is due to mainly the micropore structure, the existence of carboxylic groups and the higher charge density on the surface of the adsorbent (Franca, Oliveira, Nunes, & Alves, 2010). The adsorption of MB and iodine has been an important demonstration of adsorption capacity from the liquid phase. The MB molecules have a minimum molecular cross-section of 0.8 nm, and the minimum pore diameter that the MB molecule can enter was estimated to be 1.3 nm. Therefore, MB can enter most mesopores and the largest micropores. In contrast, the iodine molecule, because of its smaller size, is significantly adsorbed into micropores (larger than 1 nm) (Hu & Srinivasan, 2001; Wartelle, Marshall, Toles, & Johns, 2000). To review the effects of the microwave method on AC characterization, the main parameters that significantly affect the physical and chemical properties of AC particles were studied.

Microwave power, radiation time, impregnation ratio in chemical activation and agent flow rate in physical activation are the main variables that have been studied by other

authors. These parameters demonstrated more noticeable effects on the preparation of AC than the other preparation conditions. The physical characteristics of the ACs produced from agricultural wastes using the microwave heating method have been summarized for chemical activation in Table 2.1 and physical activation in Table 2.2.

#### **2.4 Effects of microwave power on the physical structure of chemically AC**

As noted above, it is nearly impossible to accurately measure the temperature of the sample in the microwave radiation method, and thus, the microwave power has been used as a preparation variable instead of the sample temperature (J. Guo & Lua, 2000). The microwave power could develop the pores that are constricted and blocked by deposits of tarry substances, resulting in highly uniform and well pronounced porous structures in the prepared AC (Foo & Hameed, 2011g; K.Y. Foo, 2011).

Higher microwave power levels cause a higher rate of reaction between the agent and precursor, which promotes the development of the pore structure and active sites (Hui Deng et al., 2009). Some researchers specifically investigated the effects of microwave power on the adsorption capacity of AC. For instance, Foo and Hameed (2011) (Foo & Hameed, 2012c) studied the effects of the power level at a constant impregnation ratio of 1.25 (wt%) and irradiation time of 5 min on the adsorption capacity of the ACs prepared by the microwave method from orange peels with  $K_2CO_3$  chemical activation (Foo & Hameed, 2012c).

They observed that at low microwave power levels of 90 and 180 W, the iodine number and MB adsorption capacity remained approximately unchanged. This lack of change indicated that there was no continual reaction (activation) between the prepared char from the carbonization step and the activation agent at these low power levels in the activation process.

Table 2.1: Summary of the yield and physical properties of the ACs produced by the microwave method under optimum conditions with chemical activation.

Precursor	Agent	S <sub>BET</sub> (m <sup>2</sup> /g)	S <sub>micro</sub> (m <sup>2</sup> /g)	S <sub>external</sub> (m <sup>2</sup> /g)	V <sub>tot</sub> (cm <sup>3</sup> /g)	V <sub>micro</sub> (cm <sup>3</sup> /g)	V <sub>meso</sub> (cm <sup>3</sup> /g)	Average pore size (Å)	Yield (%)	Langmuir (m <sup>2</sup> /g)	Ref
Pineapple Peels	KOH	1006	521	485	0.59	0.28	0.31	23.44	–	1513	(Foo & Hameed, 2012b; K.Y. Foo, 2011)
	K <sub>2</sub> CO <sub>3</sub>	680	538	142	0.45	0.28	0.17	25.97		1010	
Rice Husks	KOH	752	346	406	0.64	0.26	0.38	34.14	–	1147	(Foo & Hameed, 2011g)
	K <sub>2</sub> CO <sub>3</sub>	1165	607	558	0.78	0.33	0.45	26.89		1760	
Cotton Stalks	KOH	729.33	529.46	199.88	0.38	0.26	0.12	–	–	–	(Hui Deng, Li, et al., 2010)
	K <sub>2</sub> CO <sub>3</sub>	621.47	384.67	236.80	0.38	0.11	0.27	–		–	
Orange Peels	K <sub>2</sub> CO <sub>3</sub>	1104.45	420.09	684.36	0.615	0.247	0.368	22.27	80.99	1661.04	(Foo & Hameed, 2012c)
Sunflower Seed Oil	K <sub>2</sub> CO <sub>3</sub>	1411.55	–	–	0.836	–	–	23.60	–	2137.72	(Foo & Hameed, 2011d)
Tobacco Stems	K <sub>2</sub> CO <sub>3</sub>	2557	–	–	1.647	–	–	–	16.65	–	(W. Li et al., 2008)
Pistachio Nut Shells	KOH	700.53	–	–	0.375	–	–	–	–	1038.78	(Foo & Hameed, 2011c)
Oil palm (Elaeis) EFB	KOH	807.54	–	–	0.450	–	–	21.93	–	1209.62	(Foo & Hameed, 2011f)
Oil Palm Fibers	KOH	707.79	–	–	0.380	–	–	22.11	–	1030.25	(Foo & Hameed, 2011a)
Palm Residues	KOH	1372	821	551	0.760	0.44	0.32	22.06	73.78	2058	(Foo & Hameed)
Bamboo	H <sub>3</sub> PO <sub>4</sub>	1432	1112	–	0.696	0.503	0.193	–	47.80	–	(Q.S. Liu, P. Wang, et al., 2010)

‘Table 2.1, continued’

Precursor	Agent	S <sub>BET</sub> (m <sup>2</sup> /g)	S <sub>micro</sub> (m <sup>2</sup> /g)	S <sub>external</sub> (m <sup>2</sup> /g)	V <sub>tot</sub> (cm <sup>3</sup> /g)	V <sub>micro</sub> (cm <sup>3</sup> /g)	V <sub>meso</sub> (cm <sup>3</sup> /g)	Average pore size (Å)	Yield (%)	Langmuir (m <sup>2</sup> /g)	Ref
Cotton Stalks	ZnCl <sub>2</sub>	794.84	156.69	–	0.63	0.083	0.547	32.00	37.92	–	(Hui Deng, Yang, Tao, 2009)
Pine wood powder	ZnCl <sub>2</sub>	1459	–	–	0.70	–	–	–	–	–	(Tonghua Wang, 2009)
Industrial lignin	ZnCl <sub>2</sub>	1172.2	1002	162.4	0.64	0.457	0.174	20.82	60.73	–	(Maldhure & Ekhe, 2011)
Pomelo Skins	NaOH	1355	524	811	0.77	0.29	0.480	23.09	–	2057	(Foo & Hameed, 2011b)

Table 2.2: Summary of the yield and physical properties of the ACs produced by the microwave method under optimum conditions with physical activation.

Precursor	Agent	S <sub>BET</sub> (m <sup>2</sup> /g)	V <sub>tot</sub> (cm <sup>3</sup> /g)	V <sub>micro</sub> (cm <sup>3</sup> /g)	V <sub>meso</sub> (cm <sup>3</sup> /g)	Average pore size (Å)	Yield (%)	Ref
Coconut Shells	Steam	2079	1.212	0.974	0.238	–	42.20	(K. Yang et al., 2010)
	CO <sub>2</sub>	2288	1.299	1.012	0.287	–	37.50	
	Mixed	2194	1.293	1.010	0.283	–	39.20	
Jatropha Hulls	Steam	1350	1.070	0.436	0.634	31.00	16.56	(Xin-hui, Srinivasakannan, Jin-hui, Li-bo, & Zheng-yong, 2011a, 2011b)
	CO <sub>2</sub>	1284	0.870	–	–	–	36.60	
Oil-Palm-Stones	CO <sub>2</sub>	412.5	–	–	–	–	56.60	(J. Guo & Lua, 2000)
Coconut Shells	Steam	891.0	0.723	0.268	0.455	6.50	69.74	(W. Li et al., 2009)

However, at 360 W and 600 W, the adsorption capacity of MB showed a progressive increase. The authors proposed that the combined effect of volumetric and internal heating by microwave irradiation improved the formation of new porosity during chemical activation. They also found that at microwave power levels beyond the optimum value, the MB adsorption capacity decreased progressively due to burning of the carbon and destruction of the pore structures by higher levels of irradiation. These effects of the microwave power level are in agreement with the preparation procedure of an AC from oil palm residue (biodiesel industry solid residue) by KOH activation with the impregnation ratio of 1.00 (wt%) and irradiation time of 8 min (Foo & Hameed, 2012a).

Deng *et al.* (2010) investigated the effects of microwave power levels on the adsorption capacity of coconut shell-based AC prepared by microwave activation with KOH and  $K_2CO_3$  as chemical agents. The results obtained at low microwave power levels showed no obvious change due to insufficient development of the pore structures, whereas at high microwave powers of 480 to 660 W, the MB adsorption capacity increased gradually, irrespective of the agent. The authors inferred that the adsorption capacity decreases with an increase in the power level to 720 W for the same reason mentioned above (Hui Deng, Li, et al., 2010). The same adsorption behavior is reported by Deng *et al.* (2009) for the ACs produced at low and high microwave power levels, where they prepared ACs by the microwave method from cotton stalks with zinc chloride activation (Hui Deng et al., 2009). Liu *et al.* (2010) used bamboo to produce ACs with phosphoric acid as a chemical agent by the microwave-induced method. They found a remarkable drop in micropore formation at 400 W, while the formation of mesopores increased significantly. The development of mesopores appears to be preferred at higher levels of microwave power.



It was explained that, at high power levels, the phosphoric acid showed an intense reaction with carbon, which facilitates the development of the pore structure. The activation process promotes the removal of some components, such as tars and volatile matter, at the higher temperatures that result from increasing the microwave power (Q.S. Liu, T. Zheng, P. Wang, et al., 2010).

Deng *et al.* (2010) (Hui Deng, Zhang, et al., 2010) determined that the iodine number of cotton stalk-based ACs prepared with phosphoric acid activation increased as the microwave power increased from 320 to 400 W due to the full development of pore structure on the surface of the AC particles at 400 W. By increasing the microwave power above the optimum value (480 W), the iodine number decreased because a small quantity of carbon was burned and the pore structure was destroyed.

The authors who used non-agricultural waste as a precursor for the production of AC observed the same effects of microwave power on physical properties. For instance, Kubota *et al.* (2009) observed that the temperature of the samples undergoing microwave irradiation increased as the microwave power increased from 260 to 390 W when they used phenolic resin as the raw material with KOH activation (Kubota et al., 2009). This phenomenon augments the development of porosity in AC. The  $S_{\text{BET}}$  and  $V_{\text{tot}}$  increased when the microwave power was increased and then decreased as the microwave power was increased to 520 W.

## **2.5 Effects of microwave radiation time on the physical structure of chemically AC**

The microwave method heats uniformly with a rapid heating rate, so the sample may acquire more active sites in a shorter time by opening previously inaccessible pores, creating new pores by selective activation, and widening and merging the existing pores through pore wall breakage.

These changes in the porosity result in a high efficiency of activation (Foo & Hameed, 2012c). The variables associated with producing AC by microwave heating have different and significant effects on the pore structure. The  $S_{\text{BET}}$  decreases with the increase in activation time above the optimum microwave radiation time, possibly because the agent is not yet used up when the  $S_{\text{BET}}$  reaches the maximum value, and further increasing the activation time induces excess activation and the destruction of some micropore structures, leading to the decrease in  $S_{\text{BET}}$  (Ji et al., 2007).

Foo and Hameed (2012) produced orange peel-based ACs using a microwave-induced method with  $\text{K}_2\text{CO}_3$  as a chemical agent at a constant impregnation ratio of 1.25 (wt%) and microwave power of 600 W at different activation times. The adsorption capacity of MB increased from 193.81 mg/g to 297.16 mg/g when the microwave radiation time was increased from 4 to 6 min. The same increase in MB adsorption with an increase in the activation time was achieved by Foo and Hameed (Foo & Hameed, 2012c). They explained that, by prolonging activation time, the reaction and the devolatilization rate increased. Therefore, the adsorption capacity increases via the development of porosity and the rudimentary pore structure. They attributed a slight drop in the adsorption capacity (26.84 mg/g) at 7 min of radiation time to a dramatic rise in temperature and the opening of micropores and mesopores as the activation proceeded. The increase in the activation time apparently enlarged the average pore diameter, and the local hotspots produced by further heating led to the ablation and shrinkage of AC channels and the skeleton. Therefore, the accessibility of the active carbon sites was dramatically reduced, resulting in the reduction of the adsorption capacity (Foo & Hameed, 2012c).

Li *et al.* (2008) produced AC from tobacco stems using  $\text{K}_2\text{CO}_3$  as an activation agent, under the fixed experimental conditions of an impregnation ratio of 1.5 (wt%) and microwave power of 700 W with different activation times.

When they increased the activation time from 20 to 30 min, the iodine number of the AC increased from 1320 to 1834 mg/g, and the MB adsorption also increased from 290 to 517 mg/g. Li *et al.* found that the increase in radiation time intensified the formation of active sites inside the AC. Subsequently, by increasing the microwave radiation time to 40 min, both iodine number and MB adsorption capacity decreased to 1490 mg/g and 360 mg/g, respectively. It was explained that some pores of carbon would be burnt by increasing the microwave radiation time beyond the optimum radiation time, resulting in a decrease in adsorption capacity (W. Li et al., 2008). Deng et al. (2010) observed that the MB adsorption capacity decreased when the activation time increased beyond the optimum value in the activation stage. They produced AC from cotton stalks by chemical activation (KOH and K<sub>2</sub>CO<sub>3</sub>) with duration times of 8, 9 and 10 minutes. The formation of new pores became less significant with the activation proceeding, and the micropores enlarged and the mesopores widened continuously into larger pores. Furthermore, this phenomenon implied that the pores might be destroyed by prolonging the activation time, irrespective of the chemical activation agent (Hui Deng, Li, et al., 2010). Similar effects of radiation time on the AC properties were also reported by Deng et al. (2009), when they prepared AC from cotton stalks using microwave radiation with zinc chloride as the chemical agent (Hui Deng et al., 2009), and Liu et al. (2010), where they used bamboo as the precursor and phosphoric acid activation for the production of AC (Q.S. Liu, T. Zheng, P. Wang, et al., 2010).

The effects of microwave radiation time on the modification of bamboo-based AC were investigated by Liu et al. (2010). It was observed that by increasing the radiation time from 5 to 10 min, the number of micropores decreased while the value of  $V_{\text{tot}}$  increased, indicating that the micropores were enlarging (Liu, Zheng, Li, Wang, & Abulikemu, 2010).

The effects of radiation time on the properties of AC were investigated by He et al. (2010) (X. He et al., 2010) when they used petroleum coke (a non-biomass precursor) as a precursor and KOH as a chemical agent to prepare AC. The BET surface area of the prepared AC increased from 752 to 2312 m<sup>2</sup>/g when the microwave radiation time was increased from 27 to 35 min and then decreased to 1053 m<sup>2</sup>/g when the radiation time was increased to 37 min. The increase in S<sub>BET</sub> indicated the formation of new pores when the activation time was increased, while the reduction in S<sub>BET</sub> was explained by the enlarged micropores and the destruction of some pores.

## **2.6 Effects of impregnation ratio on the physical structure of chemically AC**

Chemical agents such as KOH, K<sub>2</sub>CO<sub>3</sub>, H<sub>3</sub>PO<sub>4</sub>, ZnCl<sub>2</sub> and NaOH have been frequently applied by researchers (Hayashi, Horikawa, Takeda, Muroyama, & Nasir Ani, 2002; Hsu & Teng, 2000; Sudaryanto, Hartono, Irawaty, Hindarso, & Ismadji, 2006). Activation agents are the main absorbers of microwave radiation at the initial stage of activation. Without using a chemical agent, the carbonaceous raw materials are hardly heated (Tonghua Wang, 2009). After the development of pore structure at the initial stages, the AC itself could receive the energy from microwave radiation during the activation process (Hui Deng, Li, et al., 2010). To investigate the effects of the impregnation ratio on the physical properties of the AC, the changes in adsorption capacity are considered a criterion by some authors.

The MB adsorption capacity was increased from 56.52 to 171.15 mg/g by increasing the impregnation ratio from 0.25 to 1.25 (wt%) at the fixed microwave power of 360 W and radiation time of 5 min to produce AC from orange peels with K<sub>2</sub>CO<sub>3</sub> activation. The increase in the adsorption capacity was attributed to the strengthening of the activation process by increasing the agent ratio. When the impregnation ratio was increased beyond the optimum value, the pores could be blocked by an excess of K<sub>2</sub>CO<sub>3</sub> and metallic potassium that was left on the surface of the carbon, leading to a reduction in

the accessible area. Widening and burning of pores could be another reason for the decreasing adsorption capacity (Foo & Hameed, 2012c).

The identical results from the KOH activation of fruit residue (biodiesel industry solid residue) showed that the diffusion of metallic potassium formed during the gasification process widens the exit pores and creates new pores. The adsorption capacity, therefore, increased from 132.74 to 253.44 mg/g by augmenting the impregnation ratio from 0.25 to 1.00 (wt%) at a microwave power level of 600 W and an activation time of 7 min. At the optimum impregnation ratio, the carbons on the active sites reacted completely with the KOH and the adsorption capacity was maximized (Foo and Hameed, 2012a).

Li et al. (2008) prepared AC from tobacco stems with  $K_2CO_3$  activation using microwave irradiation and found that few pores formed at an impregnation ratio below 1.5 (wt%). They also noticed that incomplete carbon reactions at the active sites caused a decrease in the adsorption capacity. When the impregnation ratio increased to 1.5 (wt%), the carbons on the active sites reacted completely, and the AC showed the maximum amount of adsorption. They concluded that the formation of pores was increased by (i) the creation of  $CO_2$  and  $K_2O$  from the decomposition of  $K_2CO_3$ , (ii) the reduction of  $K_2O$  by carbon to form K and  $CO_2$  and (iii) the diffusion of K into the carbon layer when the activation temperature reached the boiling point of potassium. With an increase in the impregnation ratio to 3.0 (wt%), the iodine number and MB adsorption decreased from 1834 and 517 mg/g to 1350 and 290 mg/g, respectively. This decrease was attributed to the burning and widening of more pores as a result of increasing the impregnation ratio (W. Li et al., 2008).

The effects of the impregnation ratio on the adsorption capacity of cotton stalk-based AC, was investigated by Deng et al. (2009) where zinc chloride was used as the chemical agent with a radiation time of 9 min and a microwave power level of 560 W.

By increasing the impregnation ratio from 0.8 to 1.6 (wt%), the authors described the initial effect of the zinc chloride as intensifying the release of volatile matter, resulting in higher adsorption capacity. By increasing the impregnation ratio to 2.0 (wt%), ZnCl<sub>2</sub> works as a dehydrating agent and prevents the formation of tars and other liquids that could block the pores of the carbon. The volatile matter can then move easily through the pore channels and be released from the surface of the carbon during the activation stage. This phenomenon leads to an increase in the adsorption capacity of AC (Hui Deng et al., 2009).

Phosphoric acid is also one of the more prominent agents used in the production of AC and has two important functions: (i) promotion of pyrolytic decomposition of the initial materials and (ii) organization of the cross-linked structure (Foo & Hameed, 2012c). Phosphoric acid was used with microwave energy as the chemical activation agent to produce AC from bamboo by Liu et al., 2010b). The surface area and pore volume of the AC were investigated at 350 W and 20 min of irradiation. The authors found that both the surface area and pore volume increased with an increase in the impregnation ratio owing to the penetration and occupation of potential sites by phosphoric acid, which aided in the process of widening and opening the pores. An excess dosage of acid might form an insulating layer and not promote further activation (Foo & Hameed, 2012c).

Tables 2.3 and 2.4 show that the range of optimum impregnation ratios (agent/precursor) used in producing AC from agricultural wastes by microwave-induced methods is 0.5:1 to 1.75:1 (wt%) for chemical activation agents. For physical activation, the agent flow rate/precursor and the steam flow rate range is 1.35 to 5 g/min, and the CO<sub>2</sub> flow rate range is 200 to 600 cm<sup>3</sup>/min. To compare the microwave and conventional heating methods, Maldhure and Ekhe used black liquor obtained from the Kraft pulping process as a precursor to prepare AC using both heating methods.

The  $S_{BET}$  of the AC increased from 993.0 to 1164  $m^2/g$  when the impregnation ratio was increased from 1:1 to 1:1.5 (wt%) and then decreased to 1105  $m^2/g$  when the impregnation ratio was increased to 1:2 (wt%). Conventionally activated samples showed significantly less nitrogen uptake than microwave activated samples where  $ZnCl_2$  was used with an impregnation ratio above the optimum amount of 1:1.5 (wt%) (Maldhure & Ekhe, 2011). The highest adsorption capacities for agricultural-based AC with the optimum preparation conditions for chemical activation are summarized in Table 2.3.

Table 2.3: Maximum adsorption capacity of ACs prepared from agricultural wastes by chemical activation under the optimum preparation conditions.

Precursor	Agent	Adsorption capacity (mg/g)	Adsorbent	power (w)	time (min)	*IR	Ref
Pineapple Peels	KOH	462.10	MB	600	6	1:1.25	(Foo & Hameed, 2012b), (K.Y. Foo, 2011)
	$K_2CO_3$	411.74	MB				
Rice Husks	KOH	441.52	MB	600	7	1:1.075	(Foo & Hameed, 2011g)
	$K_2CO_3$	362.60	MB				
Cotton Stalks	KOH	294.12	MB	660	10	0.6:1	(Hui Deng, Li, et al., 2010)
	$K_2CO_3$	285.71	MB				
Orange Peels	$K_2CO_3$	382.75	MB	600	6	1.25:1	(Foo & Hameed, 2012c)
Sunflower Seed Oil Residues	$K_2CO_3$	473.44	MB	600	8	1:1.5	(Foo & Hameed, 2011d)
		430.37	Acid Blue				
Tobacco Stems	$K_2CO_3$	517.50 1834	MB Iodine	700	30	1.5:1	(W. Li et al., 2008)
Pistachio Nut Shells	KOH	296.57	MB	700	7	1.75:1	(Foo & Hameed, 2011c)
Oil Palm Residues	KOH	344.83	MB	360	15	0.75:1	(Foo & Hameed, 2011f)
Fruit Residues	KOH	395.30	MB	600	7	1:1	(Foo & Hameed)
Oil Palm Fibers	KOH	312.50	MB	360	5	0.5:1	(Foo & Hameed, 2011a)
Cotton Stalks	$H_3PO_4$	245.70	MB	400	8	—	(Hui Deng, Zhang, et al., 2010)
Lotus Stalks	$H_3PO_4$	564.97	OTC	700	15	2:1	(Huang et al., 2011)
Pomelo Skins	NaOH	501.10	MB	500	5	1:1.25	(Foo & Hameed, 2011b)
		444.45	Acid Blue				
Cotton Stalks	$ZnCl_2$	193.50	MB	560	9	1.6:1	(Hui Deng et al., 2009)
		972.92	Iodine				

## **2.7 Effects of microwave power and radiation time on the physical structure of physically AC**

Physical activation generally requires a higher microwave power level and longer radiation time than chemical activation. Tables 2.3 and 2.4 show that the range of optimum microwave power used to produce AC by physical activation is 750 to 3000 W, whereas, in chemical activation, this range is between 200 and 900 W. The range of optimum microwave radiation time for physical activation is from 19 to 210 min, and this optimum time for chemical activation ranges from 30 sec to 30 min.

Guo and Lua (J. Guo & Lua, 2000) used a different microwave power level and activation time to investigate the effects of these variables on the properties of AC. At low microwave power levels of 80 W, 150 W and 300 W with an exposure time of 60 min, the microwave radiation has no effect on the density and total porosity of the prepared AC. No reaction occurs between the char and the agent at the lower power levels, but at the high microwave power levels of 450 W and 750 W, the total pore volume increased progressively with increasing microwave radiation time. They attained an increase of 20.9% in the total porosity of the AC by increasing the exposure time from 5 min to 1 h at the microwave power level of 750 W. The pores created during carbonization would, therefore, be enlarged by a combination of the effects of continual carbonization and the carbon-CO<sub>2</sub> reaction. New pores will be created and formed by increasing the reaction time. The proximate analyses of ACs prepared under different microwave power levels and times showed that the losses of volatile matter and fixed carbon are more significant at higher microwave power (750 W) than at lower power (450 W). It was also observed that at the longer activation time (60 min), the losses are larger than at a shorter activation time (40 min). For instance, at a fixed radiation time of 60 min, the volatile content weight losses (based on their respective individual starting weights in the char samples) at 450 W and 750 W increased by



60.3% and 87.2%, respectively. The fixed carbon decreased 14.7% at 450 W and 46.5% at 750 W. At the same microwave power of 750 W, the weight loss of volatile content at 5 min and 60 min was 38.5% and 87.2%, respectively. The BET surface area was increased by increasing the microwave radiation time at high power, and at the long radiation times, the rate of micropore production decreased suddenly because of the conversion of some micropores to mesopores. At higher microwave power, the BET surface area increased faster than at lower microwave power because of the higher release of volatile matter and the occurrence of the carbon-CO<sub>2</sub> reaction (J. Guo & Lua, 2000).

The same results for the effect of the variation in the activation time under microwave radiation were obtained by Yang et al., 2010. The coconut shell-based ACs, produced by the mixture of CO<sub>2</sub> and steam as the physical agent with activation times of 30 min, 60 min and 75 min have BET surface areas of 1424 m<sup>2</sup>/g, 2020 m<sup>2</sup>/g and 2194 m<sup>2</sup>/g, respectively, and total pore volumes of 0.827 cm<sup>3</sup>/g, 1.248 cm<sup>3</sup>/g and 1.293 cm<sup>3</sup>/g, correspondingly. These results demonstrate that the S<sub>BET</sub> and V<sub>tot</sub> are increased by increasing the microwave radiation time. The same increase in BET surface area and total pore volume were achieved by an increase in the reaction time when CO<sub>2</sub> and steam were used separately as activation agents. The BET surface area and pore volume increase with an increase in the activation time regardless of the activation agent. At higher activation times, the quantity of produced pores decreases, most likely indicating proximity to the optimum activation time (K. Yang et al., 2010). When Xin-hui et al. used Jatropha hulls as the raw material with steam activation to prepare AC, they found that an increase in the activation time increased the extent of the carbon-steam reaction, which, in turn, increased the porosity of the AC (Xin-hui et al., 2011b). The highest adsorption capacity of agriculturally based AC and the optimum preparation conditions for physical activation are summarized in Table 2.4.

Table 2.4: Maximum adsorption capacity of ACs prepared from agricultural waste by physical activation under the optimum preparation conditions.

Precursor	Agent	Adsorption capacity (mg/g)	Adsorbent	Microwave power (W)	time (min)	Agent flow	Ref
Jatropha Hulls	Steam	988	Iodine	3000	19	5 g/min	(Xin-hui et al., 2011a, 2011b)
	CO <sub>2</sub>	988	Iodine	3000	30	300 ml/min	
Coconut Shells	Steam	–	–	3000	75	1.35 g/min	(K. Yang et al., 2010)
	CO <sub>2</sub>	–	–	3000	210	600 ml/min	
	mixed	–	–	3000	75	600+1.35	
Oil Palm Stones	CO <sub>2</sub>	–	–	750	60	200 ml/min	(J. Guo & Lua, 2000)

## 2.8 Effects of different agents and agent flow rates on the physical structure of physically AC

The physical activation process is widely used for the commercial industrial production of AC because of the simplicity of the process and the ability to produce AC with well-developed microporosity and desirable physical characteristics such as good physical strength. In physical activation, AC is traditionally made by partial gasification of the char with steam, CO<sub>2</sub> or a combination of both. The gasification reaction leads to the oxidation of carbon atoms and, in the process, simultaneously produces a wide range of pores (mainly micropores), resulting in a porous AC (K. Yang et al., 2010).

Xin-hui et al., 2011, used Jatropha hulls as a biomass precursor to produce AC in the presence of CO<sub>2</sub> and steam as activation agents with both conventional and microwave heating methods for preparation procedures. They determined that using steam instead of CO<sub>2</sub> for activation increased the extent of the reaction for the same specific activation time. This difference is due to the higher rate of reaction between carbon and steam compared with the carbon-CO<sub>2</sub> reaction (González et al., 2006; Román, González, González-García, & Zamora, 2008). They also found that steam molecules can diffuse faster into the microstructure, encountering less diffusion resistance because of the smaller molecular size of H<sub>2</sub>O in comparison to CO<sub>2</sub>, and therefore, steam activation can produce more microporosity.

Microwave heating with steam activation produced double the pore volume and surface area compared with conventional heating methods, but the same magnitude of pore volume and surface area as with CO<sub>2</sub> activation (Xin-hui et al., 2011a).

Yang et al. used coconut shells with CO<sub>2</sub>, steam and CO<sub>2</sub>-steam mixture activation and microwave heating. From the nitrogen isotherms of the ACs prepared at the same activation time, they obtained a higher nitrogen adsorption capacity from the CO<sub>2</sub>-steam mixture activation compared to activation using CO<sub>2</sub> or steam separately because of the higher total flow rate of the CO<sub>2</sub>-steam mixture compared with the individual flows of the other agents. The AC that was produced by the mixture of CO<sub>2</sub>-steam had a higher porosity compared to that produced using only CO<sub>2</sub> or steam. This greater porosity was attributed to the higher reactivity of steam, which generates and widens micropores at a faster rate to aid the CO<sub>2</sub> diffusion within the carbon and cause the development of additional micropores (K. Yang et al., 2010).

Guo and Lua prepared AC from oil palm residue using microwave irradiation with CO<sub>2</sub> as agents. Both continual carbonization and carbon-CO<sub>2</sub> reactions were assumed to occur during microwave heating. Microwave radiation affects the reaction between carbon and CO<sub>2</sub> to develop further pore structure and surface area. They used nitrogen gas for the activation process and observed that micropores, BET surface area and the total pore structure remained almost unchanged from the values for the char, so microwave radiation appeared to produce no reaction in the absence of any oxidation gases. The flow rate of agents is another activation condition with an effect on AC porosity.

At a low flow rate of CO<sub>2</sub>, the BET and micropore surface areas and the total pore volume were marginal because of insufficient agent flow to remove gas products and react with char to produce an internal pore structure.

A very high CO<sub>2</sub> flow rate has a detrimental effect on the quality of AC by producing a severe char-CO<sub>2</sub> reaction and oxidizing much of the carbon content (J. Guo & Lua, 2000).

## 2.9 Effects of microwave-induced method on carbon yield

The carbon yield, defined as the weight of dried AC to the weight of dry raw material, is important in practical applications in the form of the following equation:

$$Yield (\%) = \frac{W_1}{W_0} \times 100 \quad (2.1)$$

where  $W_0$  is the precursor weight and  $W_1$  is the resulting AC mass (Q.S. Liu, T. Zheng, P. Wang, et al., 2010). Physical activation usually has a lower carbon yield and requires the use of higher temperatures compared with chemical activation (Dąbrowski, Podkościelny, Hubicki, & Barczak, 2005; Karim, Das, & Lee, 2006). There are two different results in comparison between microwave and thermal method in the yield of prepared AC. In the experiment that was performed by Liu, Q.S., *et al.*, 2010, the microwave heating method produced AC with a higher carbon yield than the conventional method, but the differences in yields are not so significant. It was explained that the difference in carbon yield between the microwave and the conventional heating method occurs because more of the carbon precursor is lost during the longer activation time necessary for thermal activation in comparison with the shorter activation time required for the microwave-induced method (Q.S. Liu, T. Zheng, P. Wang, et al., 2010). On the other hand, Huang *et al.*, 2011, showed that the microwave method produces AC with a lower production yield compared with the conventional heating method.

The explanation for this phenomenon was that the samples could attain a high temperature in minutes with microwave radiation, most likely because the activation reaction under microwave radiation is more intense.

Tar and volatile matter are, therefore, released rapidly from the surface of the carbon, which increases the weight loss of the carbon precursor and decreases carbon yield in comparison with the thermal method (Huang et al., 2011). The effects of the microwave power level on the yield of AC were investigated at a zinc chloride impregnation ratio of 1.2 (wt%) and a radiation time of 8 min by Liu et al., 2010 for bamboo-based AC. They determined that the carbon yield decreased from 61.2% to 45.5% when the microwave power increased from 200 to 400 W because of the greater weight loss of raw material at the higher level of microwave power. The weight loss is due to the aggressive reaction between the agent (phosphoric acid) and the carbon precursor at higher microwave power levels (Q.S. Liu, T. Zheng, P. Wang, et al., 2010). Deng et al. achieved an increase in the yield of cotton stalk-based AC from 27.25% to 32.37% with an increase in radiation power from 400 to 560 W at  $X_{ZnCl_2}$  of 1.2 g/g and microwave activation time of 8 min. At a higher power of 640 W, the yield decreased to 32.15%, which was attributed to the burning of small quantities of carbon by the excess energy at the higher level of microwave power (Hui Deng et al., 2009). The carbon yield decreased because of the increasing microwave power level in other studies where agricultural waste was used as the precursor. Foo and Hameed observed that, under low microwave power levels of 90 and 180 W, the carbon yield remained almost unchanged due to insufficient radiation power for continual activation. They also found that the carbon yield was drastically increased at higher microwave power levels of 360 and 600 W, possibly ascribed to the combined effect of internal and volumetric heating responsible for the expansion of the carbon structure. They also reported that the over gasification at high radiation power of 800 W might occur with a detrimental impact of reducing the surface area and porosity, resulting in a lower carbon yield (Foo & Hameed, 2012a). The activation time for the microwave heating method is another parameter with more effects on the carbon yield.

The yield of AC produced by Liu et al., 2010 from bamboo decreased from 58.6% to 45.3% with an increase in the activation time from 5 to 30 min, respectively. The development of pores causes an increase in weight loss and carbon yield (Q.S. Liu, T. Zheng, P. Wang, et al., 2010). Deng et al. (Hui Deng et al., 2009) achieved the same carbon yield (increased up to the optimum radiation time, then decreased beyond the optimum value) when they investigated the effects of radiation time at a microwave power of 560 W and zinc chloride impregnation ratio of 1.2 (wt%). They determined that the yield increased from 32.37% to 34.39% when the radiation time was increased from 8 to 9 min and then decreased to 33.5% when the time was increased to 10 min. Li et al. (W. Li et al., 2008) detected the same tendency for the yield in the production of AC from tobacco stems using  $K_2CO_3$  activation. Hirata et al., 2002 noted that the yield of AC decreased with increasing microwave activation time because part of the carbon in the form of coffee grounds was changed to carbon dioxide (Hirata et al., 2002). Foo and Hameed (Foo & Hameed, 2012c) produced AC from orange peels and found that the carbon yield decreased after 7 minutes of activation. Increasing the radiation time leads to a rise in the temperature of the samples and opening of the micropores and mesopores. Increasing the temperature promotes the reaction of carbon with agents (C- $K_2CO_3$ , C- $K_2O$ ) and C- $CO_2$ , assisting in the breaking of the C-O-C and C-C bonds and decreasing the carbon yield (Adinata, Wan Daud, & Aroua, 2007).

Haimour and Emeish (Haimour & Emeish, 2006) and Liu et al. (Q.S. Liu, T. Zheng, P. Wang, et al., 2010) observed that the yield of AC increased gradually when the impregnation ratio of phosphoric acid was increased.

This phenomenon demonstrated that without a sufficient agent ratio to participate in the activation process, the sample would be consumed without significant development of pore structure. White pine wood powders were used by Wang and Liang as a precursor to prepare AC with zinc chloride activation in the microwave.

They found that the yield increased from 36.2 wt % at an impregnation ratio of 0.75 (wt%) to 38.1 (wt%) at an impregnation ratio of 3.0 (wt%). The  $\text{ZnCl}_2$  could promote dehydration and a cross-linking reaction in the microwave case (Tonghua Wang, 2009). Foo and Hameed used orange peels ( $\text{K}_2\text{CO}_3$  activation) (Foo & Hameed, 2012c) and fruit residues (KOH activation) (Foo & Hameed, 2012a) to produce AC. In both experiments, the carbon yield was increased by increasing the impregnation ratio from 0.25 to 1.25 (wt%); beyond this value, the carbon yield decreased gradually with a further increase in the impregnation ratio. The same result, where the carbon yield decreased when the agent ratio was increased further, was achieved by Li et al. (W. Li et al., 2008).

Some researchers have investigated the effect of microwave irradiation on carbon yield with physical activation. Yang et al., 2011a, found that the yield of Jatropha hull-based AC decreased with the increase of the reaction between carbon and steam. The rate of the carbon-steam reaction was enhanced by increasing the activation time, activation temperature and agent flow rate. Increasing any of these three parameters caused a decrease in the yield (Xin-hui et al., 2011b). González et al. (González et al., 2006) and Román et al. (Román et al., 2008) reported that the rate of the carbon-steam reaction is higher than the rate of  $\text{CO}_2$  activation, implying that the faster reduction of yield with steam activation than with  $\text{CO}_2$  activation is a function of the activation time. The mixture of steam and  $\text{CO}_2$  was found to produce a higher reduction in yield than steam alone, possibly because of the higher net flow of activation agent that may cause the simultaneous reactions of steam and  $\text{CO}_2$  with carbon. Xin-hui et al. (Xin-hui et al., 2011a) used conventional and microwave heating methods to prepare AC from Jatropha hulls using steam and carbon dioxide. The yields using steam for conventional and microwave heating methods were 13.32% and 16.56%, respectively.

These yields for CO<sub>2</sub> activation with conventional and microwave heating methods are 18.02% and 36.60%, respectively.

The difference in the AC yield with different heating methods is clearly not very significant using steam as the agent, whereas the yield of AC doubled using CO<sub>2</sub> as an activation agent in microwave compared with a conventional heating method. In both cases, the pore volumes were in the same range. According to these results, the close correspondence of the results for each heating method with steam activation is due to insignificant changes in the rate of the carbon-steam reaction. The diffusion of steam to the active sites in the carbon could be the rate-limiting step. Microwave heating is, therefore, faster and more homogeneous and requires a shorter activation time, a lower activation temperature and a lower agent flow rate compared with the conventional method (Xin-hui et al., 2011a).

Guo and Lua investigated the effects of microwave power levels and exposure times on the yield of AC produced from oil palm stones by CO<sub>2</sub> activation. They determined that for a microwave power level of 300 W, when the microwave radiation time was increased from 5 to 60 min, the AC yield was unchanged because there was an insufficient amount of microwave energy to initiate the reactions between carbon and the agent. At microwave power levels of 450 W or 750 W and a longer exposure time, the yield of AC decreased progressively because of continual carbonization and the carbon–CO<sub>2</sub> reaction, which contributed to the release of volatile matter and the burn-off of some carbon content (J. Guo & Lua, 2000).

## **2.10 Effects of the microwave-induced method on the chemical properties of AC**

The types of raw materials, the types of heat treatments, the activation processes and the post-chemical treatments are the main factors that determine the surface chemical functional groups of AC (Izquierdo, Rubio, Mayoral, & Andrés, 2001; Szymański, Karpiński, Biniak, & Świątkowski, 2002).



The surface functional groups (FGs) (acidic and basic surface chemical properties) are important characteristics of the AC that have significant effects on the surface properties of AC as an adsorbent, applications in ion exchange and other properties (Budinova et al., 2006; Q.S. Liu, T. Zheng, P. Wang, et al., 2010).

The surface basicity is associated with the presence of carbonyls, chromene, pyrone and oxygen-free Lewis-type structures (Faria, Órfão, & Pereira, 2004), whereas the acidic behavior is related to oxygen-containing groups (mainly carboxylic acids, anhydrides, lactones and phenols) (Foo & Hameed, 2011d, 2012a; Pereira, Soares, Órfão, & Figueiredo, 2003). Basic surfaces are favorable for acidic liquids and gas adsorption for materials such as sulfur dioxide, and the acidic surfaces are suitable for the adsorption of basic liquids and gases such as ammonia (Ioannidou & Zabaniotou, 2007; T. Yang & Lua, 2003). The various types of atoms on the surface of porous carbon include oxygen, nitrogen, halogens, and hydrogen.

These atoms have significant effects on the applications of AC, which governs the surface chemistry by bonding the edge of the carbon layers (El-Sayed & Bandosz, 2004). Oxygen-containing functional groups are one of the most common groups formed on the surface of carbon with particular effects on the performance of AC as an adsorbent (Feron & Jansen, 1997; Y. H. Li, Lee, & Gullett, 2002; Mikhalev & Øye, 1996) and in catalytic reactions (Francisco, 1998).

Microwave treatment eliminates the acidic oxygen-containing functional groups and makes the carbon layer basic and very reactive (Huang et al., 2011; Menéndez et al., 1999). There is a significant decrease of the basic properties of AC prepared by the microwave method due to the elimination of some oxygen functional groups and the decomposition of volatile matter during the activation process (Chang, Chang, Hu, Cheng, & Zen, 2010; X.j. He et al., 2011; Nian & Teng, 2003; Valente Nabais, Carrott, Ribeiro Carrott, & Menéndez, 2004).

After the microwave treatment and the removal of most of the more weakly bound atoms, a small portion of the oxygen-containing groups with heteroatoms (substantially nitrogen) that are basic in nature remains within the aromatic structure of the carbon layers (Foo & Hameed, 2011b; Ji et al., 2007).

Huang et al. (2011) used lotus stalks as a raw material to prepare AC using the microwave method with  $\text{H}_3\text{PO}_4$  as a chemical agent. The FTIR results for the AC produced from the impregnated raw material and the char prepared from the carbonization step showed that AC has a smaller quantity of acidic functional groups, which is consistent with the elimination of acidic groups by microwave irradiation. (Huang et al., 2011). Foo and Hameed (2012) observed the elimination of some FTIR peaks for orange peel-based AC in comparison with char from the carbonization step. They mentioned that the microwave radiation released the volatile matter by decomposing the functional groups (Foo & Hameed, 2012c). They achieved similar results for the elimination of some peaks in FTIR spectra of AC prepared from Pomelo skins as the precursor (Foo & Hameed, 2011b). Deng et al.(2010) (Hui Deng, Zhang, et al., 2010) produced AC from cotton stalks by the microwave method with  $\text{H}_3\text{PO}_4$  for chemical activation and compared the FTIR results with those from the experiments conducted by El-Hendawy et al. (El-Hendawy, Alexander, Andrews, & Forrest, 2008) where AC was produced from cotton stalks with the conventional heating method and physical activation. They observed significant changes in the FTIR spectra of the AC. For instance, a new FTIR band appeared at  $966\text{ cm}^{-1}$  and two bands in the region between  $3500$  and  $2800\text{ cm}^{-1}$  disappeared because of the microwave activation process and the formation of polyphosphate and inorganic species in the carbon.

Foo and Hameed (2011) produced AC from sunflower seeds using  $\text{K}_2\text{CO}_3$  as a chemical agent. They prepared char from the impregnated precursor by the thermal method and then prepared AC using the microwave-induced method.

The carbon content in the char produced from the carbonization stage increased after the microwave treatment in the prepared AC. The oxygen content of the char decreased drastically and caused the carbon/oxygen ratio to increase from 1.30 to 3.01. The nitrogen and sulfur content decreased slightly with microwave radiation in the activation process, and hydrogen was the only material with a stable amount in the char and AC (Foo & Hameed, 2011d). Oil palm fibers have been used as a precursor to produce AC using KOH for chemical activation with the same microwave power level of 360 W and different activation times of 5 (Foo & Hameed, 2011a) and 15 min (Foo & Hameed, 2011f). The C/O ratio increased in the ACs prepared with different radiation times due to the elimination of the oxygen-containing groups and the increase of the carbon content. The FTIR assignments of the functional groups on the agricultural waste-based AC surface are listed in Table 2.5.

The same increase in oxygen-containing functional groups was achieved in non-biomass-based AC. Ji et al., 2007, determined from the FTIR spectra that the AC produced by microwave heating from commercial coal-tar pitch and KOH chemical activation had very weak adsorption in some regions and that there were higher peaks for electric furnace samples. The low content of oxygen-containing functional groups produced by the microwave heating method was most likely due to the different mechanism used for the heating method (Abdel-Nasser A, 2003; Aguilar, García, Soto-Garrido, & Arriagada, 2003; Boonamnuayvitaya, Sae-ung, & Tanthapanichakoon, 2005; Jerzy, 1988; Moreno-Castilla, López-Ramón, & Carrasco-Marín, 2000).

Maldhure and Ekhe (2011) investigated the FTIR spectra of the ACs prepared from industrial waste lignin with  $ZnCl_2$  chemical activation using microwave and thermal methods (Maldhure & Ekhe, 2011). They observed that the total amount of oxygen functional groups for the microwave-treated sample was approximately 18% higher than the thermal treated sample at the same impregnation ratio of 1:1.5 (wt%).

By increasing the impregnation ratio, the total amount of oxygen functional groups increased and then showed a slight decrease with a further increase in the impregnation ratio. They observed greater peak intensity and more highly developed surface functionality in microwave-irradiated samples. Mixing microwave and conventional heating methods showed beneficial effects on the formation of more active surface functional groups in comparison with using only the conventional process.

Table 2.5: Functional groups characterized by FTIR in different agricultural-based ACs produced under optimum conditions.

Precursor	Agent	Wave number assignments (cm <sup>-1</sup> )	Group or functionality	Ref
Pineapple Peels	KOH K <sub>2</sub> CO <sub>3</sub>	3234, 2867, 2376, 2361 2342, 1497, 1424, 1054, 828	N-H, C-H (alkanes), O-H (carboxylic acids), C≡C (alkyne), -COOH, in- plane O-H bend, C-N, C-O and N-O derivatives	(K.Y. Foo, 2011)
Rice Husks	KOH K <sub>2</sub> CO <sub>3</sub>	3436, 3247, 2362, 1421, 1261, 1054, 913, 802	N-H, -CH <sub>2</sub> (alkyl), C≡C (alkynes), in-plane O-H bend, -OH (hydroxyl), C-O stretch, -R-COO and out-of-plane C-H	(Foo & Hameed, 2011g)
Cotton Stalks	KOH K <sub>2</sub> CO <sub>3</sub>	1750-1630, 1300-1000, 1640-1430)	C=O (carboxylic, anhydride, lactone, and ketene groups, C-O (lactonic, ether, phenol), C=C	(Hui Deng, Li, et al., 2010)
Orange Peels	K <sub>2</sub> CO <sub>3</sub>	3436, 3237, 2361, 2343, 1649-1497, 1425, 1276, 1053, 806	N-H, -OH (hydroxyl), C≡C (alkynes), -COOH, in-plane O-H (hydroxyl), -CH <sub>2</sub> (alkyl), C-O-C (ester, ether and phenol), C-O (anhydrides) and C-H derivatives.	(Foo & Hameed)
Sunflower Seed Oil Residues	K <sub>2</sub> CO <sub>3</sub>	3233, 1650, 1424, 1276, 1053	N-H, in-plane O-H (hydroxyl), -CH <sub>2</sub> (alkyl), C-O-C (ester, ether and phenol), C-O functional groups	(Foo & Hameed, 2011d)
Pistachio Nut Shells	KOH	3413, 1999, 1567, 1384, 1102	-OH (hydroxyl), C≡C, OH bending vibrations, -NO <sub>2</sub> , and C-O-C (esters, ether or phenol) derivatives.	(Foo & Hameed, 2011c)
Oil Palm Residues	KOH	3840-3200, 2930 2357, 1053, 569	-OH (hydroxyl), C-H (alkanes and alkyls), C≡C (alkynes), C-O-C (esters, ether or phenol), and C-H (benzene derivatives)	(Foo & Hameed, 2011f)

“ Table 2.5, continued”

Precursor	Agent	Wave number assignments (cm <sup>-1</sup> )	Group or functionality	Ref
Oil Palm Fibers	KOH	3800–3200, 2361, 1429, 1053, 568	–OH (hydroxyl), C≡C (alkyne), –CH <sub>2</sub> (alkyl), C–O–C (ester, ether and phenol)	(Foo & Hameed, 2011a)
Oil Palm Residues	KOH	3234, 2377, 1420, 1277, 1053	–OH (hydroxyl), C≡C (alkyne), –CH <sub>2</sub> (alkyl), C–O–C (ester, ether and phenol)	(Foo & Hameed)
Bamboo	H <sub>3</sub> PO <sub>4</sub>	3450, 1050–1750 1300–1600, 600–900	O–H (hydroxyl), (ethers, lactone, carboxyl, aromatics and nitrate groups), C=O, out-of-plane bending mode of the C–H or O–H group	(Q.-S. Liu, T. Zheng, P. Wang, et al., 2010)
Cotton Stalks	H <sub>3</sub> PO <sub>4</sub>	1627.7, 1584.2, 1362.2, 1342.6, 966.3	C=O (lactonic and carbonyl groups), C–O (highly conjugated, carboxylic and carboxylate moieties), P=O (linear and cyclic polyphosphate and inorganic species)	(Hui Deng, Zhang, et al., 2010)
Lotus Stalks	H <sub>3</sub> PO <sub>4</sub>	1562, 1310 and 1000, 900 and 700	C=C (aromatic rings bands), C–O–C (ether), aromatic substitution.	(Huang et al., 2011)
Cotton Stalks	ZnCl <sub>2</sub>	3441.6, 2352.6 and 2336.6, 1627.7, and 1604.0, 1346.5, 1120.8 and 1053.3	–OH (hydroxyl), C≡C stretching, C=O (lactonic and carbonyl groups), highly conjugated C–O, C–O (carboxylic) and carboxylate moieties	(Hui Deng et al., 2009)
Industrial Waste Lignin	ZnCl <sub>2</sub>	500 and 850, 950 and 1300, 1400 and 1750, 1550 and 1650	aromatic substitution by aliphatic groups, (ether, phenol and lactones), (carboxylic groups, quinones, ketones, lactones, diketones and keto-ester and ketoenol), C=C (aromatic ring enhanced by polar functional groups)	(Maldhure & Ekhe, 2011)
Coconut Shells	Steam CO <sub>2</sub> Mixed	3430, 2917 1631	O–H (hydroxyl), C–H (methyl and methylene), C = C (olefinic)	(K. Yang et al., 2010)

## CHAPTER 3: METHODOLOGY

This chapter includes description of used precursors for preparation of AC, kinds of applied chemicals and physical agents and used MB and CO<sub>2</sub> for adsorption. The preparation methods such as impregnation procedures, activation process, washing steps and characterization methods are also described in this chapter.

### **3.1 PART 1: Palm shell based AC prepared by zinc chloride chemical activation using response surface methodology**

#### **3.1.1 Materials**

Oil palm shell waste as received from the palm oil factory was washed several times with distilled water to remove dust and dirt and placed in an oven at 110 °C for 24 h to remove moisture. The dried palm shell was ground and sieved to the different particle sizes (p) in the following ranges:  $p < 0.5$  mm,  $0.5 < p < 1.0$ ,  $1.0 < p < 1.5$ ,  $1.5 < p < 2.0$  and  $2.0 < p < 2.5$  mm. The proximate analysis of oil palm shell by weight percent shows a moisture content of 4.7%, a volatile matter content of 73.5%, a fixed carbon content of 13.8% and an ash content of 7.2%. Zinc chloride was purchased from Merck (M; Sdn. Bhd, Malaysia). Deionised water supplied by a USF ELGA water treatment system was used for washing steps and the preparation of all the solutions.

#### **3.1.2 Activation method**

The activation process was carried out in a quartz tubular reactor placed inside an ML-3 type sequence microwave heating apparatus produced by Sichuan University (Sichuan Province, China) with power that can be varied between 0 and 1400 W. Pure nitrogen gas (99.995%) at a preset flow rate of 300 cm<sup>3</sup>/min was used to purge air inside the reactor before and during the activation step.

The sieved oil palm shell with a particle size of 0.5–2.5 mm was mixed with a solution of zinc chloride (2 ml of deionized water per gram of the precursor) with impregnation ratios of 0.56, 1.13, 1.69, 2.25 and 2.81  $X_{ZnCl_2}$ , where  $X_{ZnCl_2}$  is the zinc mass per gram of the raw material. The prepared solutions were heated and stirred for 2 h at 85 °C, after which the temperature was increased until complete dryness (Arami-Niya *et al.*, 2010). The impregnated raw material was dried in the oven for 24 h at 110 °C to remove any remaining moisture. A 25 g sample of the impregnated raw material was placed inside the quartz reactor, which was in turn placed inside the microwave oven for the activation step with microwave powers of 750, 900, 1050, 1200 and 1300 W and activation times of 5, 10, 15, 20 and 25 min. The resultant AC was cooled at room temperature and then washed repeatedly with 0.1 M hydrochloric acid and warm and cool distilled water until reaching pH 6–7. The washed ACs were dried in the oven at 105 °C for 24 h and then stored in a desiccator for further use. The percentage of AC yield was calculated using the following equation:

$$Yield (\%) = \frac{W_1}{W_0} \times 100 \quad (3.1)$$

where  $W_1$  is the weight of the prepared AC after activation and  $W_0$  is the weight of the impregnated raw materials before activation.

### 3.1.3 Characterization methods

Proximate analysis of oil palm shell and the prepared ACs were carried out according to the ASTM D 7582-10, and the results were expressed in terms of moisture, volatile matter, fixed carbon and ash contents. Ultimate analysis was performed using a Perkin-Elmer 2400 Series II CHNS/O analyser to determine the fixed carbon, hydrogen, nitrogen, and oxygen contents of each sample.

The prepared ACs were characterized based on  $N_2$  adsorption isotherms measured at  $-196$  °C using a Micromeritics ASAP 2020 Series volumetric gas adsorption

instrument. The BET method was used to determine the specific surface area of the samples for relative pressures from 0.05 to 0.30. The nitrogen volume held at the highest relative pressure ( $P/P_0 = 0.99$ ) was used to calculate the pore volume of the ACs. The volume of the micropores was determined using the Dubinin–Radushkevich (DR) equation (Barrett, 1951; Rouquerol *et al.*, 1999). The Dollimore–Heal adsorption pore distribution method was applied to estimate the pore diameters.

### 3.1.4 Experimental design

Response surface methodology is a well known approach to optimising the effects of multiple process variables on the properties of prepared products using a combination of mathematical and statistical techniques (Xin-hui *et al.*, 2011b). The AC production parameters were studied using standard response surface methodology with a central composite design. This method was chosen for fitting a quadratic surface with a minimum number of experiments. It also helps analyse the interaction between the effective process parameters and identify the factor settings that optimise the response (Tan *et al.*, 2008b).

Table 3.1: Independent variables and their coded levels for the CCD

Natural Variables	Code	Coded variable level		
		-1	0	1
Activation time (min)	$X_1$	10	15	20
MW Power (W)	$X_2$	900	1050	1200
Ratio (g $ZnCl_2$ /g Palm shell)	$X_3$	1.13	1.69	2.25
Size (mm)	$X_4$	1.0	1.5	2.0

Table 3.1 shows the ranges and levels of the dependent variables: activation time ( $X_1$ ), microwave power ( $X_2$ ), impregnation ratio ( $X_3$ ) and particle size ( $X_4$ ).



Generally, the CCD consists of  $2^n$  factorial runs with  $2n$  axial runs and  $n_C$  centre runs (six replicates) (Eq. (3.2)).

$$N = 2^n + 2n + n_C \quad (3.2)$$

The full factorial CCD for four variables consists of 16 factorial points, 8 axial points and 6 replicates at the centre points, for a total of 30 experiments. The six replicate experiments at the centre point are used to estimate the experimental error and the duplicability of the data.

The independent variables are coded to the  $(-1, 1)$  interval, where the low and high levels are coded as  $-1$  and  $+1$ , respectively. The axial points are located at  $(\pm\alpha, 0, 0, 0)$ ,  $(0, \pm\alpha, 0, 0)$ ,  $(0, 0, \pm\alpha, 0)$  and  $(0, 0, 0, \pm\alpha)$ , where  $\alpha$  is the distance from the axial point to the centre. The value of  $\alpha$  can be calculated by Equation 3.3, which depends on the number of points in the factorial portion of the design (Montgomery, 2001).

$$\alpha = (2^n)^{0.25} \quad (3.3)$$

The  $\alpha$  value was fixed at 2 in this study, and the variables were coded as follows: microwave activation time (10 to 20 min) ( $X_1$ ), microwave power (900 to 1200 W) ( $X_2$ ), impregnation ratio (1.13 to 2.25 g ZnCl<sub>2</sub>/g precursor) ( $X_3$ ) and particle size (0.5 to 2 mm) ( $X_4$ ). The yield percentage ( $Y_1$ ) and the percentage of MB adsorption ( $Y_2$ ) were taken as the process responses.

Table 3.2: Experimental design matrix and response results.

Run	Type	Time (min), $X_1$	Power (W), $X_2$	Ratio (g ZnCl <sub>2</sub> /g) $X_3$	Size (mm), $X_4$	Adsorption (%), $Y_1$	Yield (%), $Y_2$
1	Center	15	1050	1.69	1.5	96.15	68.92
2	Center	15	1050	1.69	1.5	95.96	68.86
3	Factorial	10	900	1.13	2.0	95.18	56.03
4	Factorial	20	900	1.13	1.0	95.67	48.17
5	Factorial	10	1200	1.13	2.0	96.04	57.18
6	Factorial	10	900	2.25	1.0	95.78	73.60
7	Axial	15	1350	1.69	1.5	97.15	54.82
8	Axial	5	1050	1.69	1.5	95.06	67.00
9	Axial	15	1050	1.69	2.5	96.96	64.83
10	Factorial	10	900	2.25	2.0	95.53	64.00
11	Factorial	10	1200	1.13	1.0	95.59	56.28
12	Factorial	20	900	2.25	1.0	95.63	60.12
13	Factorial	20	900	1.13	2.0	96.33	52.50
14	Axial	15	750	1.69	1.5	96.15	60.92
15	Factorial	10	1200	2.25	1.0	96.05	62.22
16	Factorial	20	1200	1.13	2.0	97.20	50.00
17	Axial	25	1050	1.69	1.5	95.89	48.11
18	Factorial	10	1200	2.25	2.0	96.16	65.56
19	Center	15	1050	1.69	1.5	96.21	70.40
20	Factorial	20	900	2.25	2.0	95.65	58.72
21	Axial	15	1050	1.69	0.5	96.13	65.32
22	Factorial	20	1200	2.25	2.0	96.29	52.12
23	Factorial	20	1200	1.13	1.0	96.01	38.90
24	Factorial	10	900	1.13	1.0	95.46	60.78
25	Center	15	1050	1.69	1.5	96.15	71.20
26	Factorial	20	1200	2.25	1.0	95.28	45.02
27	Center	15	1050	1.69	1.5	96.20	70.00
28	Axial	15	1050	2.81	1.5	94.98	54.66
29	Center	15	1050	1.69	1.5	96.17	71.10
30	Axial	15	1050	0.56	1.5	95.55	36.20

The responses are assumed to be affected by the relation between the four independent variables, and the yield and MB adsorption data were analysed to fit the following second-order polynomial equation (Montgomery, 2001):

$$Y = b_0 + \sum_{i=1}^n b_i x_i + \sum_{i=1}^n b_{ii} x_{ii}^2 + \sum_{i=1}^{n-1} \sum_{j=i+1}^n b_{ij} x_i x_j \quad (3.4)$$

where  $Y$  is the predicted response;  $X_i$  to  $X_j$  are coded variables;  $b_0$ , the constant coefficient;  $b_i$ , the linear term coefficient;  $b_{ii}$ , the quadratic term efficient;  $b_{ij}$ , the interaction coefficient; and  $n$ , the number of AC preparation variables. Design Expert software (version 7.1.6, Stat-Ease, Inc., Minneapolis, USA) (Montgomery, 2001) was used to develop the mathematical model and estimate the subsequent regression analysis, analysis of variance (ANOVA) and response surfaces.

### 3.1.5 Batch equilibrium studies

MB adsorption experiments on prepared AC were carried out using known masses (1 g/l) of each AC sample mixed with 200 ml of MB. The initial concentration of the MB solution was 300 ppm (300 mg/l), prepared by mixing 300 mg of the solid MB, which is an odourless, dark green powder, with 1 litre of distilled water. Analytical-grade reagents were used in all cases. The stock solution was diluted as required to obtain standard solutions ranging from 5 to 30 mg/l.

The adsorption experiments were carried out in a thermal shaker at 30 °C for 24 h at 120 rpm. A 200 mg sample of each prepared AC was mixed with 200 ml of the 300 ppm MB solution.

After the adsorption process, all the samples were filtered to remove carbon and the residual concentrations of MB in the filtrate were analysed using a double-beam UV-visible spectrophotometer (Perkin Elmer) at 665 nm. The adsorbed MB per unit mass of AC under equilibrium conditions,  $q_e$  (mg/g), was calculated according to Equation 3.5:

$$q_e = \frac{(C_0 - C_e)}{M} \times V \quad (3.5)$$

where  $C_0$  and  $C_e$  are the initial and equilibrium concentrations (mg/L) of the MB solution, respectively;  $V$  is the volume of the MB solution (L); and  $W$  is the mass (g) of AC. Each sample was measured twice, and the average results were reported. To calculate the percentage of MB adsorption based on the initial and equilibrium MB concentration, Eq. 3.6 was used.

$$\text{Adsorption}(\%) = \frac{C_0 - C_e}{C_0} \times 100 \quad (3.6)$$

## **3.2 PART 2: Comparison of oil palm shell-based ACs produced by microwave and conventional heating methods using zinc chloride activation**

### **3.2.1 Materials**

Raw oil palm shell was crushed using a grinder and sieved to isolate particle sizes in the range of 1–2 mm, followed by washing with distilled water and drying at 110 °C for 24 h. Zinc chloride was purchased from Merck (M) Sdn, Bhd, Malaysia. Deionized water was supplied by a USF ELGA water treatment system, to be used during the washing stages.

### **3.2.2 Activation method**

Palm shell was impregnated according to the procedure given in part 1(3.1.1), where the raw material was first impregnated and stirred with a solution (2 ml of deionized water per gram of the precursor) of chemicals.

The concentrations of the solutions were tuned by providing different ratios of zinc chloride ( $X_{\text{ZnCl}_2}$ : 0.15, 0.28, 0.40, 0.53, 0.65, 0.78 and 0.90, where  $X_{\text{ZnCl}_2}$  is the zinc mass per gram of precursor); then, 10 g of the impregnated and dried samples were placed in a quartz reactor installed in an ML-3 type sequence microwave reactor produced by Sichuan University (Sichuan Province, China), and purged with pure nitrogen at a rate of 300 cm<sup>3</sup>/min before and during the activation process.

The activation step was carried out at a fixed microwave power of 1050 W for an irradiation time of 15 min. The prepared ACs were then cooled to room temperature and washed with distilled water until they obtained pH 6-7 and then they were dried in an oven at 105 °C for 12 h.

The preparation of conventionally treated AC has also been described elsewhere (Arami-Niya *et al.*, 2010), where the impregnated material was heated up to 500 °C at a heating rate of 10 °C/min for a hold time of 2 h under nitrogen flow rate of 100 ml/min.

The samples are identified according to the following nomenclature. (*MW*) represents AC prepared with the microwave method and (*C*) represents the AC prepared by the conventional heating method, and the chemical ratio (g ZnCl<sub>2</sub>/ g precursor) is displayed as the suffix (example: *MW*0.15 symbolizes the prepared AC with an impregnation ratio of 0.15).

### **3.2.3 Characterization methods**

The chemical functionalities of the ACs were qualitatively identified by Fourier transform infrared spectroscopy (FTIR). The FTIR spectra were recorded between 4000 and 400 cm<sup>-1</sup> by using an AVATAR 360 Spectrophotometer. The transmission spectra of the samples were recorded by using a KBr pellet containing 0.1% of each sample. SEM was performed to determine the physical morphology of the surface.

A JSM-6390LV (JEOL Ltd., Japan) SEM with a 3 kV accelerating voltage was used to characterize the morphology of the ACs, which were dried overnight at approximately 105 °C under vacuum prior to SEM analysis.

### **3.3 PART 3: Microwave-assisted production of activated carbons from oil palm shell in the presence of CO<sub>2</sub> or N<sub>2</sub> for CO<sub>2</sub> adsorption**

#### **3.3.1 Materials**

In this study, raw oil palm shell was collected from the palm oil factory. The palm shell was first washed carefully with distilled water and then dried in an oven at 283 K for 24 h. The dried sample was cut and sieved to isolate 1-2 mm particles. The potassium hydroxide chemical activation agent was purchased from Merck (M) Sdn. Bhd., Malaysia. For the washing steps, deionised water was obtained from a USF ELGA water treatment system. Pure nitrogen gas (99.995%) was flowed through the reactor at a pre-set flow rate of 300 cm<sup>3</sup>/min to purge the air inside the reactor before and during the activation step. To investigate the effects of the physical agent, carbon dioxide (99.999%) was flowed through the reactor at a pre-set flow rate of 300 cm<sup>3</sup>/min only during the activation process.

#### **3.3.2 Activation method**

The sieved palm shell was impregnated with a KOH solution (2 ml of deionized water per gram of the precursor) with an IR of 0.5, 1.5, 2.5 or 3.5 X<sub>K</sub>, where X<sub>K</sub> is the potassium mass per gram of raw material. The prepared solutions were heated and stirred for 2 h at 85 °C, and then heated to their boiling point until completely dried. The impregnated raw material was kept in an oven for 24 h at 110 °C to remove the water. The impregnated palm shell (15 g, dry weight prior to impregnation) was placed inside the quartz reactor, which was then placed inside an ML-3 type sequence microwave reactor produced by Sichuan University (Sichuan Province, China). The microwave power could be varied between 0 and 1400 W.

The resulting ACs were cooled to room temperature and then washed repeatedly with distilled water until a pH of 6-7 was achieved. They were subsequently dried in an oven

at 105 °C for 24 h. The experimental variables were the activation time (5-45 min), microwave power (550-850 W) and IR (0.5-2.5 X<sub>K</sub>). The samples are identified as follows: (C) represents ACs prepared under CO<sub>2</sub> gasification and (N) represents ACs prepared by N<sub>2</sub> gasification. Then the activation time, chemical ratio and microwave power are listed in that order. For example, C-15-1.5-750 denotes an AC prepared under CO<sub>2</sub> gasification using an activation time of 15 min, impregnation ratio of 1.5 and microwave power of 750 W.

### **3.3.3 CO<sub>2</sub> captured measurements**

CO<sub>2</sub> adsorption was used to assess the microporosity in the range (size < 0.7 nm) where N<sub>2</sub> adsorption at -196 °C can be kinetically restricted (Rodri'guez-Reinoso F, Linares-Solano., 1998). The CO<sub>2</sub> adsorption isotherms were measured at 0 °C, 25 and 50 °C using a semi-automatic adsorption apparatus (NOVA-1200, Quantachrome). The micropore parameters were calculated by fitting the Dubinin–Radushkevich equation to the CO<sub>2</sub> adsorption isotherms measured at 0 °C.

## CHAPTER 4: RESULTS AND DISCUSSION

### 4.1 PART 1: Palm shell based activated carbon prepared by zinc chloride chemical activation using response surface methodology

#### 4.1.1 Development of regression model equation and statistical analysis

Central composite design was used to correlate the variables and responses. Both response values obtained from the experiments with complex design matrix are shown in Table 3.2. The six runs at microwave power of 1050 W, activation time of 15 min, impregnation ratio of 1.69 and particle size of 1.5 mm are centre points and were used to determine the experimental error. At this point Design-Expert fits linear, two-factor interaction (2FI), quadratic and cubic polynomials to the responses. This desperation is exhibited in the Fit Summary given by Design-Expert. The program recommends quadratic model due to its superior adjusted R-squared values of 0.9328 compared with adjusted R-squared of 0.2415, 0.3446 and 0.9215 for linear, 2FI and cubic models, respectively and also, higher p-value of 0.1255 for quadratic model in contrast with p-value of 0.0006, 0.0007 and 0.0378 for linear, 2FI and cubic models, respectively. Therefore, the quadratic model was selected for both MB adsorption capacity and carbon yield, as suggested by the software. Regression analysis was performed to fit the response function of yield and MB adsorption capacity. The final empirical models for carbon yield and MB adsorption capacity in terms of coded factors after excluding the insignificant terms are shown in Eqs. (4.1) and (4.2), respectively.

$$\begin{aligned} Y_1 = & 96.14 + 0.16x_1 + 0.22x_2 - 0.094x_3 + 0.19x_4 - 0.024x_1x_2 - 0.23x_1x_3 + \\ & 0.18x_1x_4 - 0.063x_2x_3 + 0.16x_2x_4 - 0.07x_3x_4 - 0.19x_1^2 + 0.11x_2^2 - 0.24x_3^2 - \\ & 0.0082x_4^2 \end{aligned} \quad (4.1)$$



$$\begin{aligned}
Y_1 = & 70.08 - 5.33x_1 - 2.45x_2 + 4.10x_3 + 0.42x_4 - 1.27x_1x_2 - 0.54x_1x_3 + \\
& 1.95x_1x_4 - 1.02x_2x_3 + 2.12x_2x_4 - 0.76x_3x_4 - 3.16x_1^2 - 3.08x_2^2 - 6.19x_3^2 - \\
& 1.28x_4^2
\end{aligned}
\tag{4.2}$$

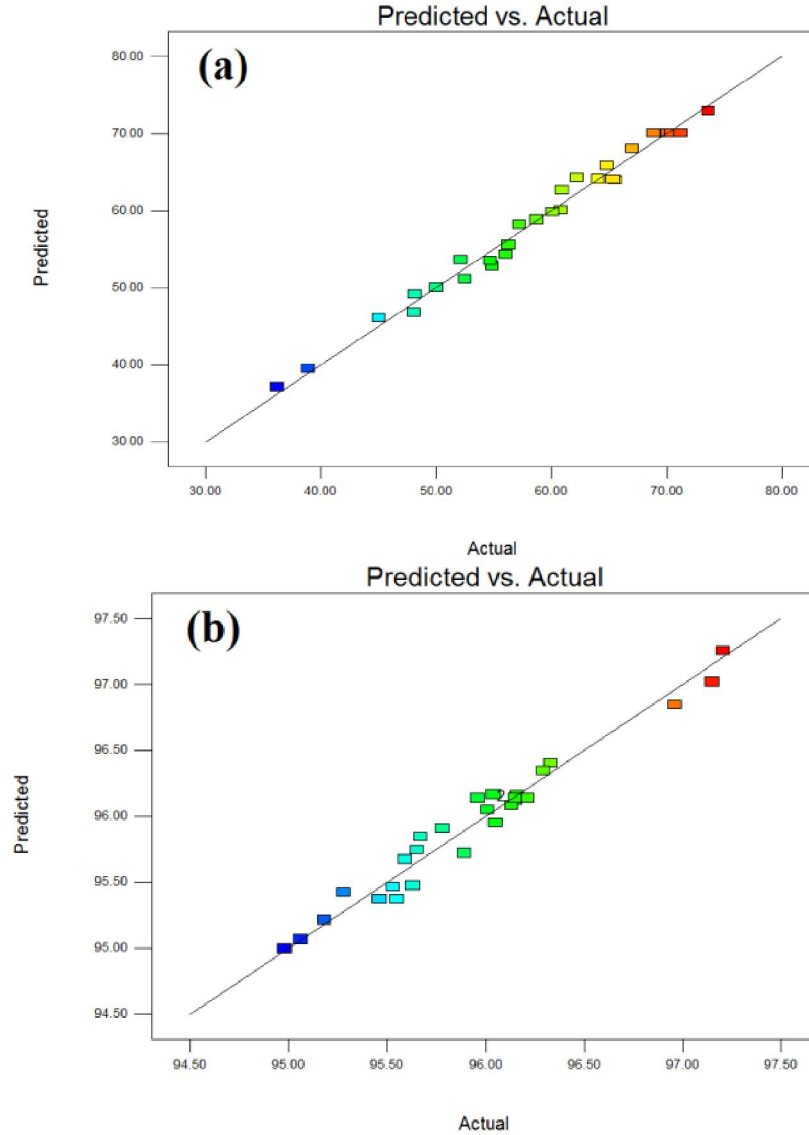


Figure 4.1: Predicted vs. experimental value of (a) AC yield (%) and (b) MB adsorption capacity

Negative signs in front of the terms indicate antagonistic effects, whereas the positive signs indicate synergistic effects. The RSM method includes the multiple regression analysis technique, which was used to determine the coefficient of the responses for the model.

The correlation coefficient is a base to evaluate the development of the quality of the models. Eq. 4.1 and 4.2 were used for the predicted yield and MB adsorption capacity, respectively, in combination with the experimental data, which are given in Fig. 4.1(a) and Fig. 4.1(b). These figures show that the excellent capability of the developed quadratic model to fit the experimental results due to very small distance between the points or point clusters and the diagonal line.

Design Expert software (DOE) was used to evaluate the coefficient of the empirical model (Eq. (3.3)) and to conduct statistical analyses to visualise the effects of the experimental variables on the MB adsorption capacity and yield of prepared ACs. The *F*-test analysis of variance was used to evaluate the statistical significance of the quadratic model equation between microwave power, activation time, impregnation ratio and particle size shown in Table 4.1 and 4.2. The determination coefficients ( $R^2$ ) were shown significant at a confidence level of close to unity (99 and 97% for  $Y_1$  and  $Y_2$ , respectively) indicate that the model predictions of the responses are near the experimental values.

The stability of the models was further justified through analysis of variance (ANOVA). The ANOVA for the quadratic models for AC yield and MB adsorption capacity are listed in Tables 4.1 and 4.2, respectively. The *F*-value and p-value were used to determine the regression coefficients, standard error and significance of each coefficient. The *F*-values of 75.65 for the AC yield ( $Y_1$ ) and 29.91 for MB adsorption ( $Y_2$ ) indicate that the models are significant. If the “p-value” value is less than 0.05, the model terms are significant, whereas a value above 0.1 denotes non-significant model terms. In the case of yield ( $Y_1$ ), the following terms were significant, with a “p-value” of less than 0.05: activation time ( $X_1$ ), microwave power ( $X_2$ ), impregnation ratio ( $X_3$ ), interaction effect between activation time and microwave power ( $X_1X_2$ ), interaction effect between activation time and particle size ( $X_1X_4$ ), interaction effect between

microwave power and particle size ( $X_2X_4$ ), squared effect of activation time ( $X_1^2$ ), squared effect of microwave power ( $X_2^2$ ), squared effect of impregnation ratio ( $X_3^2$ ) and squared effect of particle size ( $X_4^2$ ). Moreover, activation time ( $X_1$ ), microwave power ( $X_2$ ), impregnation ratio ( $X_3$ ), particle size ( $X_4$ ),  $X_1X_3$ ,  $X_1X_4$ ,  $X_2X_4$ ,  $X_1^2$ ,  $X_2^2$ ,  $X_3^2$ ,  $X_4^2$  were significant model terms in the case of MB adsorption capacity ( $Y_2$ ). Thus, the statistical results indicate that these models accurately predict the AC yield and MB adsorption capacity in the range of variables studied.

Table 4.1: Analysis of variance (ANOVA) for response surface quadratic model for AC yield

Source	Sum of Squares	Degree of Freedom	Mean of Square	F-Value	p-value Prob > F	Remarks
Model	2722.063	14	194.4330	75.65987	< 0.0001	significant
$X_1$	681.3553	1	681.3553	265.1363	< 0.0001	significant
$X_2$	144.2414	1	144.2414	56.12874	< 0.0001	significant
$X_3$	403.7927	1	403.7927	157.1281	< 0.0001	significant
$X_4$	4.197557	1	4.197557	1.633398	0.2207	Not significant
$X_1X_2$	25.74801	1	25.74801	10.01934	0.0064	significant
$X_1X_4$	60.98439	1	60.98439	23.7309	0.0002	significant
$X_2X_4$	71.64353	1	71.64353	27.8787	< 0.0001	significant
$X_1^2$	273.4521	1	273.4521	106.4086	< 0.0001	significant
$X_2^2$	259.982	1	259.9820	101.167	< 0.0001	significant
$X_3^2$	1050.521	1	1050.521	408.7899	< 0.0001	significant
$X_4^2$	44.76141	1	44.76141	17.41804	0.0008	significant
Residual	38.54746	15	2.569830	-	-	
Lack of Fit	33.30986	10	3.330986	3.179878	0.1068	Not significant
Pure Error	5.2376	5	1.047520	-	-	
Cor Total	2760.61	29	-	-	-	
R-Squares	0.9860					

Analysis of variance (ANOVA) was used for further justification of the stability of the quadratic models for AC yield and MB adsorption capacity, which are listed in Tables

4.1 and 4.2, respectively. The  $F$ -value and Prob  $> F$ -value were used to determine the regression coefficients, standard error and significance of each coefficient.

Table 4.2: Analysis of variance (ANOVA) for responses surface quadratic model for MB adsorption

Source	Sum of Squares	Degree of Freedom	Mean of Square	$F$ -Value	p-value Prob $> F$	Remarks
Model	8.18292	14	0.584494	29.91632	< 0.0001	significant
$X_1$	0.645176	1	0.645176	33.02221	< 0.0001	significant
$X_2$	1.212751	1	1.212751	62.07255	< 0.0001	significant
$X_3$	0.211876	1	0.211876	10.84451	0.0049	significant
$X_4$	0.872109	1	0.872109	44.63740	< 0.0001	significant
$X_1X_3$	0.816764	1	0.816764	41.80465	< 0.0001	significant
$X_1X_4$	0.509439	1	0.509439	26.07475	0.0001	significant
$X_2X_4$	0.427389	1	0.427389	21.87516	0.0003	significant
$X_1^2$	0.94775	1	0.94775	48.50894	< 0.0001	significant
$X_2^2$	0.319125	1	0.319125	16.33386	0.0011	significant
$X_3^2$	1.5587	1	1.5587	79.77935	< 0.0001	significant
$X_4^2$	0.1827	1	0.1827	9.351185	0.0080	significant
Residual	0.293065	15	0.019538	-	-	
Lack of Fit	0.251065	10	0.025106	2.988864	0.1193	Not significant
Pure Error	0.042	5	0.0084	-	-	
Cor Total	8.475984	29	-	-	-	
R-Squares	0.9654					

#### 4.1.2 Effects of the preparation variables on the AC yield

According to the results in Table 4.1, the activation time ( $X_1$ ), microwave power ( $X_2$ ) and impregnation ratio ( $X_3$ ) had significant effects on the AC yield, whereas the particle size ( $X_4$ ) was ineffective based on its p-value of 0.2207, which is greater than 0.05. Among the significant studied factors, activation time ( $X_1$ ), with the highest  $F$ -value of 256.13, had the greatest effect on the yield ( $Y_1$ ) followed by impregnation ratio ( $X_3$ ) with an  $F$ -value of 157.1281 and microwave power ( $X_2$ ) with an  $F$ -value of 56.13, while particle size ( $X_4$ ) had a much smaller effect ( $F$ -value of 1.63).

Furthermore, the interaction between microwave power and particle size ( $X_2X_4$ ) had a considerable effect on the yield, with the highest  $F$ -value of 27.8787, while  $X_1X_2$  and  $X_1X_4$  had less notable effects.

The quadratic function of activation time and microwave power, with close  $F$ -values (106.41 and 101.17, respectively), had similar effects on AC yield, which were less significant than that of the impregnation ratio ( $X_3^2$ ), with a higher  $F$ -value of 408.7899, which indicates a substantial effect. The quadratic function of particle size had a less noticeable effect than the other studied factors.

Fig. 4.2 a-c show the three-dimensional (3D) plots of the interaction between the effects of the studied variables on AC yield, with the real values for the  $X$ - and  $Y$ -axis. Fig. 4.2(a) displays the combined effect of activation time ( $X_1$ ) and microwave power ( $X_2$ ) on the yield, while Fig. 4.2(b) shows the effect of activation time ( $X_1$ ) and particle size ( $X_4$ ) on the yield and Fig. 4.2(c) demonstrates the effect of impregnation ratio ( $X_3$ ) and microwave power ( $X_2$ ) on the yield.

According to Figures 4.2(a) and 4.2(b), at lower activation times, the yield is not appreciably affected by the increase in the microwave power and impregnation ratio due to insufficient time for the reaction between the agent and carbon (K. Yang et al., 2010) and the lower extent of the carbon-agent reaction (Xin-hui et al., 2011b). At higher activation times, as observed in Fig. 4.2(a), the yields decreased with increasing microwave power because the pores were burnt off and the micropores and mesopores were widened under higher radiation power (Hui Deng et al., 2009; Hui Deng, Zhang, et al., 2010; Hejazifar et al., 2011; W. Li et al., 2008). Additionally, tar and volatile matter were rapidly released from the carbon surface at high microwave power and long activation times, which increased the weight loss of the carbon precursor (Huang et al., 2011).

It is evident from Fig. 4.2(b) that the particle size also has no significant effect on the carbon yield at high activation times, as this figure can depict the results obtained in Table 4.3 for an insignificant effect of particle size with low  $F$ -value of 1.63. The yield decreased as the activation time increased (Fig. 4.2(a) and 4.2(b)), and this reduction is more dramatic at higher microwave powers.

According to Fig. 4.2(c), the highest yield was found at the optimum impregnation ratio within the range studied and the interaction between microwave power and impregnation ratio does not have a strong effect on yield, which as shown in Table 4.3. The yield increased with increasing impregnation ratio to the optimum point of approximately 1.69 (g ZnCl<sub>2</sub>/g palm shell) due to the greater release of volatile products, which intensifies the dehydration and elimination reactions (Adinata et al., 2007). Additional zinc chloride could restrict the formation of tars and any liquids that could block the pore passages of the carbon surface during the activation step, decreasing the yield beyond the optimum point, as observed in Fig. 4.2(c) (Xin-hui et al., 2011b). However, except for the particle size of the raw material, the main parameters have significant effects on the prepared AC yield and the maximum yield corresponds to the lowest activation time and microwave power and the optimum impregnation ratio.

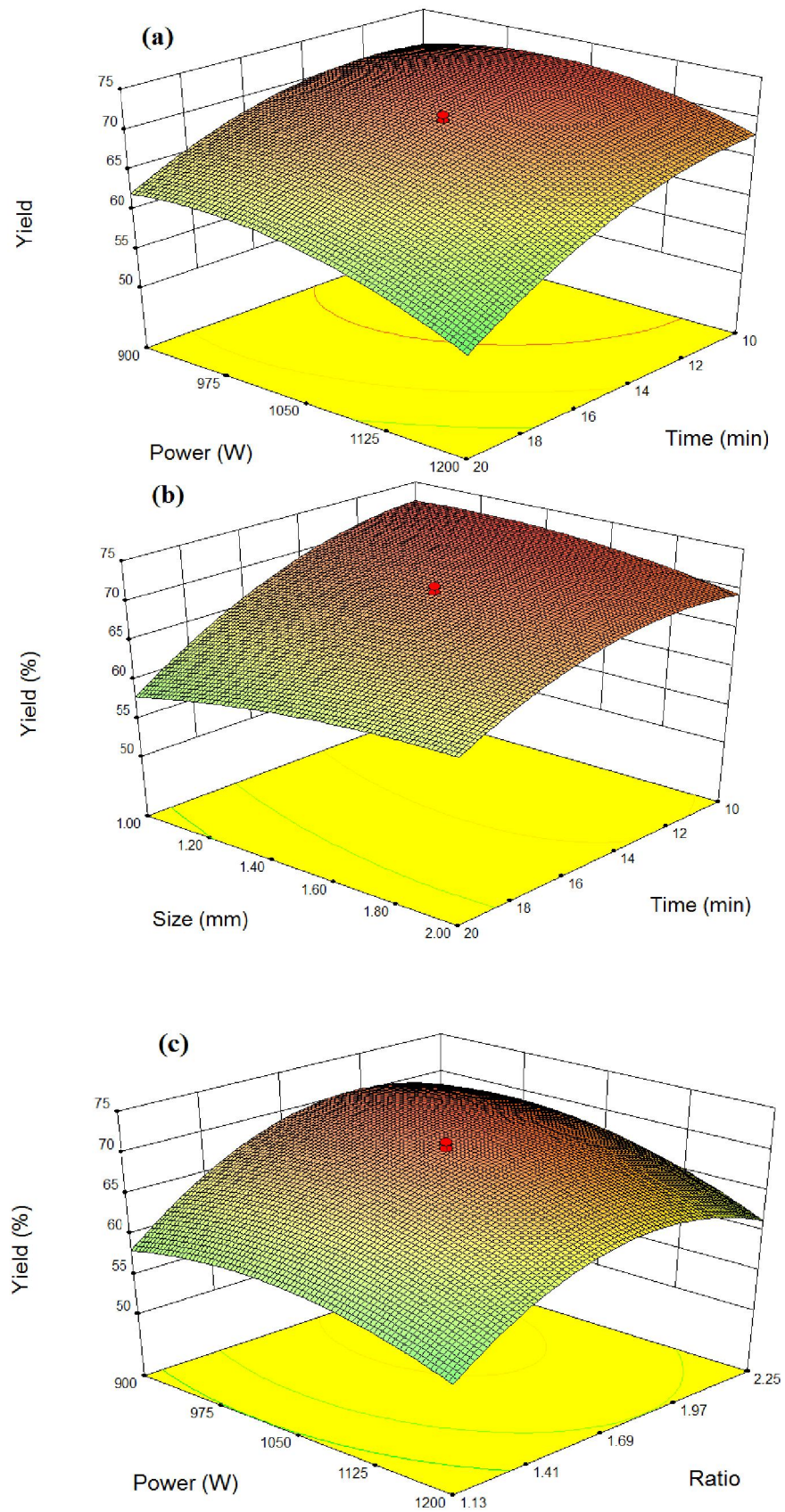


Figure 4.2: The three-dimensional response surfaces (a) the effect of activation time and microwave power (b) the effect of activation time and particle size (c) the effect of impregnation ratio and microwave power on the AC yield

### 4.1.3 Effect of preparation variables on MB adsorption capacity

The results of the MB adsorption experiments on the prepared ACs are shown in Table 4.2. According to data in Table 4.2 and based on the  $F$ -values, all four experimental parameters have considerable effects on the MB adsorption capacity. The interaction effects between  $X_1X_3$ ,  $X_1X_4$  and  $X_2X_4$  are significant, with the interaction between activation time and impregnation ratio having a higher  $F$ -value (41.80), whereas the interaction of particle size with activation time and microwave power (26.07 and 21.88, respectively) have near-zero  $F$ -values. Moreover, the quadratic effects of all four parameters ( $X_1^2$ ,  $X_2^2$ ,  $X_3^2$  and  $X_4^2$ ) were significant. The three-dimensional response surface indicating the effects of the AC preparation parameters (activation time, microwave power, impregnation ratio and particle size) on the MB adsorption capacity ( $Y_2$ ) is shown in Figs. 4.3 (a-c). As observed from Figs. 4.3(a) and 4.3(b), particle size has only a weak effect on MB adsorption capacity for lower activation times and microwave powers, respectively. The MB adsorption increased significantly for larger particle sizes at higher activation times and radiation powers. The optimum adsorption capacity was obtained at the highest particle size for the maximum radiation time and microwave power. However, the adsorption capacity exhibited no considerable changes at higher impregnation ratios with increasing activation time, whereas increasing the activation time at lower impregnation ratios increased the adsorption capacity. This phenomenon is attributed to the pores being blocked by an excess of the chemical agent remaining on the carbon surface at high impregnation ratios, reducing the accessible area for MB adsorption (Foo & Hameed, 2012c). At lower impregnation ratios, the adsorption capacity increases with increasing activation time via the development of porosity and the rudimentary pore structure and the formation of active sites inside the AC (Foo & Hameed, 2012c; W. Li et al., 2008).



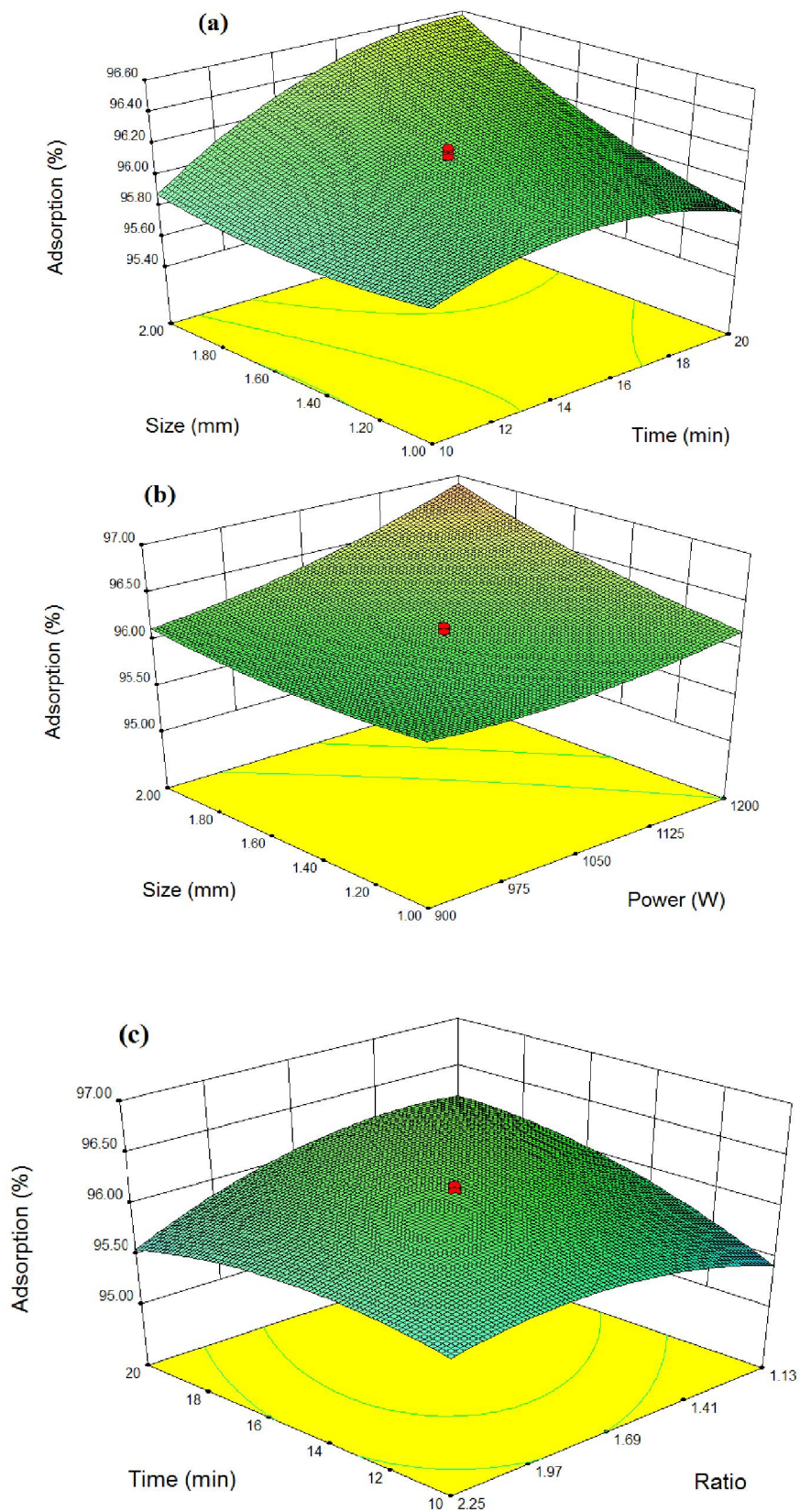


Figure 4.3: The three-dimensional response surfaces (a) the effect of activation time and particle size (b) the effect of microwave power and particle size (c) the effect of impregnation ratio and activation time on the MB adsorption capacity.

#### 4.1.4 Process optimisation

The preparation of AC with relatively high yield and adsorption efficiency is the most important aspect of its potential economic feasibility and marketing. Thus, response surface methodology was used to find the optimum conditions for the preparation of AC with high yield and acceptable adsorption capacity. Design Expert software version 7.1.5 (STAT-EASE Inc., Minneapolis, USA) was used to compromise between yield and adsorption capacity while optimising both of these values by selecting the two highest responses from the experimental results. The optimum calculated conditions were an activation time of 15.17 min, microwave power of 1200 W, ZnCl<sub>2</sub> impregnation ratio of 1.65 and particle size of 2 mm, predicting a carbon yield of 65.484% and an MB adsorption capacity of 96.93%. The AC prepared under the optimised conditions led to a carbon yield of 64% and an MB adsorption capacity of 95.95% (287.85 mg/g).

The relative errors for the carbon yield and MB adsorption capacity between the experimental and predicted values are 2.26% and 1.01%, respectively, which indicates sufficient accuracy of the process optimisation.

Arami-Niya et al.2011, achieved MB adsorption capacity of 78.285 mg/g for palm shell based AC prepared by conventional heating method at optimum operation conditions achieved by RSM method (Arami-Niya, A., Abnisa, F., Shafeeyan, M.S., Wan Daud, W.M.A., & Sahu, J.N, 2012). Oil palm fiber based AC prepared under optimum conditions attained by RSM method with physiochemical activation and conventional method presented MB adsorption capacity of 203.83 mg/g (Hameed, Tan, & Ahmad, 2008). Therefore, prepared AC from palm shell by using microwave method with zinc chloride chemical activation in this study has higher MB adsorption capacity of 287.85 mg/g compared with palm shell based AC prepared by conventional methods (78.285 mg/g) and physiochemical activation with conventional method (203.83 mg/g).

#### 4.1.5 Characterization of the AC prepared under the optimised conditions

Fig. 4.4 (a) shows the SEM images of raw palm shell, which features very small pores on the surface. The SEM image of the AC prepared under the optimum conditions (activation time of 15.00 min, microwave power of 1200 W, zinc chloride impregnation ratio of 1.65 and particle size of 2 mm) is shown in Fig. 4.4(b). As seen in this figure, the number of pores has increased significantly during the activation process, resulting in more pores available for MB adsorption.

The proximate and ultimate analyses of the oil palm shell and AC prepared under the optimum conditions are given in Table 4.3. As seen in this table, the amount of fixed carbon was greater in AC (52.1%) than in the raw material due to the release of volatile contents during the activation step, as proven by the (55.8%) decrease in volatile content in the AC sample.

Table 4.3: Proximate and ultimate analysis of oil palm shell and prepared AC under optimum conditions.

Sample	Proximate analysis (%)				Ultimate analysis (%)			
	Moisture	Volatile	Fixed carbon	Ash	C	H	N	O
Palm shell	4.7	73.5	13.2	8.6	52.05	5.37	0.49	42.10
AC	7.9	17.7	65.3	9.1	81.30	1.30	1.10	16.10

The N<sub>2</sub> adsorption isotherm of the AC prepared under the optimum conditions, shown in Fig. 4.5, is a type I isotherm based on the IUPAC classification of isotherms. Therefore, the adsorption occurred mainly in the microporous structure according to the pore-filling mechanism. In low-pressure regions ( $P/P_0 < 0.2$ ), the main increase in nitrogen adsorption occurred in the micropores. However, for higher relative pressures ( $P/P_0 > 0.2$ ), the nitrogen adsorption increased gradually, indicating a higher volume of wide micropores and the presence of small mesopores.

The pore size distribution of the AC prepared under the optimum conditions is shown in Fig. 4.6. As seen in this figure, the sample mostly contains pores between 1 and 4 nm.

Indeed, it has been estimated that the minimum pore diameter that MB can enter is 1.3 nm (Stuart S, 1987). Therefore, the high micropore volume could be the cause of the high MB adsorption. The BET surface area evaluated using nitrogen adsorption isotherms for the optimally prepared sample is 1253.5 m<sup>2</sup>/g with a pore volume of 0.83 cm<sup>3</sup>/g. The micropore volume contributed strongly (approximately 56%) to the total pore volume, and the average pore width was 2.65 nm.

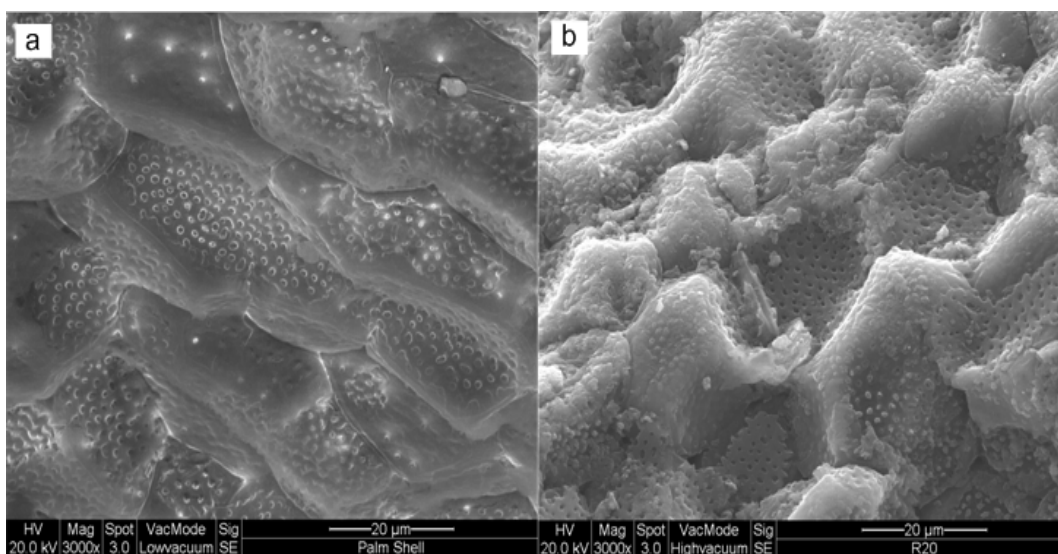


Figure 4.4: (a) SEM image of the raw palm shell. (b) SEM image of the prepared AC under optimum conditions.

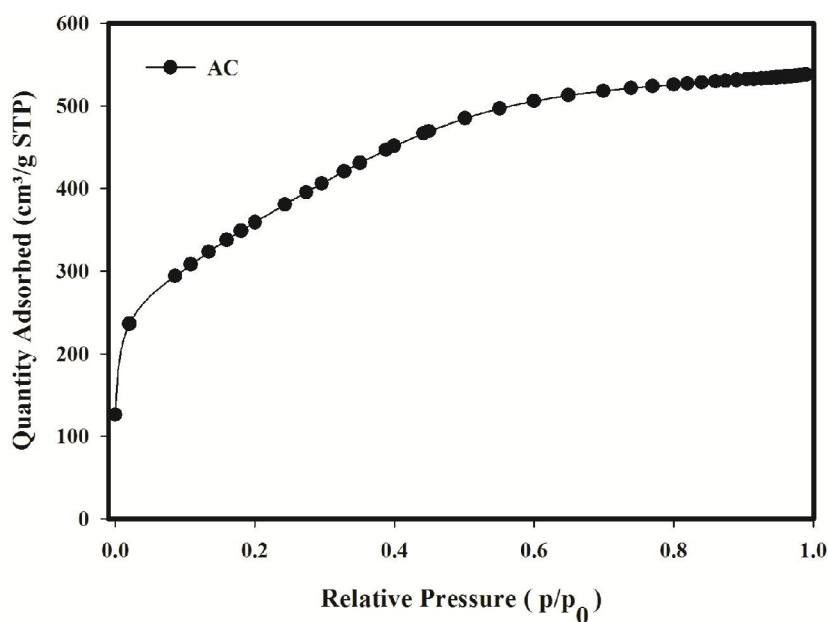


Figure 4.5: Nitrogen adsorption isotherm of prepared AC under optimum conditions

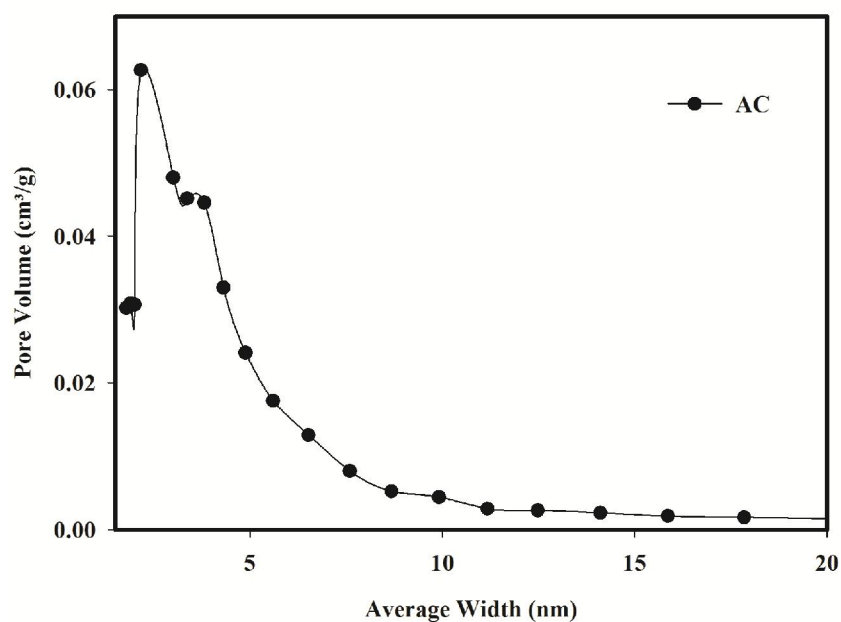


Figure 4.6: Pore width vs. pore volume of prepared AC under optimum conditions.

Fourier-transform infrared (FTIR) transmission spectra were obtained to characterise the surface groups on palm shell and AC prepared under optimum conditions. Fig. 4.7 shows the FTIR spectra of these two samples. Some peaks were absent or lower in intensity in the prepared AC relative to the palm shell sample. The peak at approximately  $3346\text{ cm}^{-1}$ , which is attributed to hydroxyl functional groups including hydrogen bonding [O–H stretching], was much lower in the prepared AC. The reduction of hydrogen bonding shows that the zinc chloride acts as a dehydrating agent, and the reaction between the chemical agent and raw materials begins as soon as both substances are mixed (Jagtoyen & Derbyshire, 1998; Suárez-García, Martínez-Alonso, & Tascón, 2002). The band at approximately  $2910\text{ cm}^{-1}$ , which is assigned to asymmetric and symmetric C–H stretching, was lower in AC, indicating that activation removed a large amount of hydrogen. The reduction of H and O contents observed by FTIR spectroscopy is in good agreement with ultimate analysis results, wherein the hydrogen and oxygen contents decreased to 75.8 and 61.75%, respectively.

The band at approximately  $1670\text{ cm}^{-1}$ , which is most likely due to the C=O stretching vibration of carbonyl groups (Sabio et al., 2004), disappeared in the prepared AC, indicating that chemical activation broke many aliphatic and aromatic bonds and eliminated much of the volatile matter (E.P. Barrett, 1951; Yagmur et al., 2008). As seen from Table 4.4, the volatile matter content decreased by 76%. A significant reduction was observed for a series of complex bands in the range of  $1000\text{--}1260\text{ cm}^{-1}$  in the prepared AC, which includes C-O in carboxylic acids, alcohols, phenols and esters (Hui Deng, Zhang, et al., 2010).

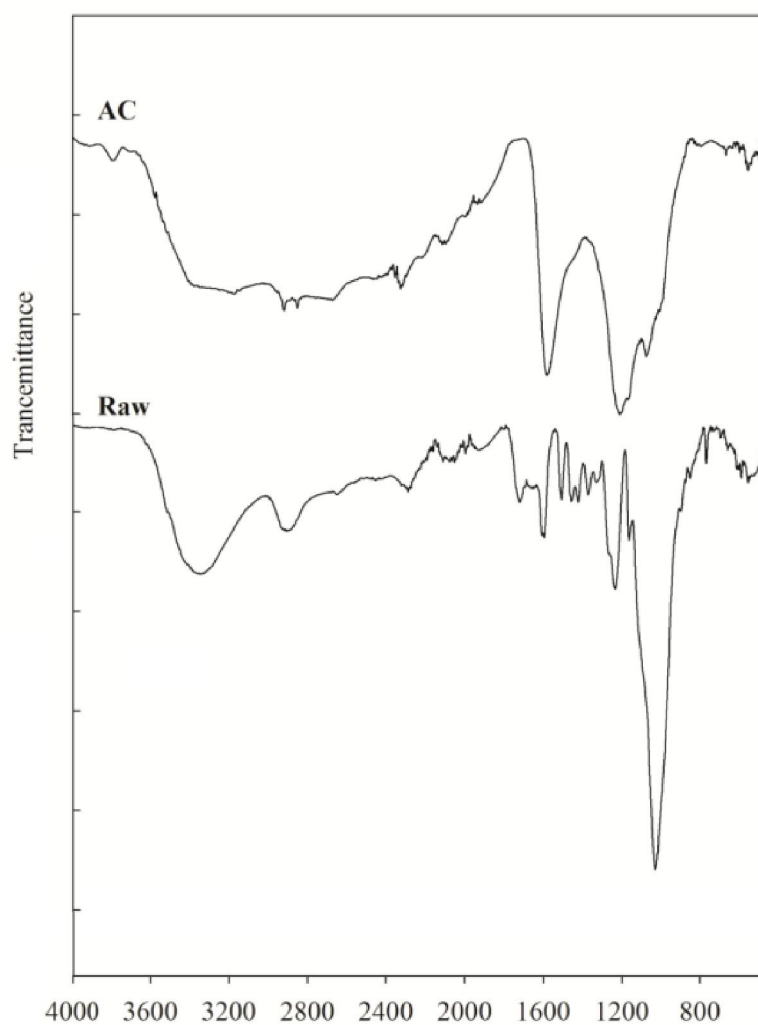


Figure 4.7: Fourier transforms infrared spectra of raw palm shell and prepared AC under optimum conditions.

## **4.2 PART 2: Comparison of oil palm shell-based ACs produced by microwave and conventional heating methods using zinc chloride activation**

### **4.2.1 Surface textural properties**

The impregnation ratio is one factor that affects the pore development in AC because the raw materials are not heated well by microwave irradiation in the absence of an activation agent (T. Wang et al., 2009). The N<sub>2</sub> adsorption isotherms of the ACs produced by microwave and conventional heating methods at different impregnation ratios are shown in Figs. 4.8 and 4.9, respectively. According to the IUPAC classification, all isotherms exhibit type I behaviour, with a sharp “knee” form at low relative pressures that tends to turn into an almost horizontal plateau at higher relative pressures, indicating microporous AC. In *MW0.15*, the nitrogen adsorption increased until a relative pressure of approximately 0.1, and then became constant with further increase in the relative pressure, indicating that the AC is only microporous.

By increasing the agent ratio up to *Zn0.53*, the isotherms did not show a significant change in the nitrogen uptake at relative pressures greater than 0.1, whereas the adsorption capacity increased to some extent at  $P/P_0 \leq 0.1$ .

This can be explained by the pyrolysis of the palm shell, which was initialized by the heat carrying properties of ZnCl<sub>2</sub>, and promoted the development of new pores (T. Wang et al., 2009). Therefore, an increase in the ratio of ZnCl<sub>2</sub> was effective in the creation and development of porosity in the AC produced. Augmenting the ratio of zinc chloride could strengthen the activation process and result in the formation of more active sites (W. Li et al., 2008). As shown in Fig. 4.8, by increasing the ratio from *MW0.53* to *MW0.65*, the nitrogen uptake increased at relative pressures  $\leq 0.1$  and also gradually increased at relative pressures  $\geq 0.1$ .

In this case, the greater amount of nitrogen adsorption at low relative pressures of 0.1 indicates the creation of a large amount of new micropores. The development of larger micropores and the formation of mesopores is the cause of the increase in nitrogen uptake at higher relative pressures. Increasing the chemical also inhibits tars and any other liquids from entering the pores, which can clog the pores of the AC. Moreover, the existing micropores can be penetrated and occupied by the extra zinc chloride, which helped promote the following pore-opening and widening processes in the existing pores (Q. S. Liu et al., 2010). A further increase to *MW0.78* showed a gradual decrease in nitrogen uptake by the micropores and mesopores compared with *MW0.65*. The reduction in nitrogen adsorption can be attributed to the burning and widening of the existing pores (W. Li et al., 2008). The pores could also be blocked by an excess of zinc chloride, which causes a decrease in the accessible area for nitrogen adsorption (Hoseinzadeh Hesas, Wan Daud, et al., 2013). *MW0.90* showed a decrease in nitrogen uptake at low relative pressures relative to *MW0.78* and *MW0.65*. The  $N_2$  adsorption of *MW0.9* is higher than that of the other samples at relative pressures greater than  $P/P_0=0.6$  due to the destruction of existing microporous structure in favor of the new mesopores. Figure 4.9 illustrates the nitrogen adsorption isotherms of the ACs prepared by the conventional method.

The shapes of the isotherms for the samples prepared with impregnation ratios of 0.15 to 0.53 are similar to that of the microwave samples, but the nitrogen uptake values are higher in the case of the conventional samples. It was demonstrated that, conventionally prepared ACs contain greater amounts of micropores compared to the microwave samples. By increasing the impregnation ratio up to *C0.65*, the nitrogen uptake reached the maximum amount of adsorption. Similar to the microwave prepared samples, agent ratios beyond *C0.65* for the conventional method resulted in a reduction in the nitrogen adsorption capacity for similar reasons.



It can be concluded that the impregnation ratio shows approximately the same effect on the pores development process in AC prepared by both heating methods, where the samples with lower impregnation ratios were mainly microporous and mesopores occurred at higher ratios.

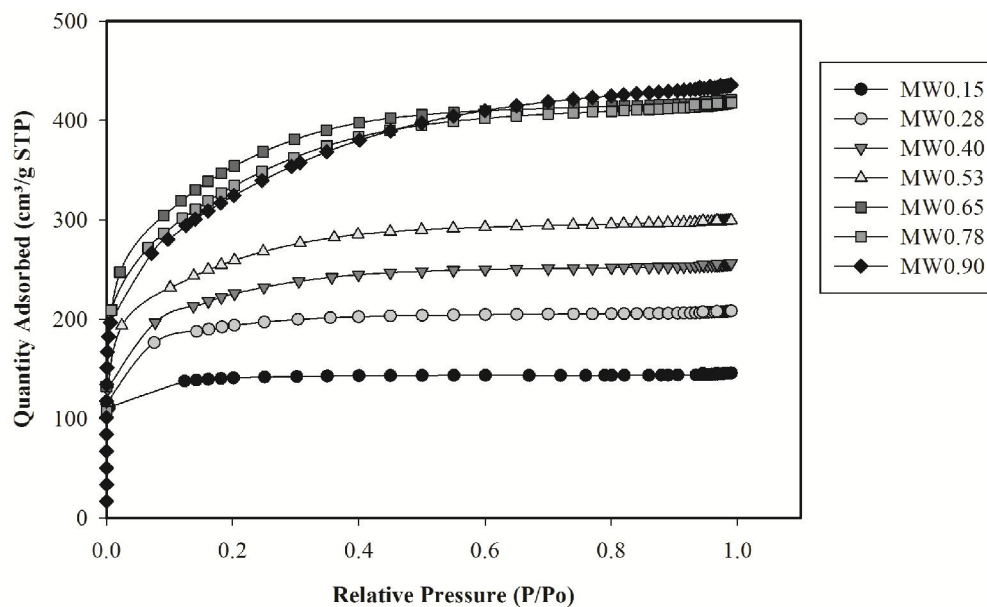


Figure 4.8: Nitrogen adsorption isotherms of ACs by microwave heating.

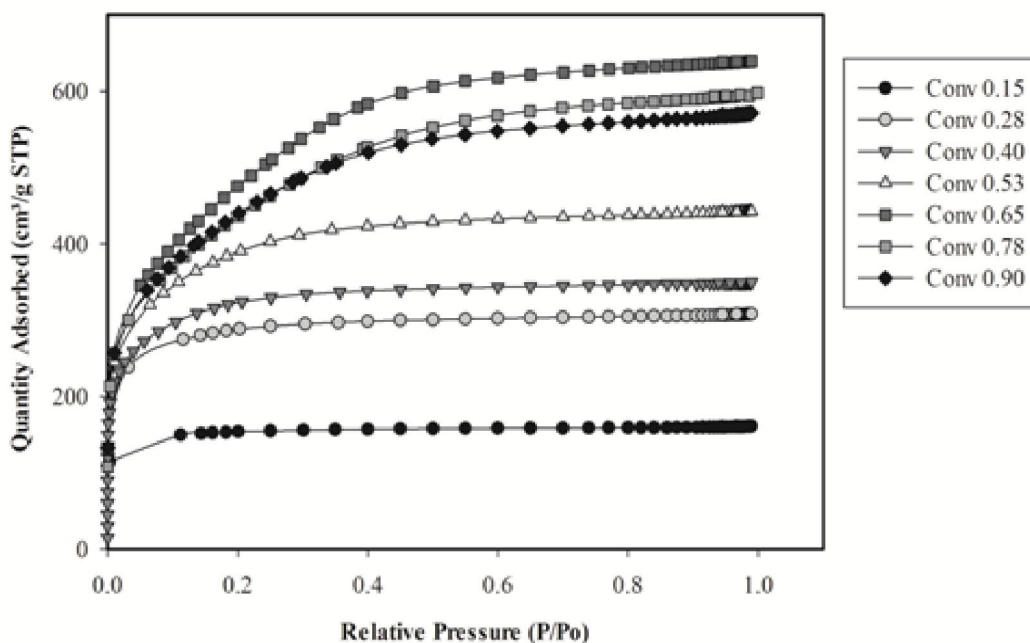


Figure 4.9: Nitrogen adsorption isotherms of ACs by conventional heating.

The specific surface area ( $S_{BET}$ ), total pore volume ( $V_{tot}$ ), micropore volume ( $V_{micro}$ ) and average pore size of the ACs prepared by microwave and conventional heating methods

are summarized in Table 4.4. By increasing the chemical ratio from *MW0.15* to *MW0.65*, the  $S_{\text{BET}}$  and  $V_{\text{micro}}$  of the prepared ACs increased gradually to 1195 ( $\text{m}^2/\text{g}$ ) and 0.63 ( $\text{cm}^3/\text{g}$ ), respectively, and then decreased with further increase to *MW0.9*. The creation of micropores and mesopores leads to an increase in  $S_{\text{BET}}$ , whereas the widening and burning of the pores and the blocking of pores by an excess of the agent on the surface of the AC can lead to a reduction in the accessible area, thus resulting in a decrease in  $S_{\text{BET}}$  (W. Li et al., 2008).

In the microwave samples  $V_{\text{tot}}$  increased gradually with increasing impregnation ratio up to *MW0.9*, despite the reduction in  $S_{\text{BET}}$  and  $V_{\text{micro}}$ . It can be concluded that the reduction is occurring only at higher impregnation ratios. Also, the microwave samples do reach their maximum level at *MW0.65* (Table 4.4). On the other hand, the trends of total and micropore volumes in Table 4.4 show obviously that some of the micropores have been destroyed and merged into larger pores (mesopores) at higher agent ratios. These results are in good agreement with the shape of the  $\text{N}_2$  isotherm of the microwave samples in Fig. 4.8, where the nitrogen adsorption increased at higher relative pressures  $\geq 0.1$  with augmenting the impregnation ratio until *MW0.9*. The average pore size of the microwave samples also increased continuously with increasing impregnation ratio, which may be attributed to the formation of wider pores. These results are in good agreement with the creation of more mesopores with increasing impregnation ratio. In conventional samples, the  $S_{\text{BET}}$ ,  $V_{\text{micro}}$  and  $V_{\text{tot}}$  increased up to 1672 ( $\text{m}^2/\text{g}$ ), 0.87 ( $\text{cm}^3/\text{g}$ ) and 0.99 ( $\text{cm}^3/\text{g}$ ), respectively, for *C0.65* and then decreased with further increases in the impregnation ratio. These trends are caused by the same reasons explained for the microwave samples.

However, the  $V_{\text{tot}}$  of the conventionally prepared ACs increased gradually up to 0.99 ( $\text{cm}^3/\text{g}$ ) at *C0.65* and then decreased continuously with further increase of the impregnation ratio.

This phenomenon could be explained as the conventional samples attaining the maximum level of micropores at the ratios up to 0.65 (Table 4.4). On the other hand, the total pore volume ( $V_{\text{tot}}$ ) reduction is indicative of a pore blockage or a structure collapse by further chemical ratio, thus resulting in a smaller internal volume (Foo & Hameed, 2012a).

As a comparison between the textural properties of the microwave and conventional samples, *MW0.9* has an average pore size of 2.43 nm, which is approximately the same as the 2.44 nm for *C0.9*, while having a much lower  $S_{\text{BET}}$  of 1079 ( $\text{m}^2/\text{g}$ ) for *MW0.9* than 1497 ( $\text{m}^2/\text{g}$ ) for *C0.9*. This phenomenon can be explained by the microwave irradiation method promoting higher concentrations of mesopores than the conventional method. This result is in good agreement with Kubota, et al (Kubota et al., 2009), where they prepared a phenolic resin based AC by both microwave and conventional methods by KOH chemical activation. They explained that due to the rapid and volumetric heating in microwave activation in contrast to slow conventional heating, volatile matter was able to released faster from the surface of the AC, resulting in a greater portion of mesoporosity in the microwave samples. Liu et al (Q. S. Liu et al., 2010), also showed that the microwave method produced AC with a slightly higher portion of mesopores than the conventional method and explained this occurrence as a more intense activation reaction under microwave radiation.

Table 4.4: Surface characteristics of AC prepared by microwave and conventional methods

Sample ID	$S_{BET}$ ( $m^2/g$ )	$V_{micro}$ ( $cm^3/g$ )	$V_{tot}$ ( $cm^3/g$ )	Average pore size (nm)
<i>MW</i> 0.15	443	0.22	0.23	2.04
<i>MW</i> 0.28	622	0.32	0.32	2.06
<i>MW</i> 0.40	738	0.38	0.39	2.14
<i>MW</i> 0.53	860	0.45	0.46	2.15
<i>MW</i> 0.65	1195	0.63	0.65	2.17
<i>MW</i> 0.78	1137	0.59	0.68	2.26
<i>MW</i> 0.90	1079	0.58	0.70	2.43
<i>C</i> 0.15	484	0.25	0.25	2.05
<i>C</i> 0.28	927	0.47	0.48	2.05
<i>C</i> 0.40	1078	0.54	0.54	2.06
<i>C</i> 0.53	1308	0.67	0.68	2.09
<i>C</i> 0.65	1672	0.87	0.99	2.36
<i>C</i> 0.78	1504	0.78	0.92	2.35
<i>C</i> 0.90	1497	0.77	0.88	2.44

The variations in  $V_{tot}$  and  $V_{micro}$  with the chemical ratio for both heating methods are shown in Fig. 4.10. According to this figure, the trends in the micropore development based on the chemical ratio are similar for both methods.

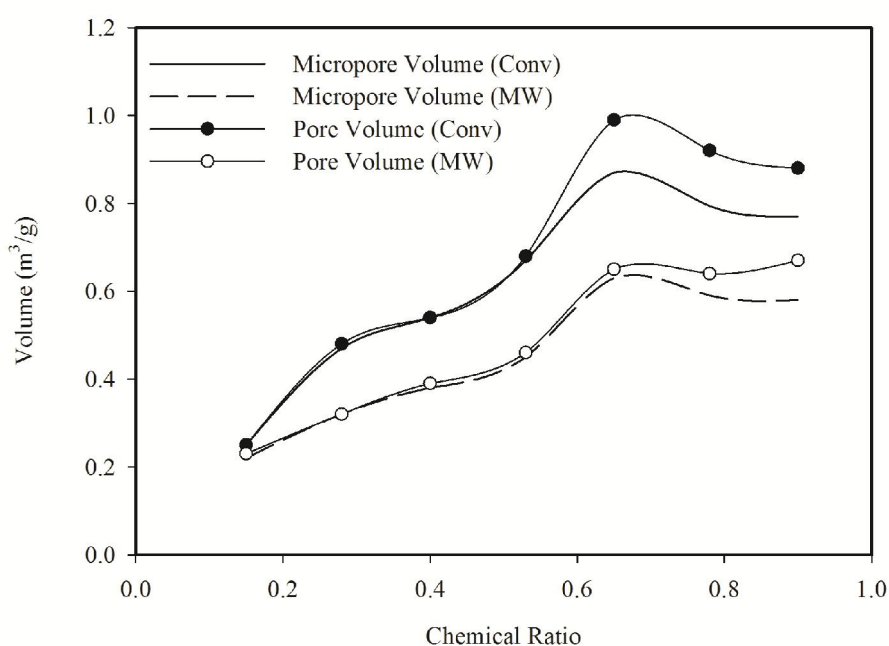


Figure 4.10: Variation of the total pore volume and micropore volume of ACs prepared by microwave and conventional heating methods.

However, the slope of the micropore development is much higher with the conventional heating method, which indicates that the conventional method more greatly promotes the development of micropores in comparison to the microwave method. This phenomenon supports the higher nitrogen adsorption in the conventional samples relative to the microwave samples.

Beyond Zn0.65, the slope of the micropore reduction in the microwave samples is lower than in the conventional samples. This can be explained that despite the widening of some micropores towards the development of mesopores with increasing impregnation ratio, new micropores were developed in the microwave samples even at higher ratios. Moreover, as shown in Fig. 4.10, in the microwave samples, the creation of mesopores (the pore volume graph is away from micropore graph) started at approximately Zn0.65 and Zn0.53 for the microwave and conventional samples, respectively.

#### **4.2.2 Pore size distribution**

The structural heterogeneity and solid internal structure can be represented by characterization of the pore size distribution (PSD) (A. Arami-Niya et al., 2010). The PSD of both the microwave and conventional samples are shown in Figs. 4.11 and 4.12, respectively. It appeared from these figures that the ratio of zinc chloride has significant effects on the pore structure of the AC prepared by both heating methods. By increasing the impregnation ratio, the microwave samples illustrated sharp peaks in the range of micropores. The ACs produced with lower ratios of Zn0.15 and Zn0.28 in the microwave samples were homogeneous microporous AC. As shown in Fig. 4.11, with a further increase in the chemical ratio, the ACs became more heterogeneous due to the opening of micropores and the creation of mesopores. The creation of wide micropores and mesopores, was enhanced by augmenting the chemical ratio up to Zn0.9, which is in good agreement with the increase in  $V_{tot}$  according to the data in Table 4.4 for the microwave samples.

The conventionally produced ACs also demonstrated a relatively broad peak in the microporous range with higher chemical ratios due to reactions at the active sites causing the creation of more pores. The conventional samples showed a similar trend of changing homogeneous to heterogeneous structures, which occurred with increasing chemical ratio in the microwave samples.

As shown in Fig. 4.12, a significant difference in the presence of wide pores started with C0.53, which is in good agreement with Fig. 4.10, where the total pore volume graph began to separate from the micropore graph at Zn0.53. According to the Table 4.4, the average pore size increased by approximately 0.9 nm from C0.78 to C0.9, while in the case of the microwave samples, MW0.9 showed a 17 nm difference from MW0.78, which is approximately double the increase of the conventional samples.

This can be explained by the entire volume of the sample having the same rate of heating with microwave irradiation, which can speed up the diffusion rate of the volatile matter and enhance its rate of release from the surface of the AC, thus resulting in the proliferation fraction of mesopores with the microwave method (Hui Deng, Zhang, et al., 2010). It is also notable that MW0.15 and C0.15 show approximately the same textural properties. This implies that at low chemical ratios, the quick and volumetric heating with the microwave method compared to the slow heating of the conventional method promotes the development of pores in a shorter time, which saves energy (Kubota et al., 2009).

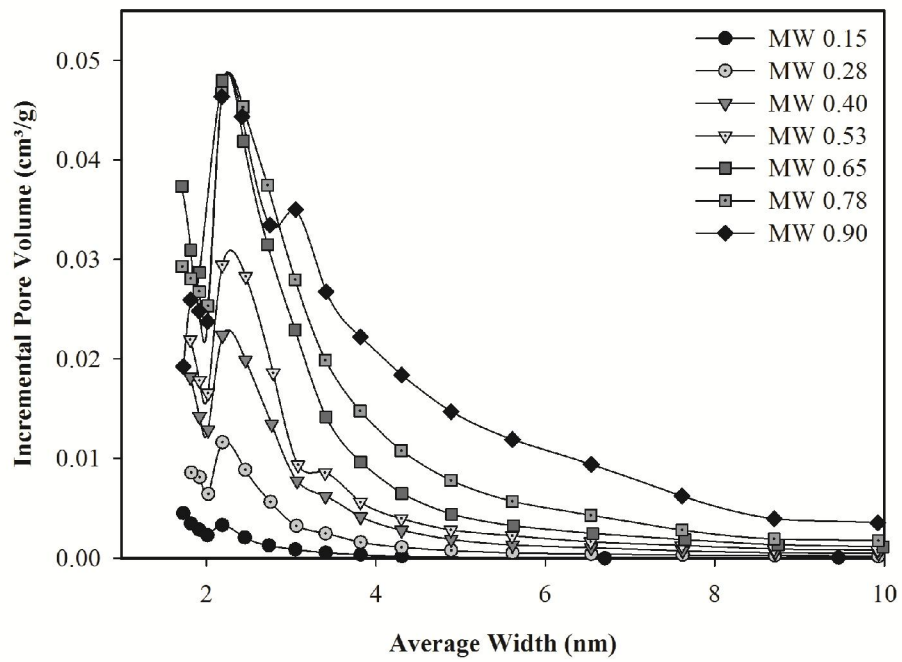


Figure 4.11: Pore size distribution of ACs prepared by microwave heating.

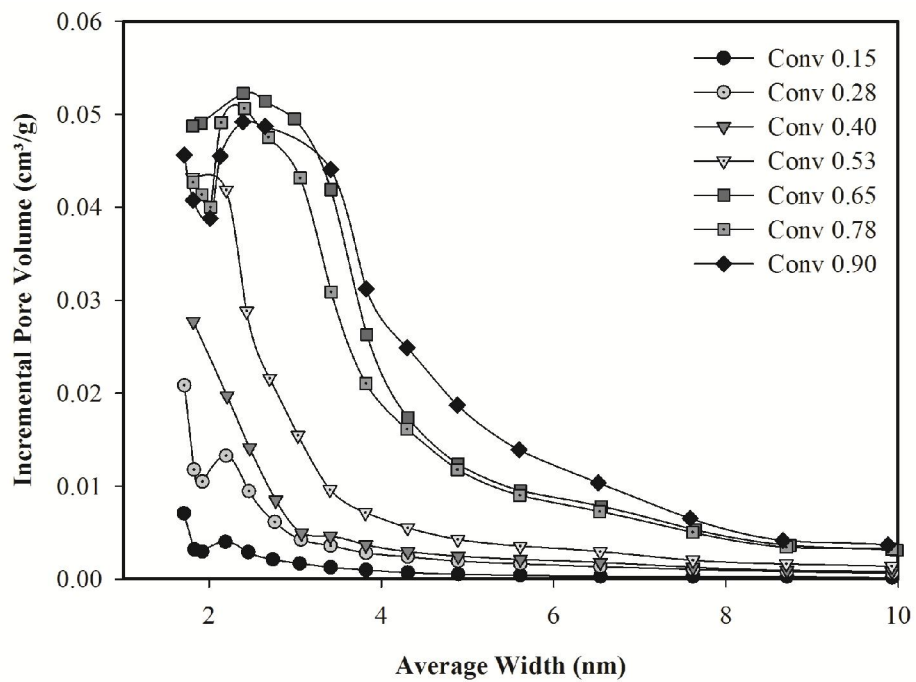


Figure 4.12: Pore size distribution of ACs prepared by conventional heating.

### 4.2.3 Proximate and ultimate analysis

Palm shell is a good precursor for the production of AC due to its high fixed carbon and volatile contents and low ash content. Table 4.5 shows the proximate and ultimate analysis results for raw palm shell and the ACs prepared with the highest surface area (Zn0.65) by the microwave and conventional methods.

It was observed that the volatile content (such as H<sub>2</sub>, CO, CO<sub>2</sub> and CH<sub>4</sub>) decreased from 74.3% in palm shell to 46.37% for *MW0.65* and 24.30% for *C0.65*, while the fixed carbon content increased from 13.8% in the palm shell to 36.64% and 53.08% for *MW0.65* and *C0.65*, respectively.

In this experiment, zinc chloride acted as a dehydration agent during the activation process, which hinders the formation of tars and other liquids that can clog pores in the sample. Therefore, volatile matter could easily pass through the pores (Hui Deng et al., 2009). According to the data in Table 4.5, *MW0.65* showed a considerable amount of fixed carbon and volatile reduction compared with higher reduction in conventional sample (*C0.65*), despite its much lower activation time of 15 min compared with 120 min with the conventional method.

This behaviour is due to the different type of heating. In the microwave heating method, the microwave energy is easily transformed into heat inside the particles by dipole rotations and ionic conduction, and creates a temperature gradient from the internal to the external portions of the samples (X. Wang et al., 2011). As a result, the interior part of the AC can be heated more violently, which facilitates the partial decomposition of volatiles compounds during the activation process (Foo & Hameed, 2011b; Huang et al., 2011). Consequently, the release of tar and volatile matter could be sped up relative to conventional heating.

The ultimate analysis results illustrate that the oxygen content decreased from 35.6% for palm shell to 17.9% and 12.33% for *MW0.65* and *C0.65*, respectively, whereas the carbon content increased from 54.7% for palm shell to 80.06% for *MW0.65* and 86.5% for *C0.65*. Therefore, the C/O ratio of 1.53 for palm shell increased to 4.47 for *MW0.65* and 7.01 for *C0.65*. The organic substances could be degraded into volatile gases and liquid tar due to pyrolysis processes at high temperature, leaving the resulting sample with higher carbon content in the ACs.



The higher carbon content indicates that the aromatic structure becomes dominant after degradation in the presence of zinc chloride (Maldhure & Ekhe, 2011).

The notable decrease in oxygen content suggests that the oxygen functional groups, which are located around the edges of the carbon layer, have a low thermal stability and can be removed during treatment (Valente Nabais et al., 2004). The hydrogen percentage decreased from 7.49% for palm shell to 1.52% for MW0.65 and 0.76% for C0.65 due to the rupturing of molecular chains at high temperatures (Maldhure & Ekhe, 2011). The nitrogen content also decreased by 74.38% and 79.8% of initial amount in palm shell in MW0.65 and C0.65, respectively, compared with palm shell. This finding shows that the microwave and conventional treatments at Zn0.65 favoured the elimination of nitrogenous compounds.

Table 4.5: Proximate and elemental analysis of raw material and ACs prepared under optimum impregnation ratio

Material	Moisture (%)	Volatile (%)	Fixed Carbon (%)	Ash (%)	C (%)	H (%)	N (%)	O (%)
Palm Shell	4.70	74.30	13.80	7.20	54.79	7.50	2.03	35.68
MW0.65	5.14	46.37	36.64	11.85	80.06	1.52	0.52	17.90
C0.65	5.98	24.30	53.08	16.64	86.50	0.76	0.41	12.33

#### 4.2.4 FTIR analysis

The surface functional groups (FG) of the AC are mainly affected by the type of raw material, types of heat treatment, activation process and post chemical treatment (Izquierdo et al., 2001; Szymański et al., 2002). Oxygen, Nitrogen, Halogen, Hydrogen, etc. are the main types of atoms on the surface of porous carbons, and these can have significant effects on the surface properties, applications as adsorbents and ion exchange by bonding the edge of the carbon layers (Budinova et al., 2006; El-Sayed & Bandoz, 2004).

Fig. 4.13 illustrates the FTIR spectra of the palm shell and Figs. 4.14(a) and 4.14(b) show the FTIR spectra of the microwave and conventional samples, respectively.

In Table 4.6, the wave numbers and assignments of the main bands observed in Figs. 4.13, 4.14(a) and 4.14(b) are summarized. As shown in Table 4.6, the peak at  $3346\text{ cm}^{-1}$  in palm shell is assigned to an O–H stretching vibration that disappears in both the microwave and conventional samples. The band at approximately  $2910\text{ cm}^{-1}$ , which is assigned to asymmetric and symmetric C–H stretching (Abnisa et al., 2013a), disappeared in the microwave samples and was reduced in the conventional samples.

The decrease in hydrogen bonding in the prepared ACs is due to the action of the zinc chloride as a dehydrating agent (Jagtøyen & Derbyshire, 1998; Suárez-García et al., 2002). The disappearance and reduction of the above mentioned bands indicates that activation removed a large amount of hydrogen and a significant amount of oxygen.

The reduction of H and O content is in good agreement with the ultimate analysis results, where in *MW0.65* the hydrogen and oxygen contents decreased to 79.62% and 49.72%, of initial amount respectively, compared with palm shell. *C0.65* showed 89.85% and 65.36% reductions in H and O contents compared with initial amount in palm shell, respectively.

The stretching absorption band at  $1710\text{ cm}^{-1}$  observed for the palm shell is associated with aldehydes and ketones (C=O) (Abnisa et al., 2013b). This band disappeared in all samples, indicating that the heat treatment removed the more weakly bound substituent's, whereas a small part of the oxygen consisting of basic natured heteroatoms (substantially nitrogen) remain within the aromatic structure of the carbon layer. Moreover, re-oxidation occurred when the samples were removed from the microwave or furnace and pyrone groups were generated on the carbon layer planes, resulting in a decrease in the oxygen content and producing highly basic samples

(Valente Nabais et al., 2004). An intense peak for a series band in the range of 1000-1260  $\text{cm}^{-1}$  for the raw palm shell, which includes carboxylic acids, alcohols, phenols and esters, showed a significant reduction in the ACs prepared by both methods.

The FTIR spectra of the ACs produced by both heating treatments showed the creation of some new peaks that were not present in the FTIR spectra of the palm shell. The peaks at 2100-2250  $\text{cm}^{-1}$  are assigned to  $\text{C}\equiv\text{C}$  stretching and appeared in the microwave treated AC at ratios of 0.15 to 0.53, but are not observed in higher ratios, whereas the  $\text{C}\equiv\text{C}$  stretching is only observed in C0.15. It can be concluded that the amount of carbon on the surface increased more by the microwave treatment than with the thermal method at lower chemical ratios (Foo & Hameed, 2011b; Ji et al., 2007). The stretching absorption band at 1550-1650  $\text{cm}^{-1}$ , which is associated with the aromatic  $\text{C}=\text{C}$  stretching, is observed in the ACs prepared by both heating methods, and may be due to an increase in the carbon content in the ACs relative to the raw material.

The appearance of the adsorption bands between 500 and 850  $\text{cm}^{-1}$  in the ACs produced by both methods corresponds to the vibration of aromatic substitution by aliphatic groups. The aromatic vibration peaks were also observed by Huang et al. (Huang et al., 2011), where they used both microwave and conventional methods to produce AC from lotus stalk by using phosphoric acid as a chemical agent.

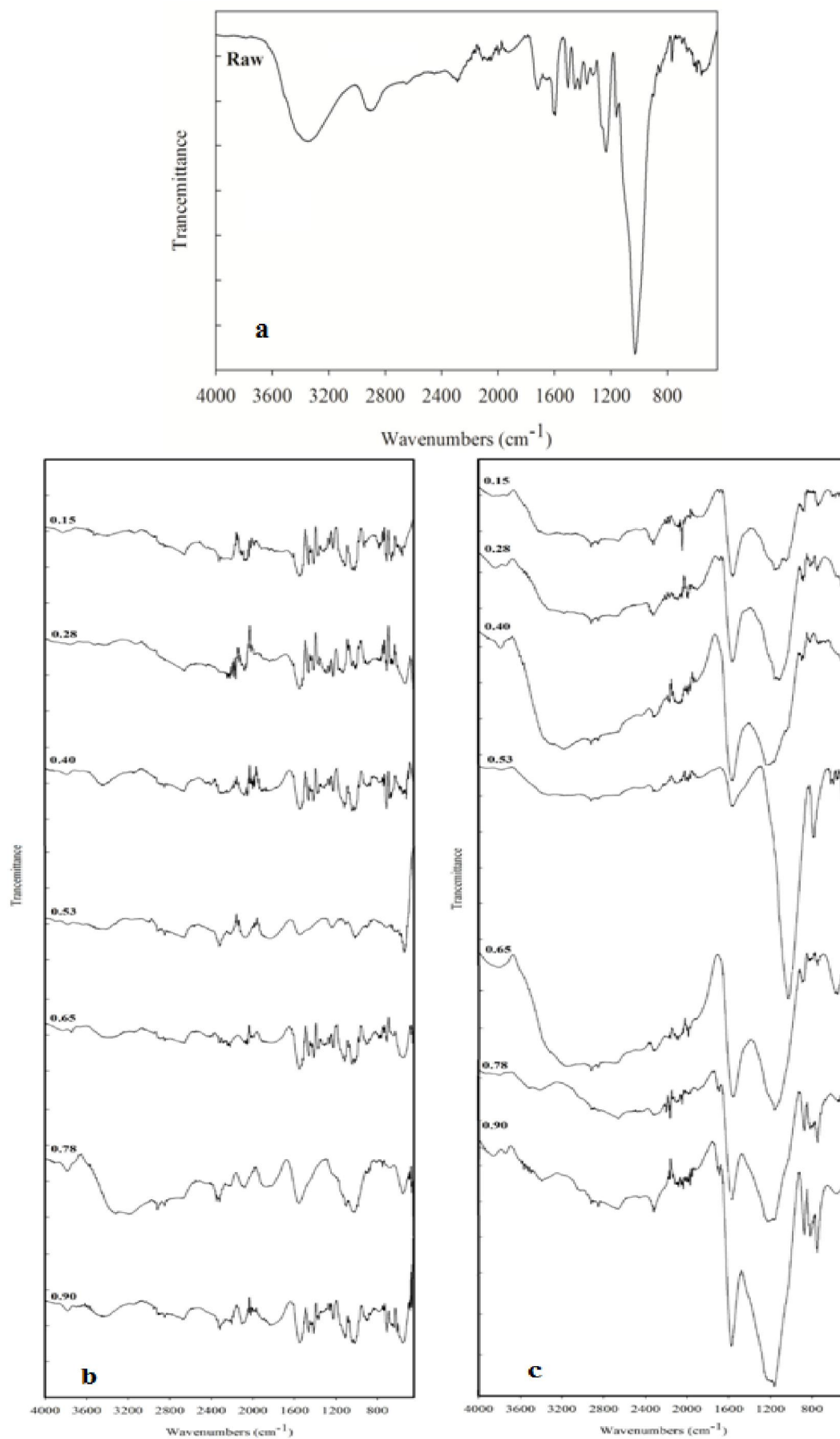


Figure 4.13: FTIR spectra of (a) palm shell, (b) prepared ACs by microwave heating and (c) prepared ACs by conventional heating

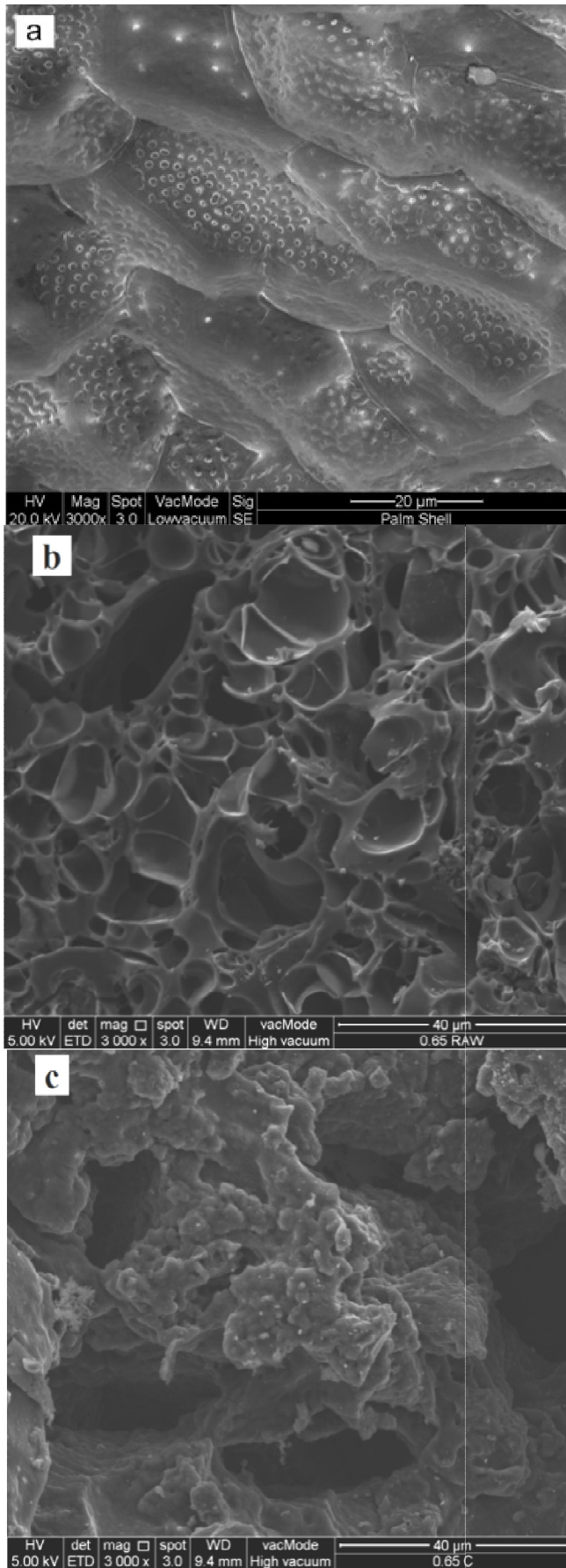


Figure 4.14: SEM micrographs (3000X) of the (a) palm shell, (b) MW0.65, (c) C0.65

#### 4.2.5 Surface morphology

SEM was used to observe the surface physical morphology of the palm shell and ACs prepared by microwave and conventional heating methods with the ratio of 0.65. The SEM micrographs of the palm shell, *MW0.65* and *C0.65* samples are shown in Figs. 4.15(a-c), respectively. As shown in Fig. 4.16(a), the surface of the palm shell has very small pores. However, the ACs are full of cavities and pores with different sizes and shapes compared to palm shell.

The pores and cavities resulted from the release of volatile components and the evaporation of zinc chloride from the spaces that were previously occupied by the  $ZnCl_2$  (Hui Deng, Zhang, et al., 2010; Maldhure & Ekhe, 2011). Fig. 4.14(b) shows that there are a large number of small and large holes with crevices and cracks on the surface of the microwave sample compared to the grainy, irregular and smoother surface of the palm shell. Moreover, the surface structure of the microwave sample shows less change compared to the palm shell surface, while the conventional sample has a completely different surface structure. The different surface structure of the ACs can be attributed to the different activation time of the heating methods. In the conventional heating method, the long activation process can destroy the surface structure of the AC compared to the short activation process in the microwave irradiation method.

Table 4.6: Wave numbers and ascription of the principal bands in the FTIR Spectra of palm shell and prepared ACs

Wave number (cm <sup>-1</sup> )	Assignments	Palm Shell	MW 0.15	MW 0.28	MW 0.40	MW 0.53	MW 0.65	MW 0.78	MW 0.90	C 0.15	C 0.28	C 0.40	C 0.53	C 0.65	C 0.78	C 0.90
3500-3300	Alcohols & Phenols, O-H Stretching	*														
2850-3000	Alkanes, H-C-H Asymmetric & Symmetric Stretch	*								*	*	*	*	*	*	*
2100-2250	Alkynes, C≡C (symmetry reduces intensity)		*	*	*	*				*						
1710-1720	Aldehydes & Ketones, C=O (saturated ketone)	*														
1550-1650	Aromatic C=C stretching		*	*	*	*	*	*	*	*	*	*	*	*	*	*
1000-1260	Carboxylic Acids & Derivatives, C-O banding	*	*	*	*	*	*	*	*	*	*	*	*	*	*	*
500-850	Aromatic substitution by aliphatic groups		*	*	*	*	*	*	*	*	*	*	*	*	*	*

### **4.3 PART 3: Production of ACs from oil palm shell via microwave-assisted KOH activation in the presence of CO<sub>2</sub> or N<sub>2</sub> for CO<sub>2</sub> adsorption**

#### **4.3.1 Effects of radiation time**

The effects of the microwave radiation time on the AC textural properties were determined using a chemical ratio of 1.5 and microwave input power of 750 W. The N<sub>2</sub> adsorption isotherms of the ACs produced using different activation times in the presence of CO<sub>2</sub> and N<sub>2</sub> are shown in Figures 4.15(a) and (b), respectively. According to the IUPAC classification, all of the isotherms in Figures 4.15(a) and (b) are type I and exhibit a sharp increase at a low relative pressure followed by a nearly horizontal plateau at a higher relative pressure, indicating the presence of micropores. The plateaus observed for the *C-15-1.5-750* and *N-45-1.5-750* samples slightly slope upwards at  $P/P_0 > 0.8$ , suggesting that these samples have mesopores.

The specific surface areas ( $S_{\text{BET}}$ ), total pore volumes ( $V_t$ ),  $V_{\text{mic}}/V_t$  ratios and average pore sizes of all of the ACs are summarised in Table 4.7. According to the results in Table 4.7, the textural properties of the end products obtained using an activation time of 5 min are very similar for both CO<sub>2</sub> and N<sub>2</sub> activation. These results might be due to insufficient carbonisation time for the removal of volatile matter from the carbon structure and development of the porosity.



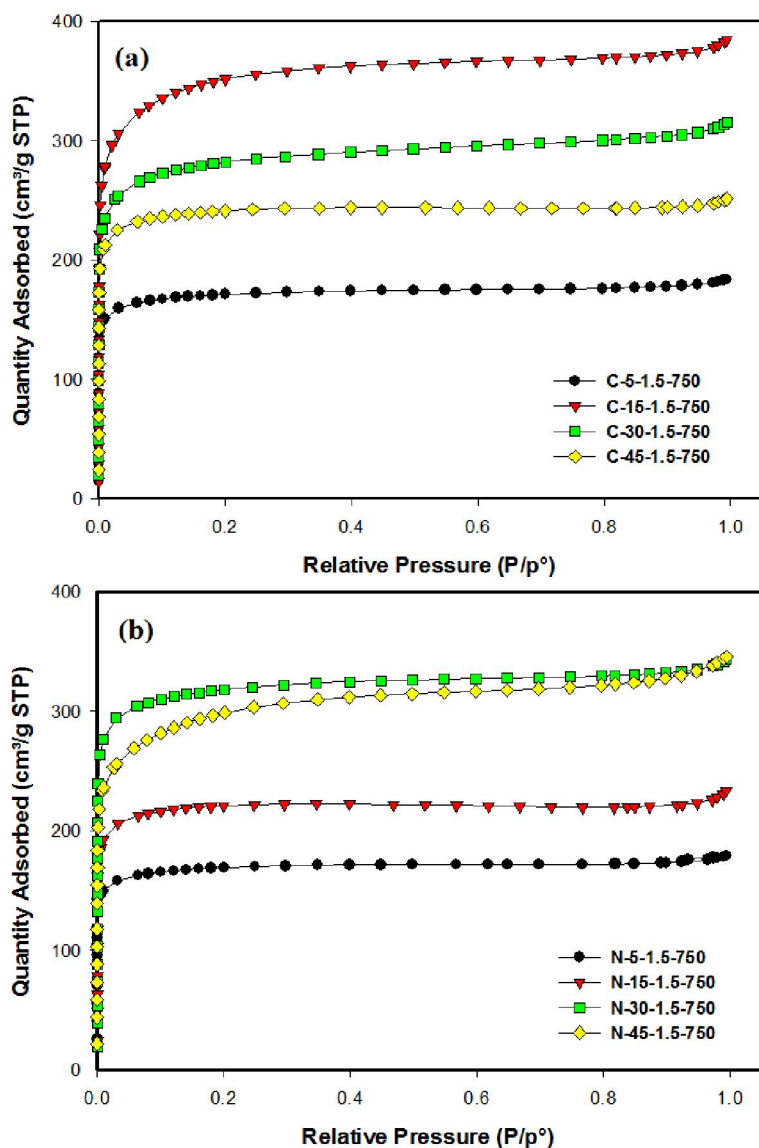


Figure 4.15: N<sub>2</sub> adsorption isotherms of ACs prepared using different activation times and a microwave power of 750 W and impregnation ratio of 1.5 in the presence of CO<sub>2</sub> (a) and N<sub>2</sub> (b).

The highest  $S_{BET}$  values are obtained for activation times of 15 and 30 min for CO<sub>2</sub> and N<sub>2</sub> activation, respectively. Above these activation times,  $S_{BET}$  decreases with increasing activation time. For both activation methods, the pore structures of the products become better developed because the extent of the reaction between the activating agent and carbon contents (C-KOH reaction) increases with increasing activation time. The porosity is developed during gasification according to the following reaction (Basta, Fierro, El-Saied, & Celzard, 2009):



Increasing the extent of the reaction allows new pores to be generated and the porosity to be developed, resulting in a higher surface area, pore volume and average pore diameter in the final AC product (X. He et al., 2010; K. Yang et al., 2010).

The results in Table 4.9 reveal that a maximum  $S_{\text{BET}}$  of 1195.6  $\text{m}^2/\text{g}$  is achieved after 15 min for the ACs produced in the presence of  $\text{CO}_2$ , while a maximum  $S_{\text{BET}}$  of 1069  $\text{m}^2/\text{g}$  is achieved after 30 min in the presence of  $\text{N}_2$  gas. This behaviour can be explained by the fact that  $\text{N}_2$  gas acts only as an inert purge gas and does not react with the raw material. Its main function is to remove the volatile matter from the reactor during the activation process (Sumathi et al., 2009). In contrast, carbon and  $\text{CO}_2$  react during the activation process, removing disorganised carbon and exposing the aromatic carbon sheets to the action of  $\text{CO}_2$  gas (Bansal, 1988). Therefore, more pores are created in less time in the presence of  $\text{CO}_2$  than in the presence of  $\text{N}_2$  because of the C- $\text{CO}_2$  reaction. When the microwave irradiation time is increased above the optimum values of 15 and 30 min for  $\text{CO}_2$  and  $\text{N}_2$  activation, respectively,  $S_{\text{BET}}$  decreases because of carbon burn-off by excessive irradiation.

Table 4.7: Textural characteristics of ACs prepared using different activation times in the presence of either  $\text{CO}_2$  or  $\text{N}_2$  measured by  $\text{N}_2$  adsorption at  $-196^\circ\text{C}$ .

Sample	$S_{\text{BET}}$ ( $\text{m}^2/\text{g}$ )	$V_t$ ( $\text{cm}^3/\text{g}$ )	$V_{\text{mic}}$ ( $\text{cm}^3/\text{g}$ )	$V_{\text{mic}}/V_t$ (%)	Average pore size (nm)
C-5-1.5-750	575.7	0.28	0.23	82.1	1.94
C-15-1.5-750	1195.6	0.58	0.41	70.6	1.95
C-30-1.5-750	951.2	0.47	0.35	74.4	2.01
C-45-1.5-750	810.3	0.38	0.33	86.8	1.88
N-5-1.5-750	567.6	0.27	0.23	85.2	1.89
N-15-1.5-750	741.5	0.35	0.30	85.2	1.92
N-30-1.5-750	1069.4	0.52	0.42	80.7	1.95
N-45-1.5-750	1023.4	0.52	0.31	59.6	2.04

The pore size distribution (PSD) can be used to characterise the structural heterogeneity and solid internal structure of the ACs (A. Arami-Niya et al., 2010). The PSDs of the CO<sub>2</sub> and N<sub>2</sub> samples are shown in Figures 4.16(a) and (b), respectively. These figures indicate that the activation time has a significant effect on the AC pore structure.

All of the samples exhibit broad pore size distributions, which reveal the presence of both micropores and mesopores. For the CO<sub>2</sub>-gasified samples (Figure 14.6(a)), the generation of micropores increases sharply when the activation time is increased to 15 min and then decreases for activation times longer than 15 min due to excessive activation.

The N<sub>2</sub>-gasified ACs produced using activation times of 5 and 10 min exhibit homogeneous microporosity. As shown in Figure 4.16(b), these ACs become more heterogeneous as the activation time is increased up to 45 min because the micropores become larger, leading to the creation of mesopores. Nitrogen uptake in larger pores is clearly observed at higher activation times (Figure 4.16(b)); the area under the curve increases with increasing microwave irradiation time and reaches a maximum for pores larger than 10 nm for *N-45-1.5-750*.

### **4.3.2 Effects of the impregnation ratio**

The effects of the chemical impregnation ratio on the AC textural properties were evaluated using a microwave input power of 750 W and irradiation time of 15 min and 30 min for CO<sub>2</sub> and N<sub>2</sub> gasification, respectively. The ACs prepared by CO<sub>2</sub> activation exhibit type I isotherms (Figure 4.17(a)).

However, when the KOH ratio is 1.5, the nitrogen uptake increases gradually at higher relative pressures ( $P/P_0 > 0.2$ ), indicating an increase in the volume of large micropores and the presence of mesopores (Hoseinzadeh Hesas, Arami-Niya, Wan Daud, & Sahu, 2013b).

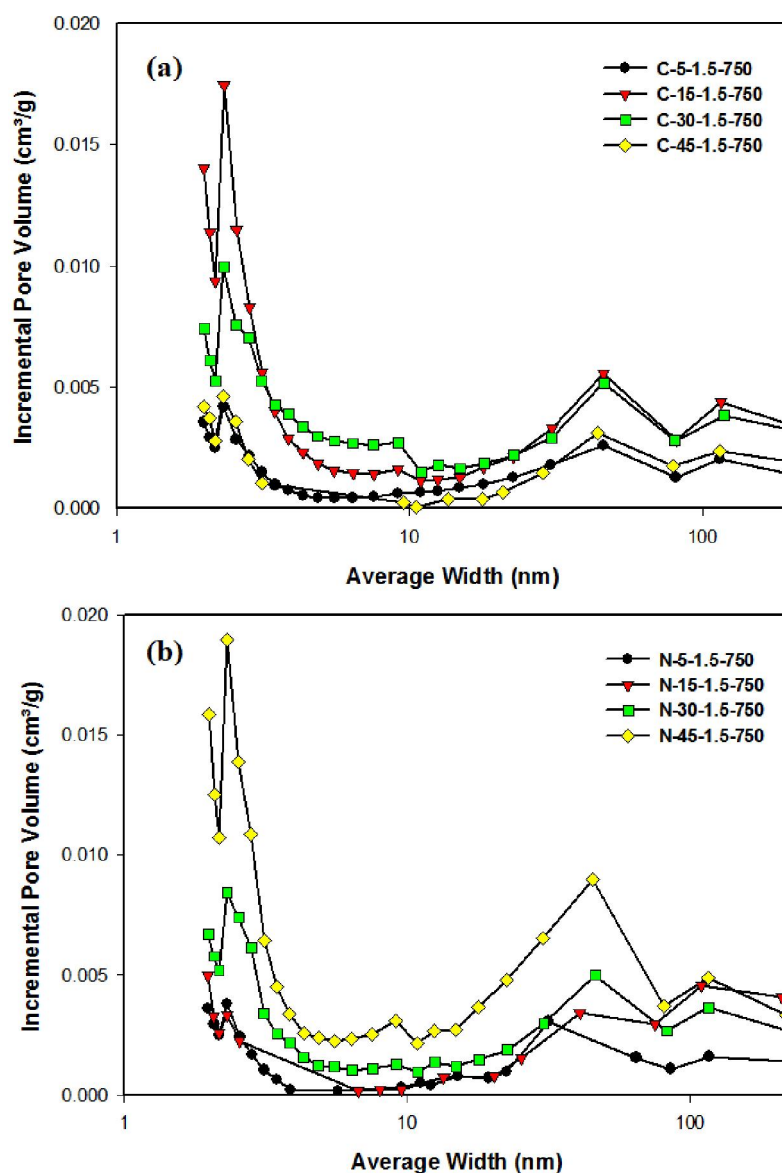


Figure 4.16: Pore size distributions of ACs prepared using different activation times and a microwave power of 750 W and agent ratio of 1.5 in the presence of CO<sub>2</sub> (a) and N<sub>2</sub> (b) derived from the N<sub>2</sub> adsorption results at -196 °C.

When the IR is 2.5, the pores are destroyed and blocked, resulting in lower nitrogen adsorption for this sample than for the other samples. Figure 4.17(b) shows that the ACs prepared by KOH activation under N<sub>2</sub> with IRs of 0.5 and 1.5 also exhibit type I isotherms, indicating the presence of micropores. When the chemical ratio is higher, a mixture of micropores and mesopores is observed as demonstrated by the results for *N*-30-2.5-750, which has a type IV isotherm. The positive slope of the plateau at high relative pressures is due to multilayer adsorption on the external surface (Foo & Hameed, 2011b).

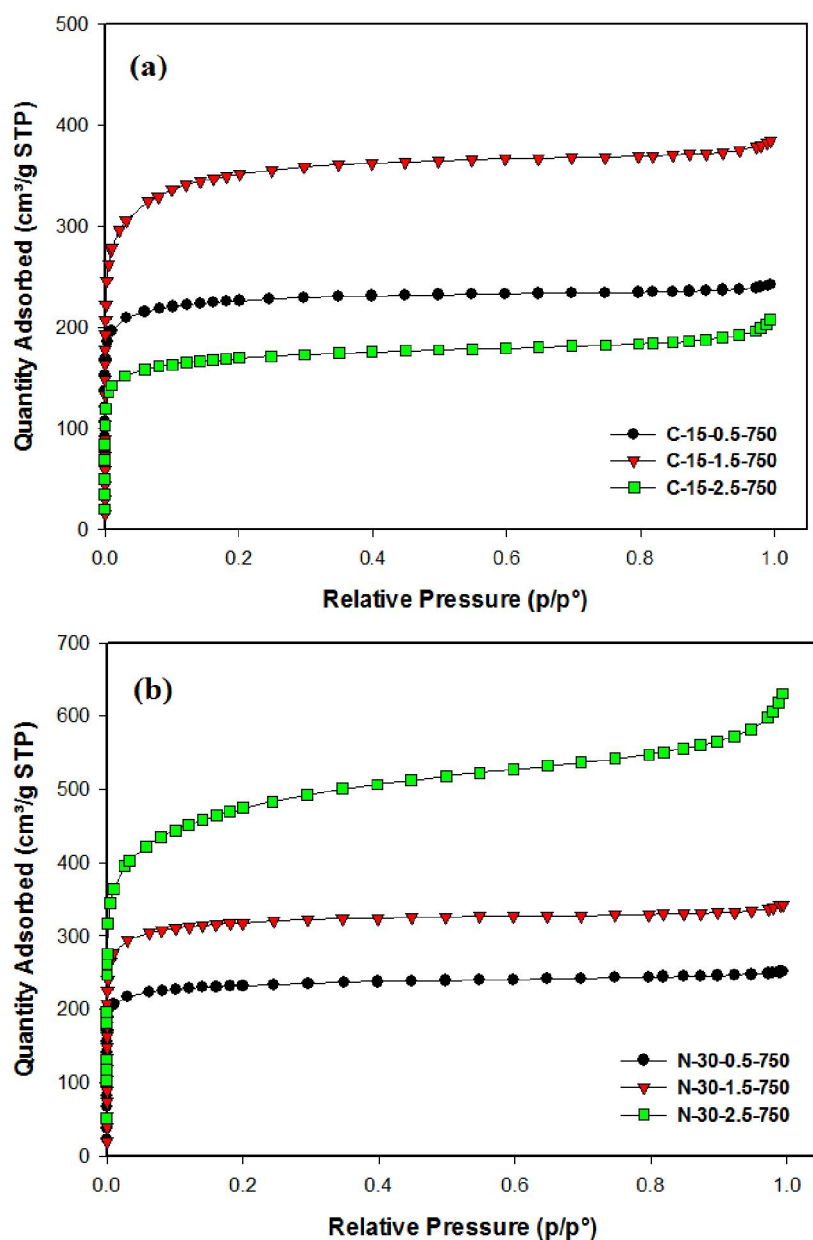


Figure 4.17:  $N_2$  adsorption isotherms of ACs prepared using different impregnation ratios and an irradiation time of 15 min and microwave input power of 750 W in the presence of  $CO_2$  (a) and an activation time of 30 min and microwave power of 750 W in the presence of  $N_2$  (b).

Table 4.8 shows that  $S_{BET}$  and  $V_t$  increase when the chemical ratio is increased from 0.5 to 1.5 and then decrease when it is further increased to 2.5 for the  $CO_2$ -activated samples. In contrast, the  $S_{BET}$  and  $V_t$  values of ACs prepared under  $N_2$  gasification increase as the KOH ratio is increased to 2.5. It is assumed that KOH was reduced to metallic potassium during the activation process and diffuses into the internal structure of the char matrix, enlarging the existing pores and creating new ones.

At lower IRs, the active site carbons partially react with KOH to form small pores. Increasing the KOH ratio should enhance the activation process and thus improve the porosity. Beyond the optimum chemical ratio, the amount of burn-off in the carbon structure increases, and the pores become larger and are destroyed (W. Li et al., 2008). For the CO<sub>2</sub>-activated samples, the combination of the carbon-CO<sub>2</sub> reaction and more extensive C-KOH reactions due to the use of larger amounts of KOH results in the destruction of the carbon structure, and thus, S<sub>BET</sub> decreases when X<sub>k</sub> is greater than 1.5. However, the microporous structure of *C-15-2.5-750* is retained due to the physical activation and creation of new small micropores.

Table 4.8: Textural characteristics of ACs prepared using different impregnation ratios in the presence of either CO<sub>2</sub> or N<sub>2</sub> measured by N<sub>2</sub> adsorption at -196 °C.

Sample	S <sub>BET</sub> (m <sup>2</sup> /g)	V <sub>t</sub> (cm <sup>3</sup> /g)	V <sub>mic</sub> (cm <sup>3</sup> /g)	V <sub>mic</sub> /V <sub>t</sub> (%)	Average pore size (nm)
C-15-0.5-750	762.2	0.37	0.30	81.1	1.94
C-15-1.5-750	1195.6	0.58	0.41	70.7	1.95
C-15-2.5-750	573.7	0.30	0.20	66.6	2.11
N-30-0.5-750	780.0	0.38	0.31	81.6	1.97
N-30-1.5-750	1069.4	0.52	0.42	80.7	1.95
N-30-2.5-750	1630.4	0.92	0.46	50.0	2.26

Note the difference in the irradiation times used for the CO<sub>2</sub> and N<sub>2</sub> gasifications (15 and 30 min, respectively).

The pore size distributions of the ACs prepared using different KOH ratios under CO<sub>2</sub> and N<sub>2</sub> flow are shown in Figures 4.18(a) and (b), respectively. Figure 4.18(a) shows that the samples have broad pore size distributions, with pores ranging from narrow micropores to large mesopores and macropores. *C-15-1.5-750* has the highest micropore volume, and thus S<sub>BET</sub>, of all of the samples in Figure 4.18(a).

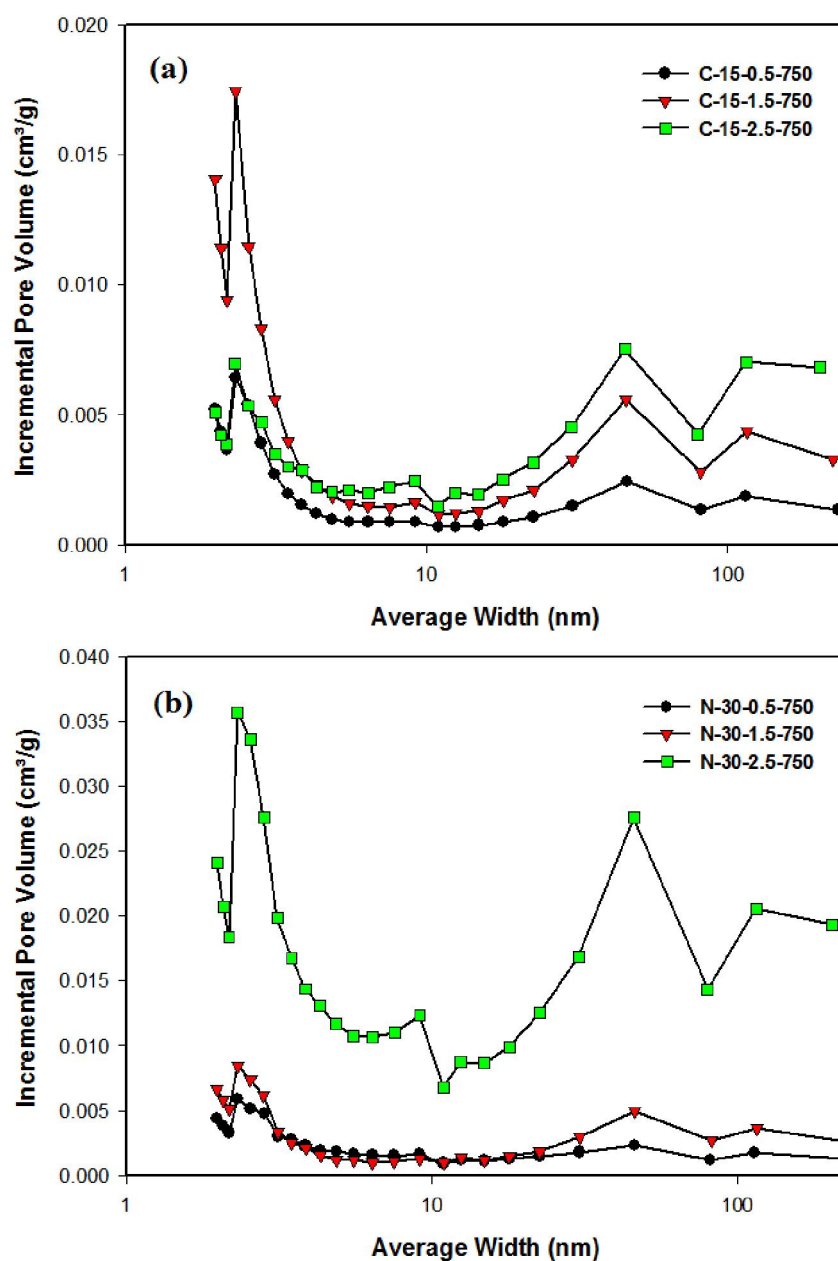


Figure 4.18: Pore size distributions of ACs prepared using different impregnation ratios and an irradiation time of 15 min and microwave input power of 750 W in the presence of CO<sub>2</sub> (a) and an activation time of 30 min and microwave power of 750 W in the presence of N<sub>2</sub> (b) derived from the N<sub>2</sub> adsorption results at -196 °C.

As the KOH ratio increases to 2.5, the pore size distribution becomes broader, and the mesopore and macropore volumes are higher due to the C-CO<sub>2</sub> reaction, which promotes carbon burn-off and increases the pore width.

As shown in Figure 4.18(b), more micropores are created, and they become larger as the KOH ratio increases to 2.5. A mesoporosity of 50% (*N-30-2.5-750*) is also observed mainly because N<sub>2</sub> acts as an inert gas and does not destroy the pore structure.

### 4.3.3 Effects of the microwave power

The effects of the microwave power levels on the textural properties of ACs prepared by KOH chemical activation were investigated using an activation time of 15 min and IR of 1.5 for CO<sub>2</sub> gasification and an irradiation time of 30 min and IR of 2.5 for N<sub>2</sub> gasification. The nitrogen adsorption isotherms of the ACs prepared using different microwave powers are shown in Figures 4.19(a) and (b). These figures show that the nitrogen adsorption isotherms of the CO<sub>2</sub>- and N<sub>2</sub>-activated samples are type I except in the case of *N-30-2.5-750*, which has a type IV isotherm, indicating microporosity and mesoporosity.

The precursor cannot be heated effectively without impregnating it with the activating agent, indicating that potassium hydroxide acts as the main microwave absorber during the initial stage of the reaction (T. Wang et al., 2009). As the pore structure develops, the AC itself can also absorb microwave energy.

The results in Table 4.7 indicate that the N<sub>2</sub>-activated samples exhibit a more developed porosity than the CO<sub>2</sub>-activated ones because of the higher IR and longer irradiation time used to prepare the N<sub>2</sub>-activated samples. Increasing the microwave power from 550 to 750 W causes a significant increase in  $S_{\text{BET}}$  and  $V_t$  (Table 4.9) for both the CO<sub>2</sub>- and N<sub>2</sub>-activated samples, mainly because of the combined effects of internal and volumetric heating, which contribute to new pore development.

However, at a high radiation power of 850 W, an excessive amount of microwave energy is absorbed, causing carbon burn-off and damaging the pore structures; thus,  $S_{\text{BET}}$  and  $V_t$  decrease. Although the pore volume of the CO<sub>2</sub>-activated sample decreases considerably when the irradiation power is 850 W, the per cent of micropores ( $V_{\text{mic}}/V_t$ ) does not change significantly, showing that the CO<sub>2</sub> activating agent effectively creates new micropores.



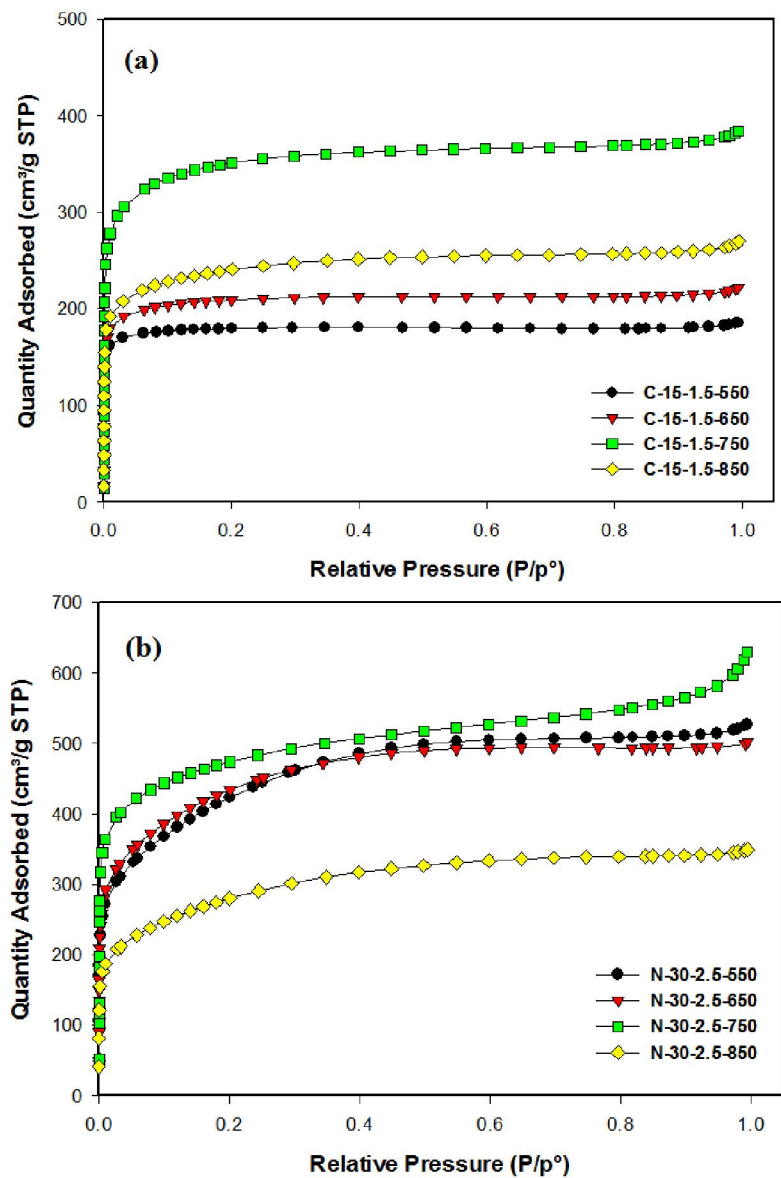


Figure 4.19:  $N_2$  adsorption isotherms of ACs prepared using different microwave powers and an irradiation time of 15 min and impregnation ratio of 1.5  $X_k$  in the presence of  $CO_2$  (a) and an activation time of 30 min and impregnation ratio of 2.5  $X_k$  in the presence of  $N_2$  (b).

However, for the  $N_2$ -activated samples,  $V_{mic}/V_t$  decreases to less than 50% when the microwave power is increased from 750 to 850 W. The same trend of reduction in micropores level at high microwave power is reported by Liu et al. (2010), where they used bamboo to produce ACs with phosphoric acid as a chemical agent by the microwave-induced method. They found a remarkable drop in micropore formation at 400 W, while the formation of mesopores increased significantly. They concluded that development of mesopores appears to be preferred at higher levels of microwave power (Q.S. Liu, T. Zheng, P. Wang, et al., 2010).

Table 4.9: Textural characteristics of ACs prepared using different microwave powers in the presence of either CO<sub>2</sub> or N<sub>2</sub> measured by N<sub>2</sub> adsorption at -196 °C.

Sample	S <sub>BET</sub> (m <sup>2</sup> /g)	V <sub>t</sub> (cm <sup>3</sup> /g)	V <sub>mic</sub> (cm <sup>3</sup> /g)	V <sub>mic</sub> /V <sub>t</sub> (%)	Average pore size (nm)
C-15-1.5-550	602.1	0.28	0.25	89.3	1.87
C-15-1.5-650	705.7	0.33	0.28	84.8	1.90
C-15-1.5-750	1195.6	0.58	0.41	70.7	1.95
C-15-1.5-850	822.14	0.40	0.27	67.5	1.98
N-30-2.5-550	1514.0	0.77	0.13	16.2	2.12
N-30-2.5-650	1538.4	0.80	0.24	31.1	2.26
N-30-2.5-750	1630.4	0.92	0.46	50.0	2.01
N-30-2.5-850	993.0	0.53	0.13	24.5	2.15

Note the differences in the irradiation times and impregnation ratios for the CO<sub>2</sub> (15 min and 1.5 X<sub>k</sub>, respectively) and N<sub>2</sub> (30 min and 2.5 X<sub>k</sub>, respectively) gasifications.

The pore size distributions of the ACs produced under CO<sub>2</sub> (Figure 4.20(a)) show that the micropore volume increases markedly with increasing microwave power. The increase in the micropore volume is higher when the power level is 750 W. Moreover, the percentage of mesopores and macropores in the CO<sub>2</sub>-activated samples increases with increasing microwave power.

#### 4.3.4 Extra surface characterisations

To determine the different effects of the CO<sub>2</sub> and N<sub>2</sub> environments on the AC textural and surface chemical properties, *C-15-1.5-750* and *N-30-2.5-750* were further characterised. Because the AC specific surface area (S<sub>BET</sub>) is one of the most important physical properties affecting the reactivity and combustion behaviour of the carbon, the samples with the highest surface areas were chosen. Based on the N<sub>2</sub> adsorption results at -196 °C for the CO<sub>2</sub>-activated samples (Tables 4.7-4.9), the AC prepared using an activation time of 15 min, IR of 1.5 and microwave power of 750 W has the highest S<sub>BET</sub> of 1195.6 m<sup>2</sup>/g. For the N<sub>2</sub> gasification, the AC produced using an activation time of 30 min, IR of 2.5 and microwave power of 750 has the highest S<sub>BET</sub> of 1630.4 m<sup>2</sup>/g.

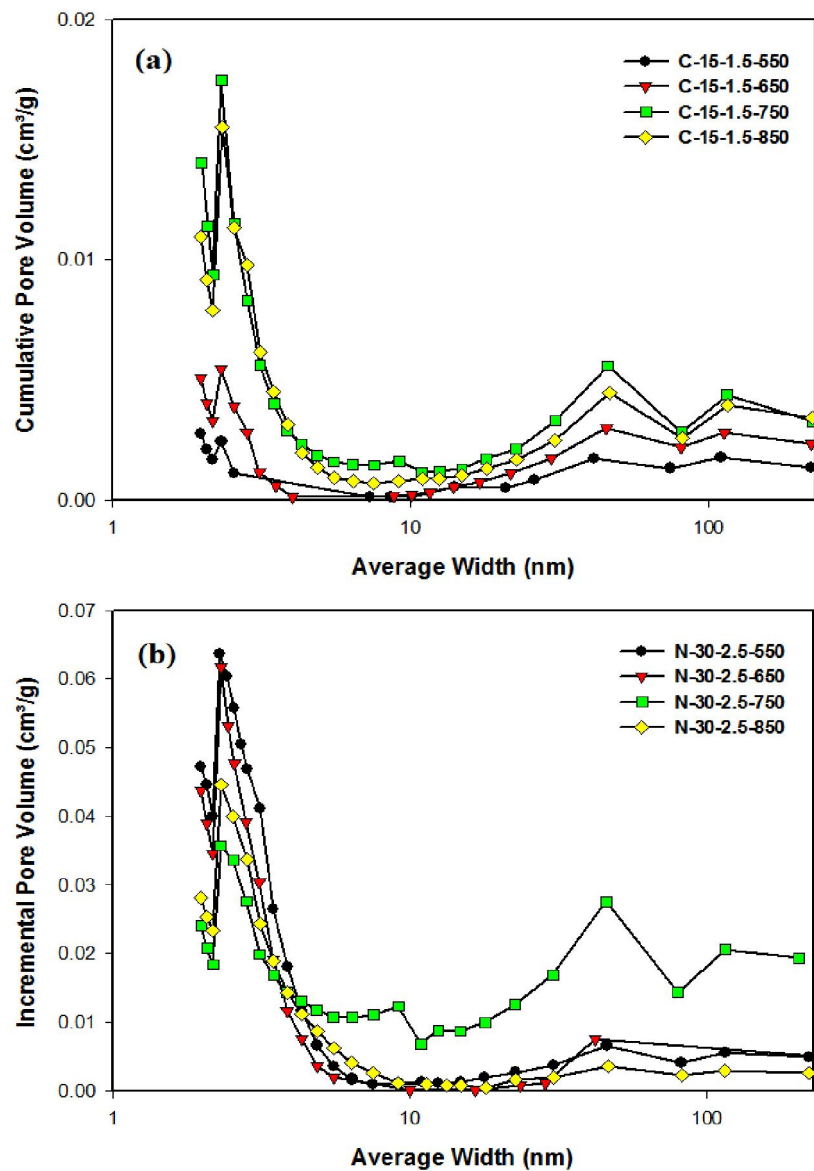


Figure 4.20: Pore size distributions of ACs prepared using different microwave powers and an irradiation time of 15 min and impregnation ratio of 1.5  $X_k$  in the presence of  $\text{CO}_2$  (a) and an activation time of 30 min and impregnation ratio of 2.5  $X_k$  in the presence of  $\text{N}_2$  (b).

#### 4.3.4.1 Surface morphology

The physical surface morphology of the raw palm shell and ACs observed by using SEM. Figures 4.21(a), (b) and (c) show the SEM photographs of the palm shell,  $\text{CO}_2$ -activated sample (*C-15-1.5-750*) and  $\text{N}_2$ -activated sample (*N-30-2.5-750*), respectively. As shown in Figure 4.21(a), the surface of the palm shell has very small pores. In contrast, the ACs have many cavities and pores of different sizes and shapes.

Figures 4.21(b) and (c) show that the AC surfaces have many small and large holes, crevices and cracks, while the surface of the palm shell is grainy, irregular and relatively smooth. These cavities, voids and pores result from the interactions between KOH and the precursor and from the removal of potassium hydroxide and its derivatives from the carbon matrix during the activation and washing steps. Moreover, the surface of the CO<sub>2</sub>-activated sample (Figure 4.21(b)) has more regular, smaller holes than that of the N<sub>2</sub>-activated sample, possibly due to the effect of CO<sub>2</sub> on the surface during activation and to differences in the activation time and KOH ratio used to produce these two samples.

For the N<sub>2</sub>-gasified sample (Figure 4.21(c)), the surface structure is completely different mainly due to the longer activation time and larger amount of the chemical agent used (more intensive C-KOH activation), which could result in greater damage to the surface structure than that observed when a shorter activation time and lower agent ratio are used to produce the CO<sub>2</sub>-gasified sample.

#### 4.3.4.2 Proximate and ultimate analyses

The proximate and ultimate analysis results for the oil palm shell and ACs (*C-15-1.5-750* and *N-30-2.5-750*) are given in Table 4.12. These results confirm that palm shell is a good precursor for AC production due to its high fixed carbon and volatile matter contents and low ash content. The ultimate analysis results show that the carbon content increases from 54.7% in the palm shell to 65.97% and 61.71% in the ACs prepared under CO<sub>2</sub> and N<sub>2</sub>, respectively. The decrease in oxygen content after activation suggests that the oxygen functional groups, which are located at the carbon layer edges, have a low thermal stability and can be easily removed during treatment (Valente Nabais et al., 2004). The C/O ratio of the products is higher than that of the precursor because the volatile substances degrade into gases and liquid tar during the pyrolysis process, which leads to higher carbon contents in the ACs (Maldhure & Ekhe, 2011).

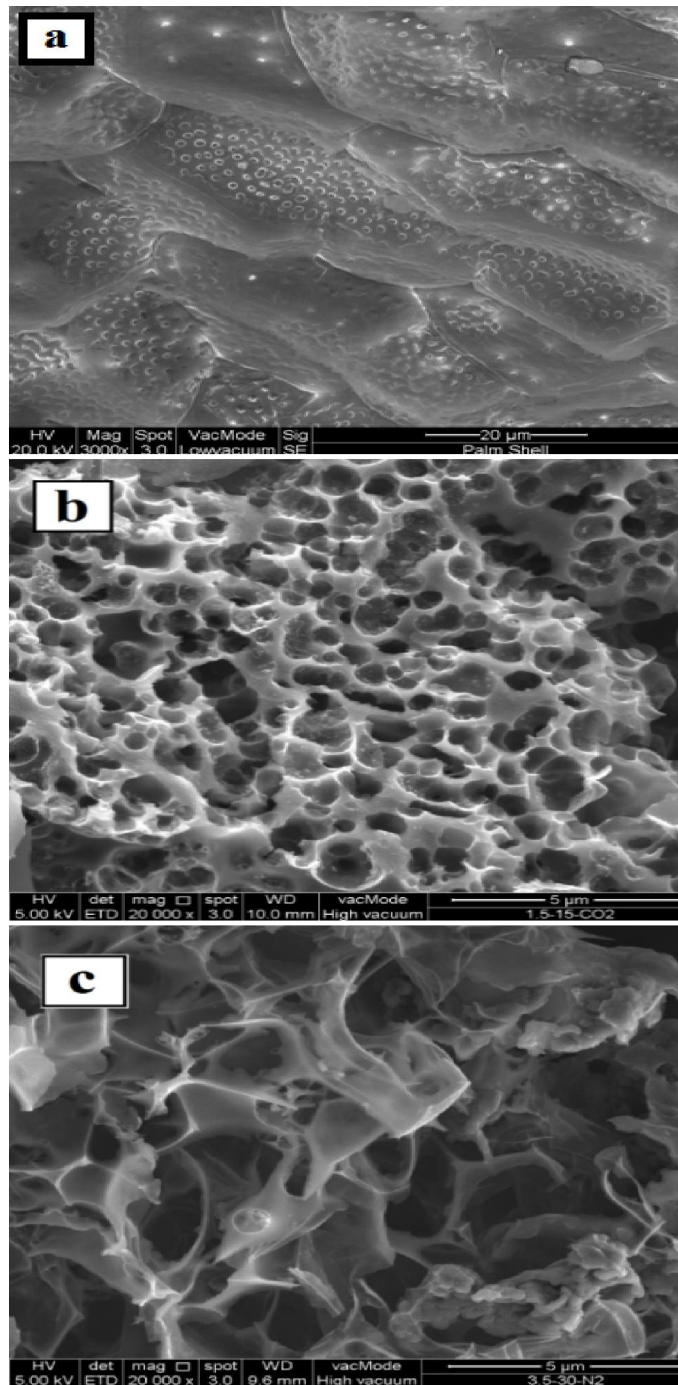


Figure 4.21: SEM images of the raw palm shell (a) and the ACs with the highest surface areas prepared under CO<sub>2</sub> (b) and N<sub>2</sub> (c).

The nitrogen content in the CO<sub>2</sub> and N<sub>2</sub> samples decreases by 0.06% and 0.58%, respectively, relative to that in the palm shell. These findings show that using an excess of the chemical activation agent helps to eliminate more of the nitrogenous compounds in the N<sub>2</sub>-activated sample (Hoseinzadeh Hesas, Arami-Niya, Wan Daud, & Sahu,

2013a; Yagmur, Ozmak, & Aktas, 2008). Also, the per cent of hydrogen in the ACs decreases relative to that in the palm shell because the molecular chains in the precursor are broken at high temperatures. The proximate analysis results in Table 4.10 show that the loss of volatile matter is greater for the N<sub>2</sub>-activated sample than for the CO<sub>2</sub>-activated sample, probably due to the longer activation time and higher chemical: precursor ratio used to prepare the N<sub>2</sub>-activated sample. The volatile matter can then move easily through the pore channels and be released from the carbon surface during the activation stage as indicated by the results in Table 4.10. The amount of fixed carbon is greater in the N<sub>2</sub> sample than in the CO<sub>2</sub> sample because more volatile compounds are released during the longer activation time.

Table 4.10: Proximate and elemental analyses of the raw palm shell and ACs prepared under the optimum CO<sub>2</sub> and N<sub>2</sub> gasification conditions.

Material	Volatile Matter (%)	Fixed Carbon (%)	Ash (%)	C (%)	H (%)	N (%)	O (%)
Palm Shell	78	14.5	7.5	54.7	7.49	2.03	35.6
C-15-1.5-750	64.3	26.7	9.0	65.97	2.81	1.97	29.25
N-30-2.5-750	55.3	33.9	10.8	61.71	3.50	1.48	33.31

#### 4.3.4.3 FTIR analysis

The types of AC surface functional groups (FG) obtained are mainly affected by the type of raw material, type of heat treatment, activation process and post-chemical treatment (Izquierdo et al., 2001; Szymański et al., 2002). The FTIR spectra of the palm shell, C-15-1.5-750 and N-30-2.5-750 samples are shown in Figure 4.22. The wave numbers and assignments of the main bands observed in this figure are summarised in Table 4.11. A broad band at approximately 3400 cm<sup>-1</sup>, which is assigned to the O–H stretching vibration of hydroxyl functional groups and hydrogen bonding, is observed for the precursor but is nearly absent in the AC spectra.

The band in the palm shell spectrum at approximately  $2910\text{ cm}^{-1}$ , which is assigned to asymmetric and symmetric C–H stretching, disappears in both AC spectra, indicating that a significant amount of hydrogen is removed during the thermal degradation of the precursor (Franca et al., 2010; Roozbeh Hoseinzadeh Hesas, 2013). These results are consistent with those showing a reduction in hydrogen content in Table 4.11. The bands located at approximately  $2100\text{--}2250\text{ cm}^{-1}$  are assigned to alkyne  $\text{C}\equiv\text{C}$  stretching and are observed for all of the samples (Hoseinzadeh Hesas, Arami-Niya, et al., 2013a). The stretching absorption band at  $1710\text{ cm}^{-1}$  observed for the palm shell is associated with aldehydes and ketones ( $\text{C}=\text{O}$ ). This band disappears in both the *C-15-1.5-750* and *N-30-2.5-750* spectra, indicating that the heat treatment removes these more weakly bound substituents.

However, some oxygen remains within the aromatic structure of the carbon layer. Moreover, the samples are reoxidised when they are removed from the microwave or furnace, and pyrone groups are generated on the carbon layer planes, resulting in a decrease in the oxygen content and the production of highly basic samples (Valente Nabais et al., 2004). An absorption band at  $1550\text{--}1650\text{ cm}^{-1}$ , which is associated with aromatic  $\text{C}=\text{C}$  stretching, is observed in the AC spectra and might be due to the higher carbon contents in the ACs relative to that in the raw material. An intense band in the range of  $1000\text{--}1260\text{ cm}^{-1}$  due to carboxylic acid, alcohol, phenol and ester groups is significantly reduced in the AC spectra. The C–C stretching band at  $400\text{--}700\text{ cm}^{-1}$  observed for the palm shell decreases considerably for the  $\text{CO}_2$  sample and disappears completely for the  $\text{N}_2$  sample.

Table 4.11: Wavenumbers and descriptions of the principal FTIR bands of the palm shell and the ACs with the highest surface areas.

Wavenumber (cm <sup>-1</sup> )	Assignment	Palm Shell	C	N
3500–3300	Alcohols & Phenols, O–H Stretching	*		
2850-3000	Alkanes, H-C-H Asymmetric & Symmetric Stretching	*		
2100-2250	Alkynes, C≡C (symmetry reduces the intensity)	*	*	*
1710-1720	Aldehydes & Ketones, C=O (saturated ketone)	*		
1550-1650	Aromatic C=C Stretching		*	*
1000–1260	Carboxylic Acids & their Derivatives, C–O Band	*	*	*
400-700	C–C Stretching	*		

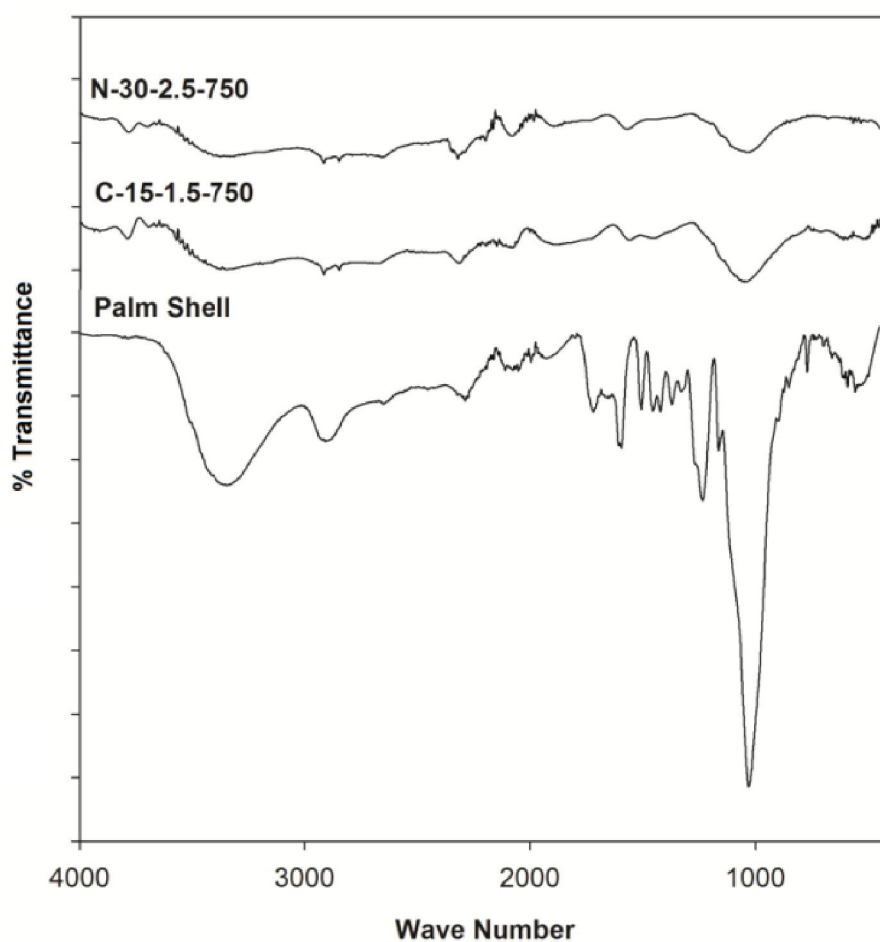


Figure 4.22: Fourier transform infrared spectra of the raw palm shell and the ACs with the highest surface areas prepared under CO<sub>2</sub> and N<sub>2</sub>.



#### 4.3.4.4 CO<sub>2</sub> adsorption

Generally, ACs can be used in gas-phase adsorption because of their high surface areas and large micropore volumes. Most gas pollutant molecules have diameters of approximately 0.4 to 0.9 nm; hence, for gas-phase processes, ACs should be predominantly microporous and have high pore volumes. Because most of the internal surface is due to micropores, adsorption mainly occurs within them (Sumathi et al., 2009). CO<sub>2</sub> adsorption at 0 °C can be used to assess narrow micropores (pore width,  $w < 0.7$  nm) where N<sub>2</sub> adsorption at -196 °C can be kinetically restricted (Puziy et al., 2005). The data in Table 4.12 show that the Dubinin–Radushkevich micropore volume and surface area calculated from the N<sub>2</sub> adsorption isotherms are higher than the Dubinin–Astakhov (DA) micropore volume and DR surface area calculated from the CO<sub>2</sub> adsorption isotherms. These results indicate the presence of large micropores that are only partially filled with CO<sub>2</sub> at 0 °C and subatmospheric pressures because of the low relative pressures ( $P/P_0 < 0.035$ ) attained under these conditions (Puziy et al., 2007). The AC micropore volumes obtained from CO<sub>2</sub> adsorption are very different, while those obtained from N<sub>2</sub> adsorption are similar. Therefore, it is concluded that the AC prepared under N<sub>2</sub> contains more ultramicropores than that prepared under CO<sub>2</sub>. This result can be attributed to the oxidising behaviour of CO<sub>2</sub>, which penetrates the carbon surface and possibly enlarges the ultramicropores created during the KOH activation. N<sub>2</sub>, on the other hand, is inert and does not interfere with the activation process.

Table 4.12: Textural parameters of the ACs with the highest surface areas obtained from N<sub>2</sub> adsorption at -196 °C and CO<sub>2</sub> adsorption at 0 °C.

Sample	N <sub>2</sub>				CO <sub>2</sub>	
	S <sub>BET</sub> (m <sup>2</sup> /g)	V <sub>t</sub> (cm <sup>3</sup> /g)	DR Method		DR S <sub>mic</sub> (m <sup>2</sup> /g)	DA V <sub>mic</sub> (cm <sup>3</sup> /g)
			S <sub>mic</sub> (m <sup>2</sup> /g)	V <sub>mic</sub> (cm <sup>3</sup> /g)		
C-15-1.5-750	1195.6	0.58	899.6	0.41	439.5	0.36
N-30-2.5-750	1630.4	0.92	1020.9	0.46	628.6	0.61

The absolute adsorption capacities of the ACs (*C-15-1.5-750* and *N-30-2.5-750*) measured at 0, 25 and 50 °C over the pressure range of 0 – 120 kPa are presented in Figures 4.23(a) and (b). The maximum CO<sub>2</sub> adsorptions by *C-15-1.5-750* and *N-30-2.5-750* samples are 9 and 12 (mol/kg), respectively. All of these CO<sub>2</sub> adsorption isotherms are type I according to the IUPAC classification. At all pressures, the AC produced under N<sub>2</sub> adsorbs more CO<sub>2</sub> than the AC produced under CO<sub>2</sub>, indicating that *N-30-2.5-750* has higher micropore and ultramicropores volumes than *C-15-1.5-750* (Ello, de Souza, Trokourey, & Jaroniec, 2013). The CO<sub>2</sub> adsorption capacity of these ACs is reasonable compared to those of other carbon adsorbents produced from different raw materials reported in the literature (Esteves, Lopes, Nunes, & Mota, 2008; Vargas, Giraldo, & Moreno-Piraján, 2012).

The ability of a temperature-dependent equilibrium isotherm model, the Toth model, to predict the measured CO<sub>2</sub> adsorption capacity of the ACs over the pressure range and temperatures measured in this study was determined (Duong, 1998). The model consists of the following equation:

$$Q_i = Q_{mi} \frac{K_i P}{[1+(K_i P)^{n_i}]^{\frac{1}{n_i}}} \quad (4.4)$$

Where,

$$K_i = K_i^0 \exp\left(-\frac{\Delta H_i}{RT}\right) \quad (4.5)$$

Here,  $Q_i$  and  $Q_{mi}$  are the absolute and maximum amounts of component  $i$  adsorbed,  $\Delta H_i$  is the isosteric heat of adsorption at zero loading,  $n_i$  is a parameter describing the surface heterogeneity,  $R$  is the gas constant,  $T$  is the measurement temperature and  $K_i^0$  is the Henry adsorption constant at infinite temperature. The isosteric heat of adsorption decreases with adsorbate loading for  $n_i < 1$ .

The best-fit parameters for Equations (4.4) and (4.5) were determined using a least-squares regression method to minimise the standard deviation (SD) between the measured and calculated capacities ( $Q_i$  and  $Q_i^{Calc}$ , respectively)

$$(SD = \left( \left( \frac{1}{N} \right) \sqrt{\sum (Q_i^{meas} - Q_i^{calc})^2} \right)), \text{ where } N \text{ is the number of regressed data points.}$$

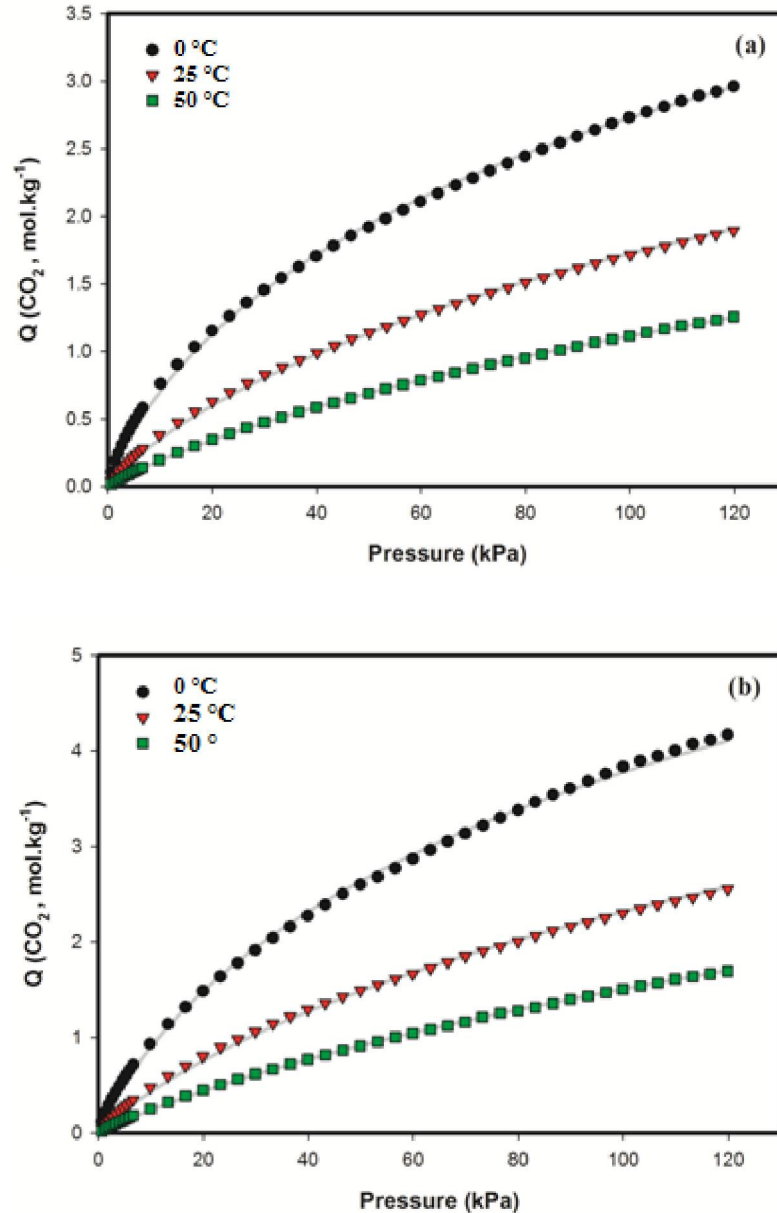


Figure 4.23: Carbon dioxide adsorption isotherms of the ACs with the highest surface areas prepared under (a) CO<sub>2</sub> and (b) N<sub>2</sub> at 0 °C, 25 °C and 50 °C; solid lines, Toth model.

The optimised parameters obtained from the model regression are listed in Table 4.13.

The deviations of the calculated capacities from the measured data ( $Q_i^{meas} - Q_i^{calc}$ ) are

presented in Figure 4.24. As shown in Figures 4.23(a) and (b), the empirical Toth model fits the data very well at the investigated temperatures. The deviations between the measured and calculated capacities shown in Figure 4.24 are in the range of  $\pm 0.1$  for most of the pressure points (especially at low pressures). A good regression of the model in the low pressure range is critical for describing the multicomponent data properly. The standard deviations (SDs) of the Toth model listed in Table 4.13 are small, showing that this model fits the equilibrium adsorption data well. The model predictions of the CO<sub>2</sub> adsorption capacities of *C-15-1.5-750* and *N-30-2.5-750* made from the best-fit parameters are shown as solid lines in Figures 4.23(a) and (b), respectively.

Table 4.13: Fitting parameters of the Toth model.

Sample	Toth Model				
	$Q_{mi}$ (mol/kg)	$K_i^0 \times 10^8$ (MPa)	$-\Delta H_i$ (kJ/mol)	$n_i$	SD (mol/kg)
C-15-1.5-750	9	1.45	31.5	0.5	0.02
N-30-2.5-750	12	1.4	34	0.55	0.08

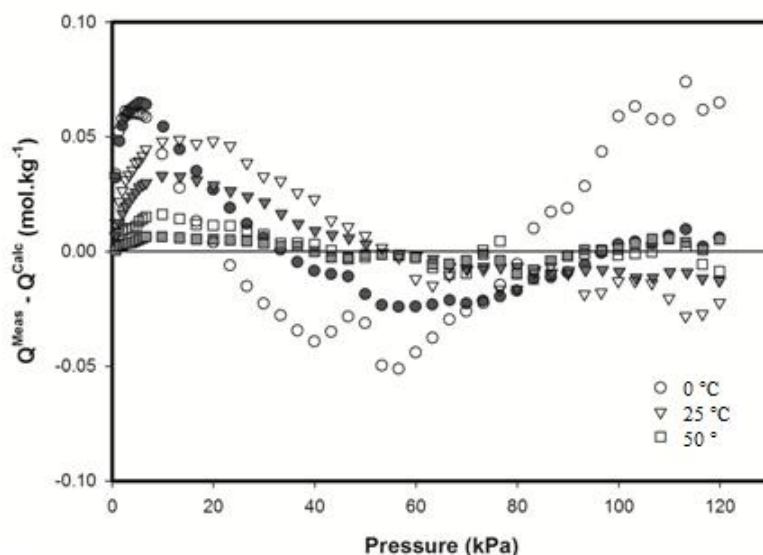


Figure 4.24: Deviations between the measured and the calculated carbon dioxide adsorption capacities of Toth Model for the ACs prepared under CO<sub>2</sub>; filled symbols; and under N<sub>2</sub>, empty symbols.

## CHAPTER IV: CONCLUSION

### 5.1 PART 1: Palm shell based AC prepared by zinc chloride chemical activation using response surface methodology

In this study, RSM was used to optimise the process conditions for palm-shell-based AC. A CCD was conducted to study the effects of four variables on the properties of the prepared AC: microwave power, microwave radiation time, impregnation ratio ( $\text{ZnCl}_2$ : precursor), and particle size. Through process optimisation, it was found that the experimental values for the MB adsorption and yield agreed satisfactory with the predicted value. The optimum conditions for the production of AC from oil palm shell by microwave radiation and zinc chloride activation have been identified as the following: microwave power of 1200 W, activation time of 15 min, impregnation ratio of 1.65 and particle size of 2 mm. Based on these results, microwave power and activation time were the most significant factors affecting on carbon yield and MB adsorption, respectively. The AC prepared under optimum conditions exhibited a type I isotherm, indicating that it is a microporous adsorbent.

### 5.2 PART 2: Comparison of oil palm shell-based ACs produced by microwave and conventional heating methods using zinc chloride activation

Microporous ACs with high  $S_{\text{BET}}$  were prepared from palm shell by microwave and conventional heating methods. The textural properties of the ACs were analyzed by  $\text{N}_2$  adsorption at  $-196\text{ }^\circ\text{C}$  and SEM to investigate the effects of the different treatments. The optimum specific surface area ( $S_{\text{BET}}$ ) was achieved at  $\text{ZnCl}_2 0.65$  for both heating methods, and both showed microporous structures. The textural characterization indicated that by increasing the chemical ratio, the adsorption capacity of the microwave and conventional samples increased to an optimum point due to the formation of new pores, and then decreased owing to a widening and burning of the

existing pores. The microwave samples illustrated higher portions of wide micropores and mesopores than the conventional samples at a high impregnation ratio of Zn0.9.

SEM micrographs showed that the external surface structure of the microwave and conventional samples were totally different due to the different types of heating. FTIR spectra of the ACs prepared by both methods showed that the microwave samples contain less weak bands than the conventional samples, indicating the ready and quick release of weak bands in microwave activation due to energy dissipation processes through dipole rotations and ionic conduction at the molecular level.

### **5.3 PART 3: Production of ACs from oil palm shell via microwave-assisted KOH activation in the presence of CO<sub>2</sub> or N<sub>2</sub> for CO<sub>2</sub> adsorption**

Oil palm shell was chemically activated with KOH using a microwave heat source. The effects of the preparation variables; activation time, impregnation ratio and microwave power level were investigated on the textural and surface chemical properties of the prepared ACs. According to the characterization results a maximum  $S_{\text{BET}}$  of 1630.4  $\text{m}^2/\text{g}$  is obtained using an irradiation time of 30 min, IR of 2.5 and microwave power of 750 W. The CO<sub>2</sub> activation requires a shorter activation time to reach the maximum  $S_{\text{BET}}$  than the N<sub>2</sub> activation because CO<sub>2</sub> reacts with the carbon to generate more pores. The ACs prepared under N<sub>2</sub> have more ultramicropores than those activated under CO<sub>2</sub>. This result can be attributed to the oxidising behaviour of CO<sub>2</sub>, which penetrates the carbon surface and enlarges the ultramicropores created during the KOH activation. In contrast, N<sub>2</sub> does not interfere with the activation process. The ACs produced under N<sub>2</sub> and CO<sub>2</sub> adsorb similar amounts of CO<sub>2</sub> at low pressures (up to 140 kPa), and their high CO<sub>2</sub> adsorption capacities are comparable to those of other adsorbents reported in the literature.

## REFERENCES

- Abdel-Nasser A, El-Hendawy. (2003). Influence of HNO<sub>3</sub> oxidation on the structure and adsorptive properties of corncob-based activated carbon. *Carbon*, 41(4), 713-722.
- Abdel-Nasser A, El-Hendawy. (2009). An insight into the KOH activation mechanism through the production of microporous activated carbon for the removal of Pb<sup>2+</sup> cations. *Applied Surface Science*, 255(6), 3723-3730.
- Abnisa, Faisal, Arami-Niya, Arash, Daud, W. M. A. Wan, & Sahu, J. N. (2013a). Characterization of Bio-oil and Bio-char from Pyrolysis of Palm Oil Wastes. *BioEnergy Research*, 6(2), 830-840. doi: 10.1007/s12155-013-9313-8.
- Abnisa, Faisal, Arami-Niya, Arash, Wan Daud, W. M. A. Sahu, J. N., Noor, I. M. (2013b). Utilization of oil palm tree residues to produce bio-oil and bio-char via pyrolysis. *Energy Conversion and Management*, 76(0), 1073-1082.
- Adinata, Donni, Wan Daud, Wan Mohd Ashri, & Aroua, Mohd Kheireddine. (2007). Preparation and characterization of activated carbon from palm shell by chemical activation with K<sub>2</sub>CO<sub>3</sub>. *Bioresource Technology*, 98(1), 145-149.
- Aguilar, Croswel, García, Rafael, Soto-Garrido, Gabriela, & Arriagada, Renán. (2003). Catalytic wet air oxidation of aqueous ammonia with activated carbon. *Applied Catalysis B: Environmental*, 46(2), 229-237.
- Albin, Pintar. (2003). Catalytic processes for the purification of drinking water and industrial effluents. *Catalysis Today*, 77(4), 451-465.
- Almansa, C., Molina-Sabio, M., & Rodríguez-Reinoso, F. (2004). Adsorption of methane into ZnCl<sub>2</sub>-activated carbon derived discs. *Microporous and Mesoporous Materials*, 76(1-3), 185-191.
- Ania, C. O., Menéndez, J. A., Parra, J. B., & Pis, J. J. (2004). Microwave-induced regeneration of activated carbons polluted with phenol. A comparison with conventional thermal regeneration. *Carbon*, 42(7), 1383-1387.
- Ania, C. O., Parra, J. B., Menéndez, J. A., & Pis, J. J. (2005). Effect of microwave and conventional regeneration on the microporous and mesoporous network and on the adsorptive capacity of activated carbons. *Microporous and Mesoporous Materials*, 85(1-2), 7-15.
- Ania, C. O., Parra, J. B., Menéndez, J. A., & Pis, J. J. (2007). Microwave-assisted regeneration of activated carbons loaded with pharmaceuticals. *Water Research*, 41(15), 3299-3306.
- Appleton, T. J., Colder, R. I., Kingman, S. W., Lowndes, I. S., & Read, A. G. (2005). Microwave technology for energy-efficient processing of waste. *Applied Energy*, 81(1), 85-113.
- Arami-Niya, A., Abnisa, F., Shafeeyan, M.S., Wan Daud, W.M.A., & Sahu, J.N. (2012). Optimization of synthesis and characterization of palm shell-based bio-char as a by-product of bio-oil production process. *Bioresources*, 7, 246-264.
- Arami-Niya, Arash, Daud, Wan Mohd Ashri Wan, & Mjalli, Farouq S. (2010). Using granular activated carbon prepared from oil palm shell by ZnCl<sub>2</sub> and physical activation for methane adsorption. *Journal of Analytical and Applied Pyrolysis*, 89(2), 197-203.
- Arami-Niya, A., Wan Daud, W.M.A, Mjalli, S. F, Abnisa, F., & Shafeeyan, M.S. (2011) Production of microporous palm shell based activated carbon for methane adsorption: Modeling and optimization using response surface methodology. *Chemical Engineering Research and Design*, 90(6), 776-784.
- Bansal, R.C., Donnet, J.B., Stoeckli, F. (1988). Activated Carbon. *Marcel Dekker, Inc., New York*, 482.

- Basta, A. H., Fierro, V., El-Saied, H., & Celzard, A. (2009). 2-Steps KOH activation of rice straw: An efficient method for preparing high-performance activated carbons. *Bioresource Technology*, *100*(17), 3941-3947.
- Biniak, S., Szymański, G., Siedlewski, J., & Świątkowski, A. (1997). The characterization of activated carbons with oxygen and nitrogen surface groups. *Carbon*, *35*(12), 1799-1810.
- Boonamnuyvitaya, Virote, Sae-ung, Srisuda, & Tanthapanichakoon, Wiwut. (2005). Preparation of activated carbons from coffee residue for the adsorption of formaldehyde. *Separation and Purification Technology*, *42*(2), 159-168.
- Budinova, T., Ekinci, E., Yardim, F., Grimm, A., Björnbom, E., Minkova, V., & Goranova, M. (2006). Characterization and application of activated carbon produced by H<sub>3</sub>PO<sub>4</sub> and water vapor activation. *Fuel Processing Technology*, *87*(10), 899-905.
- Chang, Jen-Lin, Chang, Kuo-Hsin, Hu, Chi-Chang, Cheng, Wan-Ling, & Zen, Jyh-Myng. (2010). Improved voltammetric peak separation and sensitivity of uric acid and ascorbic acid at nanoplatelets of graphitic oxide. *Electrochemistry Communications*, *12*(4), 596-599.
- Dąbrowski, A., Podkościelny, P., Hubicki, Z., & Barczak, M. (2005). Adsorption of phenolic compounds by activated carbon—a critical review. *Chemosphere*, *58*(8), 1049-1070.
- Deng, Hui , Yang, Le , Tao, Guanghui , & Dai, Jiulei. (2009). Preparation and characterization of activated carbon from cotton stalk by microwave assisted chemical activation—Application in methylene blue adsorption from aqueous solution. *Journal of Hazardous Materials*, *166*(2-3), 1514-1521.
- Deng, Hui, Li, Guoxue, Yang, Hongbing, Tang, Jiping, & Tang, Jiangyun. (2010). Preparation of activated carbons from cotton stalk by microwave assisted KOH and K<sub>2</sub>CO<sub>3</sub> activation. *Chemical Engineering Journal*, *163*(3), 373-381.
- Deng, Hui, Zhang, Genlin, Xu, Xiaolin, Tao, Guanghui, & Dai, Jiulei. (2010). Optimization of preparation of activated carbon from cotton stalk by microwave assisted phosphoric acid-chemical activation. *Journal of Hazardous Materials*, *182*(1-3), 217-224.
- Dias, Joana M., Alvim-Ferraz, Maria C. M., Almeida, Manuel F., Rivera-Utrilla, José, & Sánchez-Polo, Manuel. (2007). Waste materials for activated carbon preparation and its use in aqueous-phase treatment: A review. *Journal of Environmental Management*, *85*(4), 833-846.
- Duong, D. D. . (1998). Adsorption analysis: equilibria and kinetics;. *Imperial College Press: London*, xxi.
- E.P. Barrett, L.G. Joyner, P.P. Halenda. (1951). The determination of pore volume and area distributions in porous substances I. Computations from nitrogen isotherms. *J. Am. Cem. Soc.* , *73*, 373-380.
- El-Hendawy, Abdel-Nasser A., Alexander, Andrew J., Andrews, Robert J., & Forrest, Gavin. (2008). Effects of activation schemes on porous, surface and thermal properties of activated carbons prepared from cotton stalks. *Journal of Analytical and Applied Pyrolysis*, *82*(2), 272-278.
- El-Hendawy, Abdel-Nasser A., Samra, S. E., & Girgis, B. S. (2001). Adsorption characteristics of activated carbons obtained from corncobs. *Colloids and Surfaces A: Physicochemical and Engineering Aspects*, *180*(3), 209-221.
- El-Sayed, Yehya, & Bandosz, Teresa J. (2004). Adsorption of valeric acid from aqueous solution onto activated carbons: role of surface basic sites. *Journal of Colloid and Interface Science*, *273*(1), 64-72.



- El-Sheikh, Amjad H., Newman, Alan P., Al-Daffae, Hafid K., Phull, Suki, & Cresswell, Neil. (2004). Characterization of activated carbon prepared from a single cultivar of Jordanian Olive stones by chemical and physicochemical techniques. *Journal of Analytical and Applied Pyrolysis*, 71(1), 151-164.
- Ello, Aimé Serge, de Souza, Luiz K. C., Trokourey, Albert, & Jaroniec, Mietek. (2013). Development of microporous carbons for CO<sub>2</sub> capture by KOH activation of African palm shells. *Journal of CO<sub>2</sub> Utilization*, 2(0), 35-38.
- Esteves, Isabel A. A. C., Lopes, Marta S. S., Nunes, Pedro M. C., & Mota, José P. B. (2008). Adsorption of natural gas and biogas components on activated carbon. *Separation and Purification Technology*, 62(2), 281-296.
- Faria, P. C. C., Órfão, J. J. M., & Pereira, M. F. R. (2004). Adsorption of anionic and cationic dyes on activated carbons with different surface chemistries. *Water Research*, 38(8), 2043-2052.
- Feron, P. H. M., & Jansen, A. E. (1997). The production of carbon dioxide from flue gas by membrane gas absorption. *Energy Conversion and Management*, 38, Supplement(0), S93-S98.
- Figueiredo, J. L., Pereira, M. F. R., Freitas, M. M. A., & Órfão, J. J. M. (1999). Modification of the surface chemistry of activated carbons. *Carbon*, 37(9), 1379-1389.
- Foo, K. Y., & Hameed, B. H. Microwave-assisted preparation and adsorption performance of activated carbon from biodiesel industry solid residue: Influence of operational parameters. *Bioresource Technology*, 103(1), 398-404.
- Foo, K. Y., & Hameed, B. H. (2011a). Microwave-assisted preparation of oil palm fiber activated carbon for methylene blue adsorption. *Chemical Engineering Journal*, 166(2), 792-795.
- Foo, K. Y., & Hameed, B. H. (2011b). Microwave assisted preparation of activated carbon from pomelo skin for the removal of anionic and cationic dyes. *Chemical Engineering Journal*, 173(2), 385-390.
- Foo, K. Y., & Hameed, B. H. (2011c). Preparation and characterization of activated carbon from pistachio nut shells via microwave-induced chemical activation. *Biomass and Bioenergy*, 35(7), 3257-3261.
- Foo, K. Y., & Hameed, B. H. (2011d). Preparation and characterization of activated carbon from sunflower seed oil residue via microwave assisted K<sub>2</sub>CO<sub>3</sub> activation. *Bioresource Technology*, 102(20), 9794-9799.
- Foo, K. Y., & Hameed, B. H. (2011e). Preparation of activated carbon from date stones by microwave induced chemical activation: Application for methylene blue adsorption. *Chemical Engineering Journal*, 170(1), 338-341.
- Foo, K. Y., & Hameed, B. H. (2011f). Preparation of oil palm (*Elaeis*) empty fruit bunch activated carbon by microwave-assisted KOH activation for the adsorption of methylene blue. *Desalination*, 275(1-3), 302-305.
- Foo, K. Y., & Hameed, B. H. (2011g). Utilization of rice husks as a feedstock for preparation of activated carbon by microwave induced KOH and K<sub>2</sub>CO<sub>3</sub> activation. *Bioresource Technology*, 102(20), 9814-9817.
- Foo, K. Y., & Hameed, B. H. (2012a). Microwave-assisted preparation and adsorption performance of activated carbon from biodiesel industry solid residue: Influence of operational parameters. *Bioresource Technology*, 103(1), 398-404.
- Foo, K. Y., & Hameed, B. H. (2012b). Porous structure and adsorptive properties of pineapple peel based activated carbons prepared via microwave assisted KOH and K<sub>2</sub>CO<sub>3</sub> activation. *Microporous and Mesoporous Materials*, 148(1), 191-195.

- Foo, K. Y., & Hameed, B. H. (2012c). Preparation, characterization and evaluation of adsorptive properties of orange peel based activated carbon via microwave induced K<sub>2</sub>CO<sub>3</sub> activation. *Bioresource Technology*, 104(0), 679-686.
- Franca, Adriana S., Oliveira, Leandro S., Nunes, Anne A., & Alves, Cibele C. O. (2010). Microwave assisted thermal treatment of defective coffee beans press cake for the production of adsorbents. *Bioresource Technology*, 101(3), 1068-1074.
- Francisco, Rodríguez-reinoso. (1998). The role of carbon materials in heterogeneous catalysis. *Carbon*, 36(3), 159-175.
- G.Chih-Ju, Jou. (1998). Application of activated carbon in a microwave radiation field to treat trichloroethylene. *Carbon*, 36(11), 1643-1648.
- González, Juan F., Encinar, José M., González-García, Carmen M., Sabio, E., Ramiro, A., Canito, José L., & Gañán, José. (2006). Preparation of activated carbons from used tyres by gasification with steam and carbon dioxide. *Applied Surface Science*, 252(17), 5999-6004.
- Guo, Jia, & Lua, Aik Chong. (2000). Preparation of activated carbons from oil-palm-stone chars by microwave-induced carbon dioxide activation. *Carbon*, 38(14), 1985-1993.
- Guo, Jia, & Lua, Aik Chong. (2002). Microporous Activated Carbons Prepared from Palm Shell by Thermal Activation and Their Application to Sulfur Dioxide Adsorption. *Journal of Colloid and Interface Science*, 251(2), 242-247.
- Guo, Yupeng, Zhao, Jingzhe, Zhang, Hui, Yang, Shaofeng, Qi, Jurui, Wang, Zichen, & Xu, Hongding. (2005). Use of rice husk-based porous carbon for adsorption of Rhodamine B from aqueous solutions. *Dyes and Pigments*, 66(2), 123-128.
- Haimour, N. M., & Emeish, S. (2006). Utilization of date stones for production of activated carbon using phosphoric acid. *Waste Management*, 26(6), 651-660.
- Hameed, B. H., Tan, I. A. W., & Ahmad, A. L. (2008). Optimization of basic dye removal by oil palm fibre-based activated carbon using response surface methodology. *Journal of Hazardous Materials*, 158(2-3), 324-332.
- Hayashi, Jun'ichi, Horikawa, Toshihide, Takeda, Isao, Muroyama, Katsuhiko, & Nasir Ani, Farid. (2002). Preparing activated carbon from various nutshells by chemical activation with K<sub>2</sub>CO<sub>3</sub>. *Carbon*, 40(13), 2381-2386.
- He, Xiao-jun, Wang, Ting, Qiu, Jie-shan, Zhang, Xiao-yong, Wang, Xiao-ting, & Zheng, Ming-dong. (2011). Effect of microwave-treatment time on the properties of activated carbons for electrochemical capacitors. *New Carbon Materials*, 26(4), 313-319.
- He, Xiaojun, Geng, Yejing, Qiu, Jieshan, Zheng, Mingdong, Long, Suan, & Zhang, Xiaoyong. (2010). Effect of activation time on the properties of activated carbons prepared by microwave-assisted activation for electric double layer capacitors. *Carbon*, 48(5), 1662-1669.
- Hejazifar, Mahtab, Azizian, Saeid, Sarikhani, Hassan, Li, Qiang, & Zhao, Dongyuan. (2011). Microwave assisted preparation of efficient activated carbon from grapevine rhytidome for the removal of methyl violet from aqueous solution. *Journal of Analytical and Applied Pyrolysis*, 92(1), 258-266.
- Hirata, Mizuho, Kawasaki, Naohito, Nakamura, Takeo, Matsumoto, Kazuoki, Kabayama, Mineaki, Tamura, Takamichi, & Tanada, Seiki. (2002). Adsorption of Dyes onto Carbonaceous Materials Produced from Coffee Grounds by Microwave Treatment. *Journal of Colloid and Interface Science*, 254(1), 17-22.
- Hoseinzadeh Hesas, Roozbeh, Arami-Niya, Arash, Wan Daud, Wan Mohd Ashri, & Sahu, J. N. (2013a). Comparison of oil palm shell-based activated carbons produced by microwave and conventional heating methods using zinc chloride activation. *Journal of Analytical and Applied Pyrolysis*, 104(0), 176-184.

- Hoseinzadeh Hesas, Roozbeh, Arami-Niya, Arash, Wan Daud, Wan Mohd Ashri, & Sahu, J. N. (2013b). Preparation of granular activated carbon from oil palm shell by microwave-induced chemical activation: Optimisation using surface response methodology. *Chemical Engineering Research and Design*, *91*(12), 2447-2456.
- Hoseinzadeh Hesas, Roozbeh, Wan Daud, Wan Mohd Ashri, Sahu, J. N., & Arami-Niya, Arash. (2013). The effects of a microwave heating method on the production of activated carbon from agricultural waste: A review. *Journal of Analytical and Applied Pyrolysis*, *100*(0), 1-11.
- Hsu, Li-Yeh, & Teng, Hsisheng. (2000). Influence of different chemical reagents on the preparation of activated carbons from bituminous coal. *Fuel Processing Technology*, *64*(1-3), 155-166.
- Hu, Zhonghua, & Srinivasan, M. P. (2001). Mesoporous high-surface-area activated carbon. *Microporous and Mesoporous Materials*, *43*(3), 267-275.
- Huang, Lihui, Sun, Yuanyuan, Wang, Weiliang, Yue, Qinyan, & Yang, Tao. (2011). Comparative study on characterization of activated carbons prepared by microwave and conventional heating methods and application in removal of oxytetracycline (OTC). *Chemical Engineering Journal*, *171*(3), 1446-1453.
- Ioannidou, O., & Zabaniotou, A. (2007). Agricultural residues as precursors for activated carbon production—A review. *Renewable and Sustainable Energy Reviews*, *11*(9), 1966-2005.
- Izquierdo, M. T., Rubio, B., Mayoral, C., & Andrés, J. M. (2001). Modifications to the surface chemistry of low-rank coal-based carbon catalysts to improve flue gas nitric oxide removal. *Applied Catalysis B: Environmental*, *33*(4), 315-324.
- Jagtøyen, Marit, & Derbyshire, Frank. (1998). Activated carbons from yellow poplar and white oak by H<sub>3</sub>PO<sub>4</sub> activation. *Carbon*, *36*(7-8), 1085-1097.
- Jerzy, Zawadzki. (1988). Infrared studies on the adsorption of n-butylamine on carbon films. *Carbon*, *26*(2), 183-188.
- Ji, Yongbin, Li, Tiehu, Zhu, Li, Wang, Xiaoxian, & Lin, Qilang. (2007). Preparation of activated carbons by microwave heating KOH activation. *Applied Surface Science*, *254*(2), 506-512.
- Jones, D. A., Lelyveld, T. P., Mavrofidis, S. D., Kingman, S. W., & Miles, N. J. (2002). Microwave heating applications in environmental engineering—a review. *Resources, Conservation and Recycling*, *34*(2), 75-90.
- K.Y. Foo, B.H. Hameed. (2011). Porous structure and adsorptive properties of the pineapple peel based activated carbons prepared via microwave assisted KOH and K<sub>2</sub>CO<sub>3</sub> activation. *Microporous and Mesoporous Materials*, *148*(1), 191-195.
- Kalderis, Dimitrios, Bethanis, Sophia, Paraskeva, Panagiota, & Diamadopoulos, Evan. (2008). Production of activated carbon from bagasse and rice husk by a single-stage chemical activation method at low retention times. *Bioresource Technology*, *99*(15), 6809-6816.
- Karim, Mohammad Mainul, Das, Ajoy Kumar, & Lee, Sang Hak. (2006). Treatment of colored effluent of the textile industry in Bangladesh using zinc chloride treated indigenous activated carbons. *Analytica Chimica Acta*, *576*(1), 37-42.
- Kazi E, Haque. (1999). Microwave energy for mineral treatment processes—a brief review. *International Journal of Mineral Processing*, *57*(1), 1-24.
- Kubota, Mitsuhiro, Hata, Atsushi, & Matsuda, Hitoki. (2009). Preparation of activated carbon from phenolic resin by KOH chemical activation under microwave heating. *Carbon*, *47*(12), 2805-2811.
- Li, Dawei, Zhang, Yaobin, Quan, Xie, & Zhao, Yazhi. (2009). Microwave thermal remediation of crude oil contaminated soil enhanced by carbon fiber. *Journal of Environmental Sciences*, *21*(9), 1290-1295.

- Li, Wei, Peng, Jinhui, Zhang, Libo, Yang, Kunbin, Xia, Hongying, Zhang, Shimin, & Guo, Sheng-hui. (2009). Preparation of activated carbon from coconut shell chars in pilot-scale microwave heating equipment at 60 kW. *Waste Management*, 29(2), 756-760.
- Li, Wei, Zhang, Li-bo, Peng, Jin-hui, Li, Ning, & Zhu, Xue-yun. (2008). Preparation of high surface area activated carbons from tobacco stems with K<sub>2</sub>CO<sub>3</sub> activation using microwave radiation. *Industrial Crops and Products*, 27(3), 341-347.
- Li, Y. H., Lee, C. W., & Gullett, B. K. (2002). The effect of activated carbon surface moisture on low temperature mercury adsorption. *Carbon*, 40(1), 65-72.
- Liu, Qing-Song, Zheng, Tong, Li, Nan, Wang, Peng, & Abulikemu, Gulizhaer. (2010). Modification of bamboo-based activated carbon using microwave radiation and its effects on the adsorption of methylene blue. *Applied Surface Science*, 256(10), 3309-3315.
- Liu, Qing Song, Zheng, Tong, Wang, Peng, & Guo, Liang. (2010). Preparation and characterization of activated carbon from bamboo by microwave-induced phosphoric acid activation. *Industrial Crops and Products*, 31(2), 233-238.
- Maldhure, Atul V., & Ekhe, J. D. (2011). Preparation and characterizations of microwave assisted activated carbons from industrial waste lignin for Cu(II) sorption. *Chemical Engineering Journal*, 168(3), 1103-1111.
- Menéndez, J. A., Arenillas, A., Fidalgo, B., Fernández, Y., Zubizarreta, L., Calvo, E. G., & Bermúdez, J. M. (2010). Microwave heating processes involving carbon materials. *Fuel Processing Technology*, 91(1), 1-8.
- Menéndez, J. A., Menéndez, E. M., Iglesias, M. J., García, A., & Pis, J. J. (1999). Modification of the surface chemistry of active carbons by means of microwave-induced treatments. *Carbon*, 37(7), 1115-1121.
- Menezes, Romualdo R., Souto, Pollyane M., & Kiminami, Ruth H. G. A. (2007). Microwave hybrid fast sintering of porcelain bodies. *Journal of Materials Processing Technology*, 190(1-3), 223-229.
- Métivier-Pignon, Hélène, Faur-Brasquet, Catherine, & Le Cloirec, Pierre. (2003). Adsorption of dyes onto activated carbon cloths: approach of adsorption mechanisms and coupling of ACC with ultrafiltration to treat coloured wastewaters. *Separation and Purification Technology*, 31(1), 3-11.
- Mikhalev, Yuri, & Øye, Harald A. (1996). Adsorption of metallic sodium in carbon cathode materials. *Carbon*, 34(1), 37-41.
- Montgomery, D.C. (2001). Design and Analysis of Experiments. *John Wiley and Sons Inc, 5th ed. , New york*.
- Moreno-Castilla, C., López-Ramón, M. V., & Carrasco-Marín, F. (2000). Changes in surface chemistry of activated carbons by wet oxidation. *Carbon*, 38(14), 1995-2001.
- Namasivayam, C., & Sangeetha, D. (2006). Recycling of agricultural solid waste, coir pith: Removal of anions, heavy metals, organics and dyes from water by adsorption onto ZnCl<sub>2</sub> activated coir pith carbon. *Journal of Hazardous Materials*, 135(1-3), 449-452.
- Nian, Yau-Ren, & Teng, Hsisheng. (2003). Influence of surface oxides on the impedance behavior of carbon-based electrochemical capacitors. *Journal of Electroanalytical Chemistry*, 540(0), 119-127.
- Oghbaei, Morteza, & Mirzaee, Omid. (2010). Microwave versus conventional sintering: A review of fundamentals, advantages and applications. *Journal of Alloys and Compounds*, 494(1-2), 175-189.
- Pereira, Manuel Fernando R., Soares, Samanta F., Órfão, José J. M., & Figueiredo, José L. (2003). Adsorption of dyes on activated carbons: influence of surface chemical groups. *Carbon*, 41(4), 811-821.

- Pütün, Ayşe E., Özbay, Nurgül, Önal, Eylem P., & Pütün, Ersan. (2005). Fixed-bed pyrolysis of cotton stalk for liquid and solid products. *Fuel Processing Technology*, 86(11), 1207-1219.
- Puziy, Alexander M., Poddubnaya, Olga I., Martínez-Alonso, Amelia, Castro-Muñiz, Alberto, Suárez-García, Fabian, & Tascón, Juan M. D. (2007). Oxygen and phosphorus enriched carbons from lignocellulosic material. *Carbon*, 45(10), 1941-1950.
- Puziy, Alexander M., Poddubnaya, Olga I., Martínez-Alonso, Amelia, Suárez-García, Fabian, & Tascón, Juan M. D. (2005). Surface chemistry of phosphorus-containing carbons of lignocellulosic origin. *Carbon*, 43(14), 2857-2868.
- Ravikumar, K., Deebika, B., & Balu, K. (2005). Decolourization of aqueous dye solutions by a novel adsorbent: Application of statistical designs and surface plots for the optimization and regression analysis. *Journal of Hazardous Materials*, 122(1–2), 75-83.
- Rodríguez-Reinoso, F., & Molina-Sabio, M. (1992). Activated carbons from lignocellulosic materials by chemical and/or physical activation: an overview. *Carbon*, 30(7), 1111-1118.
- Rodríguez-Reinoso, F., & Molina-Sabio, M. (1998). Textural and chemical characterization of microporous carbons. *Advances in Colloid and Interface Science*, 76-77(0), 271-294.
- Román, S., González, J. F., González-García, C. M., & Zamora, F. (2008). Control of pore development during CO<sub>2</sub> and steam activation of olive stones. *Fuel Processing Technology*, 89(8), 715-720.
- Roosbeh Hoseinzadeh Hesas, Arash Arami-Niya, Wan Mohd Ashri Wan Daud, J.N. Sahu. (2013). Preparation and characterization of activated carbon from apple wastes by microwave- assisted phosphoric acid activation: Application in methylene blue adsorption. *bioresources*, 8(2), 2950-2966.
- Rouquerol, F., Rouquerol, J., Sing, K. (1999). Adsorption by Powders & Porous Solids: Principles, Methodology and Applications. Academic, London.
- Rouquerol, Françoise, Rouquerol, Jean, & Sing, Kenneth. (1999). Chapter 6 - Assessment of Surface Area *Adsorption by Powders and Porous Solids* (pp. 165-189). London: Academic Press.
- Rodríguez-Reinoso F, Linares-Solano A. (1998). Microporous structure of activated carbons as revealed by adsorption methods. In: Thrower PA, editor. *Chemistry and physics of carbon*,. New York: Marcel Dekker, 21, 1–146.
- S.J. Gregg, K.S. Sing. (1982). Adsorption, Surface Area and Porosity. *Academic Press, London*.
- Sabio, E., González, E., González, J. F., González-García, C. M., Ramiro, A., & Gañan, J. (2004). Thermal regeneration of activated carbon saturated with p-nitrophenol. *Carbon*, 42(11), 2285-2293.
- Sahu, J. N., Acharya, Jyotikusum, & Meikap, B. C. (2010). Optimization of production conditions for activated carbons from Tamarind wood by zinc chloride using response surface methodology. *Bioresource Technology*, 101(6), 1974-1982.
- Savova, D., Apak, E., Ekinçi, E., Yardim, F., Petrov, N., Budinova, T., Minkova, V. (2001). Biomass conversion to carbon adsorbents and gas. *Biomass and Bioenergy*, 21(2), 133-142.
- Sing, Kenneth S. W. (1998). Adsorption methods for the characterization of porous materials. *Advances in Colloid and Interface Science*, 76–77(0), 3-11.
- Stavropoulos, G. G., & Zabaniotou, A. A. (2009). Minimizing activated carbons production cost. *Fuel Processing Technology*, 90(7-8), 952-957.
- Stuart S, Barton. (1987). The adsorption of methylene blue by active carbon. *Carbon*, 25(3), 343-350.

- Suárez-García, F., Martínez-Alonso, A., & Tascón, J. M. D. (2002). A comparative study of the thermal decomposition of apple pulp in the absence and presence of phosphoric acid. *Polymer Degradation and Stability*, 75(2), 375-383.
- Sudaryanto, Y., Hartono, S. B., Irawaty, W., Hindarso, H., & Ismadji, S. (2006). High surface area activated carbon prepared from cassava peel by chemical activation. *Bioresource Technology*, 97(5), 734-739.
- Sumathi, S., Bhatia, S., Lee, K. T., & Mohamed, A. R. (2009). Optimization of microporous palm shell activated carbon production for flue gas desulphurization: Experimental and statistical studies. *Bioresource Technology*, 100(4), 1614-1621.
- Szymański, Grzegorz S., Karpiński, Zbigniew, Biniak, Stanisław, & Świątkowski, Andrzej. (2002). The effect of the gradual thermal decomposition of surface oxygen species on the chemical and catalytic properties of oxidized activated carbon. *Carbon*, 40(14), 2627-2639.
- Tan, I. A. W., Ahmad, A. L., & Hameed, B. H. (2008a). Enhancement of basic dye adsorption uptake from aqueous solutions using chemically modified oil palm shell activated carbon. *Colloids and Surfaces A: Physicochemical and Engineering Aspects*, 318(1-3), 88-96.
- Tan, I. A. W., Ahmad, A. L., & Hameed, B. H. (2008b). Optimization of preparation conditions for activated carbons from coconut husk using response surface methodology. *Chemical Engineering Journal*, 137(3), 462-470.
- Tan, I. A. W., Hameed, B. H., & Ahmad, A. L. (2007). Equilibrium and kinetic studies on basic dye adsorption by oil palm fibre activated carbon. *Chemical Engineering Journal*, 127(1-3), 111-119.
- Thakur, Sanjay Kumar, Kong, Tung Siew, & Gupta, Manoj. (2007). Microwave synthesis and characterization of metastable (Al/Ti) and hybrid (Al/Ti+SiC) composites. *Materials Science and Engineering: A*, 452-453(0), 61-69.
- Thostenson, E. T., & Chou, T. W. (1999). Microwave processing: fundamentals and applications. *Composites Part A: Applied Science and Manufacturing*, 30(9), 1055-1071.
- Timur, Serkan, Kantarli, Ismail Cem, Onenc, Sermin, & Yanik, Jale. (2010). Characterization and application of activated carbon produced from oak cups pulp. *Journal of Analytical and Applied Pyrolysis*, 89(1), 129-136.
- Tonghua Wang, Suxia Tan, Changhai Liang. (2009). Preparation and characterization of activated carbon from wood via microwave-induced ZnCl<sub>2</sub> activation. *Carbon*, 47, 1880-1883.
- Tsai, W. T., Chang, C. Y., & Lee, S. L. (1998). A low cost adsorbent from agricultural waste corn cob by zinc chloride activation. *Bioresource Technology*, 64(3), 211-217.
- Valente Nabais, J. M., Carrott, P. J. M., Ribeiro Carrott, M. M. L., & Menéndez, J. A. (2004). Preparation and modification of activated carbon fibres by microwave heating. *Carbon*, 42(7), 1315-1320.
- Vargas, Diana P., Giraldo, L., & Moreno-Piraján, J. C. (2012). CO<sub>2</sub> adsorption on granular and monolith carbonaceous materials. *Journal of Analytical and Applied Pyrolysis*, 96(0), 146-152.
- Venkatesh, M. S., & Raghavan, G. S. V. (2004). An Overview of Microwave Processing and Dielectric Properties of Agri-food Materials. *Biosystems Engineering*, 88(1), 1-18.
- Vitolo, Sandra, & Seggiani, Maurizia. (2002). Mercury removal from geothermal exhaust gas by sulfur-impregnated and virgin activated carbons. *Geothermics*, 31(4), 431-442.

- Wang, Tonghua, Tan, Suxia, & Liang, Changhai. (2009). Preparation and characterization of activated carbon from wood via microwave-induced ZnCl<sub>2</sub> activation. *Carbon*, 47(7), 1880-1883.
- Wang, Xuejiang, Liang, Xia, Wang, Yin, Wang, Xin, Liu, Mian, Yin, Daqiang, . . . Zhang, Yalei. (2011). Adsorption of Copper (II) onto activated carbons from sewage sludge by microwave-induced phosphoric acid and zinc chloride activation. *Desalination*, 278(1-3), 231-237.
- Wartelle, L. H., Marshall, W. E., Toles, C. A., & Johns, M. M. (2000). Comparison of nutshell granular activated carbons to commercial adsorbents for the purge-and-trap gas chromatographic analysis of volatile organic compounds. *Journal of Chromatography A*, 879(2), 169-175.
- Xie, Zhipeng, Yang, Jinlong, Huang, Xiangdong, & Huang, Yong. (1999). Microwave processing and properties of ceramics with different dielectric loss. *Journal of the European Ceramic Society*, 19(3), 381-387.
- Xin-hui, Duan, Srinivasakannan, C., Jin-hui, Peng, Li-bo, Zhang, & Zheng-yong, Zhang. (2011a). Comparison of activated carbon prepared from Jatropha hull by conventional heating and microwave heating. *Biomass and Bioenergy*, 35(9), 3920-3926.
- Xin-hui, Duan, Srinivasakannan, C., Jin-hui, Peng, Li-bo, Zhang, & Zheng-yong, Zhang. (2011b). Preparation of activated carbon from Jatropha hull with microwave heating: Optimization using response surface methodology. *Fuel Processing Technology*, 92(3), 394-400.
- Yadoji, Purushotham, Peelamedu, Ramesh, Agrawal, Dinesh, & Roy, Rustum. (2003). Microwave sintering of Ni-Zn ferrites: comparison with conventional sintering. *Materials Science and Engineering: B*, 98(3), 269-278.
- Yagmur, Emine, Ozmak, Meryem, & Aktas, Zeki. (2008). A novel method for production of activated carbon from waste tea by chemical activation with microwave energy. *Fuel*, 87(15-16), 3278-3285.
- Yang, Jie, Shen, Zengmin, & Hao, Zibiao. (2004). Preparation of highly microporous and mesoporous carbon from the mesophase pitch and its carbon foams with KOH. *Carbon*, 42(8-9), 1872-1875.
- Yang, Kunbin, Peng, Jinhui, Srinivasakannan, C., Zhang, Libo, Xia, Hongying, & Duan, Xinhui. (2010). Preparation of high surface area activated carbon from coconut shells using microwave heating. *Bioresource Technology*, 101(15), 6163-6169.
- Yang, Ting, & Lua, Aik Chong. (2003). Characteristics of activated carbons prepared from pistachio-nut shells by physical activation. *Journal of Colloid and Interface Science*, 267(2), 408-417.
- Yu, V. B., Rybakov, K. I., & Semenov, V. E. . (2001). High-temperature microwave processing of materials. *Journal of Physics D: Applied Physics*, 34(13), R55.
- Yuen, Foo Keng, & Hameed, B. H. (2009). Recent developments in the preparation and regeneration of activated carbons by microwaves. *Advances in Colloid and Interface Science*, 149(1-2), 19-27.
- Zhang-Steenwinkel, Y., van der Zande, L. M., Castricum, H. L., Blik, A., van den Brink, R. W., & Elzinga, G. D. (2005). Microwave-assisted in-situ regeneration of a perovskite coated diesel soot filter. *Chemical Engineering Science*, 60(3), 797-804.



Contents lists available at SciVerse ScienceDirect

## Journal of Analytical and Applied Pyrolysis

journal homepage: [www.elsevier.com/locate/jaap](http://www.elsevier.com/locate/jaap)

## Review

## The effects of a microwave heating method on the production of activated carbon from agricultural waste: A review

Roozbeh Hoseinzadeh Hesas<sup>a</sup>, Wan Mohd Ashri Wan Daud<sup>a,\*</sup>, J.N. Sahu<sup>a,b</sup>, Arash Arami-Niya<sup>a</sup><sup>a</sup> Department of Chemical Engineering, Faculty of Engineering, University of Malaya, Kuala Lumpur 50603, Malaysia<sup>b</sup> Department of Chemical Engineering, Indian Institute of Technology (IIT), P.O. Kharagpur Technology, Kharagpur, West Bengal 721302, India

## ARTICLE INFO

## Article history:

Received 13 April 2012

Accepted 14 December 2012

Available online 24 December 2012

## Keywords:

Activated carbon

Agricultural waste

Microwave heating

Pore structure

Functional groups

## ABSTRACT

A review of the effect of a microwave treatment on the production of activated carbon (AC) from agricultural waste is presented in this study. Although the thermal heating method is one of the most usual and applicable methods for the production of AC, this method has some disadvantages such as a thermal gradient from the surface to the interior of a particle, high cost of heating, long preparation time and fast firing. A microwave radiation method has been used recently by many researchers as an alternative method for heating. In this review, these two different methods of producing AC were compared. Previous studies on the preparation of AC using a microwave radiation method showed that the more significant parameters are the microwave radiation time, the microwave power level, the impregnation ratio and the agent flow rate. Accordingly, in this review, the effects of these parameters on the physical and chemical properties of AC, such as the pore structure, the adsorption capacity, the carbon yield and the surface functional groups, were discussed. In general, the physical properties of AC (adsorption capacity, pore volume and carbon yield) improved when these parameters were enhanced up to their optimum points, and then these properties decreased when these parameters were increased beyond their optimum values. The carbon/oxygen ratio was increased by the microwave method due to the elimination of acidic oxygen-containing functional groups on the surfaces of the ACs.

© 2013 Elsevier B.V. All rights reserved.

## Contents

1. Introduction .....	2
2. Microwave heating methods .....	2
3. Effects of the microwave heating method on the physical properties of AC .....	3
3.1. Effects of microwave power on the physical structure of chemically activated carbon .....	4
3.2. Effects of microwave radiation time on the physical structure of chemically activated carbon .....	4
3.3. Effects of impregnation ratio on the physical structure of chemically activated carbon .....	5
3.4. Effects of microwave power and radiation time on the physical structure of physically activated carbon .....	5
3.5. Effects of different agents and agent flow rates on the physical structure of physically activated carbon .....	7
4. Effects of microwave-induced method on carbon yield .....	7
5. Effects of the microwave-induced method on the chemical properties of activated carbon .....	8
6. Conclusions .....	10
Acknowledgment .....	10
References .....	10

\* Corresponding author. Tel.: +60 3 79675297; fax: +60 3 79675319.

E-mail addresses: [roozbehhasas@gmail.com](mailto:roozbehhasas@gmail.com) (R. Hoseinzadeh Hesas), [ashri@um.edu.my](mailto:ashri@um.edu.my) (W.M.A. Wan Daud), [jay\\_sahu@yahoo.co.in](mailto:jay_sahu@yahoo.co.in) (J.N. Sahu), [arash.arami@yaho.com](mailto:arash.arami@yaho.com) (A. Arami-Niya).





Contents lists available at ScienceDirect

Chemical Engineering Research and Design

IChemE

journal homepage: [www.elsevier.com/locate/cherd](http://www.elsevier.com/locate/cherd)

# Preparation of granular activated carbon from oil palm shell by microwave-induced chemical activation: Optimisation using surface response methodology

Roozbeh Hoseinzadeh Hesas<sup>a</sup>, Arash Arami-Niya<sup>a</sup>, Wan Mohd Ashri Wan Daud<sup>a,\*</sup>, J.N. Sahu<sup>a,b</sup>

<sup>a</sup> Department of Chemical Engineering, Faculty of Engineering, University of Malaya, Kuala Lumpur 50603, Malaysia

<sup>b</sup> Department of Chemical Engineering, Indian Institute of Technology (IIT), Kharagpur, P.O. Kharagpur Technology, West Bengal 721302, India

## A B S T R A C T

In this study, waste palm shell was used to produce activated carbon (AC) using microwave radiation and zinc chloride as a chemical agent. The operating parameters of the preparation process were optimised by a combination of response surface methodology (RSM) and central composite design (CCD). The influence of the four major parameters, namely, microwave power, activation time, chemical impregnation ratio and particle size, on methylene blue (MB) adsorption capacity and AC yield were investigated. Based on the analysis of variance, microwave power and microwave radiation time were identified as the most influential factors for AC yield and MB adsorption capacity, respectively. The optimum preparation conditions are a microwave power of 1200 W, an activation time of 15 min, a ZnCl<sub>2</sub> impregnation ratio of 1.65 (g Zn/g precursor) and a particle size of 2 mm. The prepared AC under the optimised condition had a BET surface area ( $S_{\text{BET}}$ ) of 1253.5 m<sup>2</sup>/g with a total pore volume ( $V_{\text{tot}}$ ) of 0.83 cm<sup>3</sup>/g, which 56% of it was contributed to the micropore volume ( $V_{\text{mic}}$ ).

© 2013 The Institution of Chemical Engineers. Published by Elsevier B.V. All rights reserved.

**Keywords:** Activated carbon; Agricultural waste; Microwave heating; Pore structure; Functional groups; Chemical activation

## 1. Introduction

The discharge and effluence of dyes into the environment by some industries, including paper, leather and plastic, is a major concern of the government and the public (Métivier-Pignon et al., 2003; Ravikumar et al., 2005). Among the hazardous dyes, methylene blue (MB) is a particularly common substance in many dyeing industries and has strong effects on the human body, such as causing vomiting and inducing shock (Tan et al., 2008). Therefore, the treatments of such dyes are a significant issue. One of the most common methods used to treat dyes is adsorption, which is a simple approach to eliminate pollutants. Activated carbon (AC) has been heavily used as a solid adsorbent in many gas and liquid processes due to its highly desirable physical and chemical properties, such as its

controllable and highly developed porosity, large surface area, high surface reactivity and highly modifiable surface, which facilitates a broad range of surface chemistries (Abdel-Nasser, 2009; Arami-Niya et al., 2012a; Dias et al., 2007). Therefore, due to the abovementioned properties of AC and other characteristics, including its low acid/base reactivity and thermostability, AC is used in a variety of applications, including a catalyst or catalyst support and in purification and separation processes, especially for pollutants that are difficult to colour and the recovery or purification of chemicals (Hejazifar et al., 2011; Huang et al., 2011; Ioannidou and Zabaniotou, 2007; Stavropoulos and Zabaniotou, 2009). The adsorption capacity of AC is determined by its internal porosity, surface area, pore size distribution and pore volume, all of which are significantly affected by the physical and chemical properties of the

\* Corresponding author. Tel.: +60 3 79675297; fax: +60 3 79675319.

E-mail addresses: [roozbehhesas@gmail.com](mailto:roozbehhesas@gmail.com) (R. Hoseinzadeh Hesas), [arash.araminiya@yahoo.com](mailto:arash.araminiya@yahoo.com) (A. Arami-Niya), [ashri@um.edu.my](mailto:ashri@um.edu.my) (W.M.A. Wan Daud), [jay.sahu@yahoo.co.in](mailto:jay.sahu@yahoo.co.in) (J.N. Sahu).

Received 4 February 2013; Received in revised form 20 May 2013; Accepted 4 June 2013

0263-8762/\$ – see front matter © 2013 The Institution of Chemical Engineers. Published by Elsevier B.V. All rights reserved.  
<http://dx.doi.org/10.1016/j.cherd.2013.06.004>



Contents lists available at ScienceDirect

# Journal of Analytical and Applied Pyrolysis

journal homepage: [www.elsevier.com/locate/jaap](http://www.elsevier.com/locate/jaap)



## Comparison of oil palm shell-based activated carbons produced by microwave and conventional heating methods using zinc chloride activation

Roozbeh Hoseinzadeh Hesas<sup>a</sup>, Arash Arami-Niya<sup>a</sup>, Wan Mohd Ashri Wan Daud<sup>a,\*</sup>, J.N. Sahu<sup>a,b</sup>

<sup>a</sup> Department of Chemical Engineering, Faculty of Engineering, University of Malaya, 50603 Kuala Lumpur, Malaysia

<sup>b</sup> Department of Chemical Engineering, Indian Institute of Technology (IIT), Kharagpur, P.O. Kharagpur Technology, West Bengal 721302, India

### ARTICLE INFO

#### Article history:

Received 26 March 2013

Accepted 13 August 2013

Available online xxx

#### Keywords:

Oil palm shell  
Activated carbon  
Microwave  
Zinc chloride

### ABSTRACT

Oil palm shell was used to prepare activated carbons by microwave irradiation and conventional heating methods using zinc chloride as the activation agent. The effects of the weight ratio of zinc chloride to palm shell on the textual and surface chemical properties of prepared activated carbon by both heating treatments were studied and compared in this study. The textual properties were investigated using nitrogen adsorption, ultimate and proximate analysis, and scanning electron microscopy (SEM), and Fourier transform infrared spectroscopy (FT-IR) was used to study the surface chemical properties. For both the microwave and conventionally prepared samples, the BET surface area was enhanced to a maximum at an impregnation ratio of 0.65 (Zn/palm shell) and then decreased with further increases in the chemical ratio. The total pore volume in the microwave samples increased continuously with increasing zinc chloride, while in the conventional samples, the total pore volume increased up to impregnation ratio of 0.65 and then decreased. The results showed that at the impregnation ratios of higher than 0.65, the rate of mesopore creation in microwave method is higher than that of conventional methods. FTIR spectra demonstrated that the C–H stretching of the palm shell disappeared completely in the microwave samples, where it was only reduced in the case of the conventional samples as a result of the different types of heating.

© 2013 Elsevier B.V. All rights reserved.

### 1. Introduction

Activated carbon is widely used to remove a variety of organic pollutants in gas and liquid phases due to its significant properties such as its large surface area, high porosity, internal structure and the presence of various surface functional groups [1,2]. Natural materials, such as coal or wood, are usually used as precursors for the production of commercial activated carbon, which can result in high costs of the adsorbents. Recently, the preparation of inexpensive activated carbons was achieved by the use of cheap precursor materials obtained from agricultural by-products and waste materials such as cotton stalk [3], coconut shell [4] and industrial waste lignin [5]. Palm shell is a by-product of the palm oil industry and was used as a raw material in this study due to its high carbon content, high density and low ash content. Palm shell is available

in large quantities of approximately 2 million tonnes annually in Malaysia.

Generally, two main methods are used to prepare activated carbon, which involve chemical and physical activation. In physical activation, the carbonaceous material is first pyrolyzed under an inert atmosphere and then activated by carbon dioxide, steam or a mixture of the two. In chemical activation, dehydrating reagents such as KOH, K<sub>2</sub>CO<sub>3</sub>, ZnCl<sub>2</sub> and H<sub>3</sub>PO<sub>4</sub> are used to impregnate the raw materials, which influence their pyrolytic decomposition and inhibit tar formation [6–8]. Chemical activation generally results in the preparation of activated carbon with a higher carbon yield and a better developed pore structure relative to physical activation [9]. Zinc chloride is an activation agent that results in a high yield and a high surface area, and thus is widely used in the chemical activation method [10,11].

In addition to the raw materials and preparation methods, the method of heating during activation can strongly affect the physical and chemical structure of the activated carbon produced. Conventional and microwave heating treatments constitute two different types of preparation methods. In conventional heating, the heat source is located outside the carbon bed and energy is transferred to

\* Corresponding author. Tel.: +60 3 79675297; fax: +60 3 79675319.  
E-mail addresses: [roozbehhesas@gmail.com](mailto:roozbehhesas@gmail.com) (R. Hoseinzadeh Hesas),  
[arash.araminiya@yahoo.com](mailto:arash.araminiya@yahoo.com) (A. Arami-Niya), [ashri@um.edu.my](mailto:ashri@um.edu.my)  
(W.M.A. Wan Daud), [jnsahu@um.edu.my](mailto:jnsahu@um.edu.my) (J.N. Sahu).



Contents lists available at ScienceDirect

# Journal of Industrial and Engineering Chemistry

journal homepage: [www.elsevier.com/locate/jiec](http://www.elsevier.com/locate/jiec)



## Microwave-assisted production of activated carbons from oil palm shell in the presence of CO<sub>2</sub> or N<sub>2</sub> for CO<sub>2</sub> adsorption

Roozbeh Hoseinzadeh Hesas<sup>a</sup>, Arash Arami-Niya<sup>a,\*</sup>, Wan Mohd Ashri Wan Daud<sup>a</sup>,  
J.N. Sahu<sup>a,b</sup>

<sup>a</sup> Department of Chemical Engineering, Faculty of Engineering, University of Malaya, 50603 Kuala Lumpur, Malaysia

<sup>b</sup> Department of Petroleum and Chemical Engineering, Faculty of Engineering, Institut Teknologi Brunei, Tungku Gadong, P.O. Box 2909, Brunei Darussalam

### ARTICLE INFO

#### Article history:

Received 16 June 2014  
Received in revised form 9 September 2014  
Accepted 22 September 2014  
Available online xxx

#### Keywords:

Biomass  
Chemical activation  
Microwave irradiation  
Adsorption

### ABSTRACT

Activated carbon (AC) was prepared from oil palm shell using different ratios of KOH as an activation agent and various microwave irradiation powers. To study the effects of physical agents, the impregnated precursors were activated under a flow of CO<sub>2</sub> or N<sub>2</sub>. Maximum BET surface areas of 1196 and 1630 m<sup>2</sup>/g were achieved in the presence of CO<sub>2</sub> and N<sub>2</sub>, respectively. The textural properties of the samples with the highest surface areas were investigated using ultimate and proximate analyses, SEM and FTIR. The CO<sub>2</sub> adsorption results suggest that the ACs are promising adsorbents for gas separation or storage applications.

© 2014 The Korean Society of Industrial and Engineering Chemistry. Published by Elsevier B.V. All rights reserved.

### Introduction

Activated carbons (ACs) have been widely used as solid adsorbents in many gas and liquid processes due to their highly desirable textural and surface chemical properties. ACs are good adsorbents because of their large specific surface areas ( $S_{\text{BET}}$ ), high micropore volumes ( $V_{\text{mic}}$ ), favourable pore size distributions, thermal stability and controllable and highly developed porosity [1–3]. Due to the high cost of commercial ACs, many researchers have focused on preparing low-cost ACs using inexpensive precursors with a high carbon content and low levels of inorganic compounds. Waste materials and agricultural by-products such as cotton stalk [4], almond shell and orange peel [5], pomelo skin [6] and coconut shell [7] have been utilised as low-cost precursors for AC production.

In addition to the nature of the raw material, the preparation method also plays an important role in determining the textural and surface chemical properties of the end products. One of the most widely used AC preparation techniques is conventional heating. In this method, the heat source is located outside the carbon bed, and energy is transferred to the samples via

convection, conduction and radiation, which produces a negative temperature gradient from the particle surface to its interior [8,9]. Gaseous products cannot be easily removed due to the thermal gradient, resulting in long preparation times and high energy consumption [10]. Recently, microwave irradiation has been used to prepare ACs because it provides volumetric and internal heating. During microwave heating, materials receive energy through dipole rotations and ionic conduction, which create a negative thermal gradient from the centre of the sample to its surface, thereby saving energy and requiring less activation time [11].

Activation methods are generally classified as either physical or chemical. In physical activation, the raw materials are carbonised in a furnace at a high temperature under an inert atmosphere such as pure nitrogen. The chars produced from the carbonisation are then activated in the presence of oxidising gases, such as carbon dioxide, steam, air or mixtures of these gases, to produce ACs [12]. In chemical activation, an acidic or basic solution, such as a H<sub>3</sub>PO<sub>4</sub>, ZnCl<sub>2</sub>, KOH or K<sub>2</sub>CO<sub>3</sub> solution, is used to decompose the precursors pyrolytically [12]. Generally, chemical activation results in a higher carbon yield and better developed pore structure than physical activation [13].

In this study, oil palm fruit waste (palm shell), which is a common low-cost agricultural waste in Malaysia (more than 4.7 million tonnes in 2007 [14]) was used as a raw material to produce ACs via microwave irradiation and KOH chemical activation. To study the effects of the synthesis conditions, the activation time, impregnation ratio (IR) and microwave power were varied. Carbon

\* Corresponding author. Tel.: +60 3 79675297; fax: +60 3 79675319.

E-mail addresses: [roozbehhesas@gmail.com](mailto:roozbehhesas@gmail.com) (R. Hoseinzadeh Hesas), [arash\\_araminiya@yahoo.com](mailto:arash_araminiya@yahoo.com) (A. Arami-Niya), [ashri@um.edu.my](mailto:ashri@um.edu.my) (W.M.A. Wan Daud), [jnsahu@um.edu.my](mailto:jnsahu@um.edu.my) (J.N. Sahu).